UCSF
UC San Francisco Electronic Theses and Dissertations

Title
Defining the interplay between hepatic enzymes and transporters in vitro and in vivo

Permalink
https://escholarship.org/uc/item/0b39t0qz

Author
Lam, Justine Lu

Publication Date
2006

Peer reviewed|Thesis/dissertation

eScholarship.org Powered by the California Digital Library
University of California

Defining the Interplay Between Hepatic Enzymes and Transporters *In Vitro* and *In Vivo*

by

Justine Lu Lam

DISSERTATION

Submitted in partial satisfaction of the requirements for the degree of

DOCTOR OF PHILOSOPHY

in

PHARMACEUTICAL SCIENCES AND PHARMACOGENOMICS

in the

GRADUATE DIVISION

of the

UNIVERSITY OF CALIFORNIA, SAN FRANCISCO

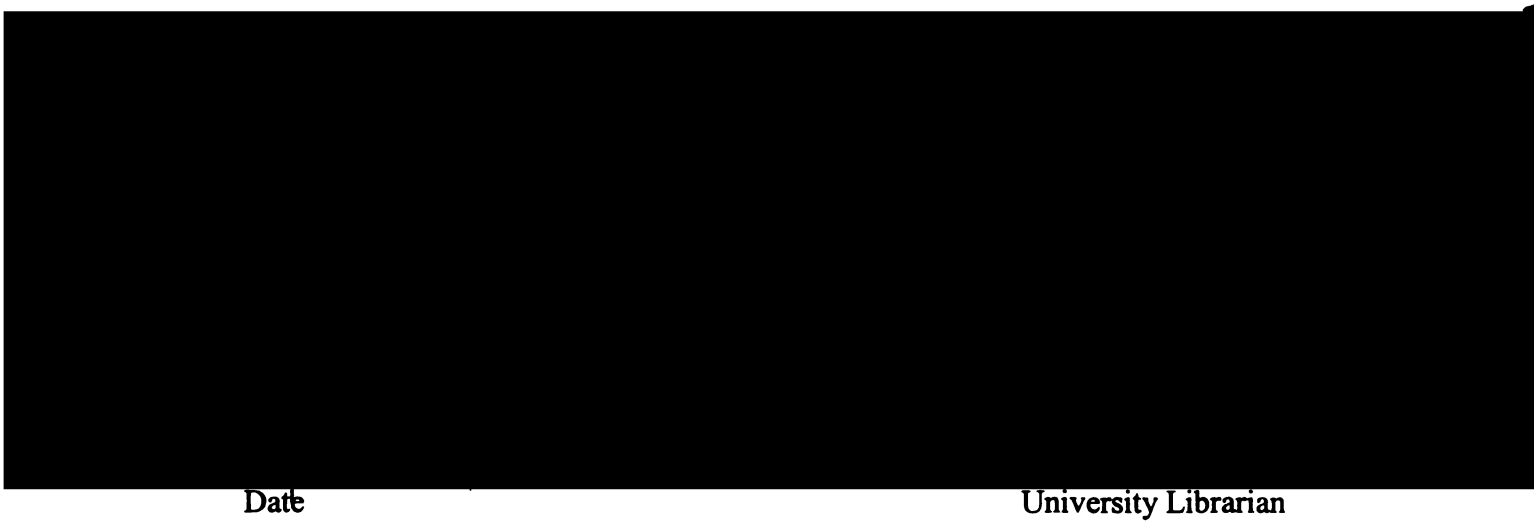

Date University Librarian

Degree Conferred: .....

To my parents

and

my loving husband

Acknowledgments

Going back to graduate school was the best career decision I have ever made. In 2001, God brought me to the beautiful city of San Francisco, which I will dearly miss. During the past five years, so many people have touched my life and shaped me to be who I am today. My deepest gratitude goes to my advisor Dr. Leslie Benet, who over the years has guided me through the ups and downs of my graduate career and personal life. From someone who had never heard of pharmacokinetics to an independent thinking scientist, I have been so blessed to have such a wonderful mentor whom I will continue to benefit from for the rest of my career.

I would like to extend my appreciation to my thesis and oral committee members: Dr. Betty-Ann Hoener, Dr. Alan Verkman, Dr. Kathleen Giacomini, and Dr. M. Almira Correia for their advice and recommendations. I am very grateful for their timely and critical reviews of this thesis research.

Special thanks to many former and present Benet group members: Dr. Carolyn Cummins and Dr. Chi-Yuan Wu for helping with my rotation projects; Dr. Muhammad Baluom, Dr. Yong Huang, and Dr. Emil Lin for their help with LC-MS assays; Dr. Hideaki Okochi for teaching me animal surgery techniques and cell line studies; Dr. Hong Sun and Dr. Nobuaki Watanabe for many insightful scientific discussions; Sarah Shugarts and Alan Wolfe for being the third hand for me whenever I need them.

My classmates - Cory Adams, Illaria Badagnani, Peter Chang, Kim Fife, Sharon Haynes, Jason Held, Eric Peters, Tom Urban and Yvonne Lau – had made my first year experience in UCSF pleasant and fruitful. Special thanks to Yvonne, my classmate, my

labmate, my roommate and my bridesmaid, for being the friend she is. Friendships of many encouraging friends – Dr. Jae Chang, Dr. Winnie Kim, Joseph Custodio, Debbie Acoba and Frances Peterson – go beyond the scope of research.

Lastly, I would like to thank my friends and family for their support as I complete this chapter of my life. My friends from San Francisco Mandarin Baptist Church, Wing, Cindy, Bernice, Mandy, Raymond, David, have grown with me spiritually and enriched my life with peace and joy. I thank God for my loving parents who left China so that I could have a good education in America. For their unconditional love and support, this thesis is dedicated to them. Finally, my love and most heartfelt thanks goes to my husband, Fleming, who is always there for me every step along this journey, without him all of this would not have been possible.

I am the scientist that I am because all of your help.

Justine Lu Lam

May 2006

Abstract

Defining the Interplay of Hepatic Enzymes and Transporters In Vitro and In Vivo

Justine L. Lam

Liver is a major site of metabolism of many xenobiotics, since the great majority of drug metabolizing enzymes are localized in the hepatocytes. Recently, several hepatic uptake and efflux transporters were found on the sinusoidal and canalicular membranes of hepatocytes, respectively. Furthermore, the substrate specificities of enzymes and transporters overlap significantly. The goal of this thesis research is to investigate the interplay of hepatic enzymes and transporters and the resulting potential clinical implications.

In specific aim one, we hypothesized that hepatic microsome studies are insufficient to characterize *in vivo* hepatic metabolic clearance; rather, studies in freshly isolated hepatocytes are needed because intact hepatic uptake and efflux transporters, which are not found in microsomes, modulate drug disposition and metabolism. Using the model compound digoxin, hepatic metabolic clearance determined using hepatocytes, but not using microsomes, correlated well with *in vivo* data.

In specific aim two, we hypothesized that metabolic drug-drug interactions at the hepatic uptake or efflux transporter levels, independent of any change in enzymatic activity, would alter the metabolism and pharmacokinetics of substrate compounds. In hepatocytes, inhibition of uptake transporters reduced substrate metabolism compared to controls, whereas inhibition of efflux transporters resulted in increased drug metabolism relative to controls. Co-administration of uptake or efflux transporter inhibitors with a model compound, erythromycin, in rats resulted in similar pharmacokinetic profiles.

However the changes versus control resulted from very different mechanisms, inhibition of hepatic uptake and inhibition of biliary excretion, confirming our prediction.

In specific aim three, we hypothesized that because rifampin induces hepatic enzymes and inhibits uptake transporters, dosing of a drug that is a dual substrate of enzymes and uptake transporters on the final day of an inducing regimen should exhibit less inductive effect than dosing on the following day in the absence of rifampin. We tested this hypothesis *in vitro* and *in vivo* in rats. Concomitant dosing of rifampin and a model compound, digoxin, completely diminished the induction effect in hepatocytes and in whole animals. Therefore, to observe the full induction effect, an uptake transporter substrate should be administered one day following the completion of an inducing regimen.

UNC LIBRARY

Table of Contents

List of Tables

NOT TRADEN

List of Figures

UCL LIBRARY

Chapter 1

Hepatic Enzymes and Transporters Modulate Drug Disposition and Metabolism

1.1 Introduction

The liver is a major site for metabolism of many endogenous compounds and xenobiotics. Drug metabolism is catalyzed by oxidative drug metabolizing enzymes (phase I enzymes) and conjugative drug metabolizing enzymes (phase II enzymes). Phase I and phase II enzymes have very broad substrate specificities, which makes the liver the chief detoxification organ in the body.

With rapid advances in molecular biology, scientists have recently cloned several families of transport proteins that are localized on the membranes of various organs. In general, 2 types of transporters are found in the liver cells, the uptake transporters and the efflux transporters. Uptake and efflux refers to the movement of substrate into and out of cells, respectively. The uptake transporters are localized on the sinusoidal (basolateral) domain, whereas the efflux transporters are present primarily on the bile canalicular (apical) domain, although several isoforms have been found on the basolateral domain.

Compared to the existing extensive knowledge of enzymes, less is known about the transporters and their significance to overall drug metabolism.

Previously, our laboratory was one of the first to recognize and to demonstrate that transporter-enzyme interplay in the intestine regulates pre-systemic metabolism (Cummins et al., 2002; Cummins et al., 2003; Cummins et al., 2004). We further hypothesize that hepatic transporters and enzymes work synergistically to detoxify xenobiotics in the liver. The goal of this project is to investigate the interplay between hepatic transporters and enzymes in vitro and in vivo.

1.2 Hepatic Enzymes

In the liver, drug metabolizing enzymes consist primarily of oxidative enzymes (phase I) and conjugative enzymes (phase II). Classically, phase I enzymes mediate the biotransformation of polar and lipophilic compounds to their more non-polar and hydrophilic metabolites by inserting an oxygen molecule into the substrates, and these enzymes are also designated as monooxygenases. Phase II enzymes catalyze bimolecular conjugation reactions to form conjugates such as glucuronides and sulfates that are more hydrophilic and easier to excrete. Traditionally, conjugative reactions are thought to occur following oxidative reactions, but many compounds do not require prior oxidation because they already possess functional groups that can be readily conjugated. The metabolites resulting from these reactions are usually inactive; however, some metabolites are not only pharmacologically active, but also even more therapeutically

potent. In some instances, to achieve better solubility, prodrugs are cleverly formulated such that bioactivation by one or more metabolizing enzymes are required to generate the active form of the drug.

1.2.1 Oxidative and Hydrolytic Enzymes (Phase I Enzymes)

1.2.1.1 Cytochrome P450

1.2.1.1.1 Background

Cytochrome P450 (CYP in human/cyp in rodents) is the largest family of monooxygenases and includes the most important drug metabolizing enzymes in the phase I category. Forty years ago, Garfinkel (1958) and Klingenberg (1958) discovered an unusual cytochrome, which later received its name P450 due to its characteristic UV absorption at 450 nm of its carbon monoxide adduct (Omura and Sato, 1962; Omura and Sato, 1964). Since then, more than two thousand CYP genes have been identified across species of bacteria, plants, fungi, insects, and mammals. As many as 57 human CYPs have been found and classified into 29 families. Families are then sub-divided into sub-families and denoted A, B, or C (i.e. CYP3A). Subsequently, each gene in each sub-family receives a number following the sub-family name (i.e. CYP3A4). All CYP isoforms in the same family have at least 40% structural similarity, and those in the same subfamily have at least 60% structural similarity. Only CYP1, 2, and 3 families are involved in metabolism of xenobiotics. The rest of the families are involved in

biotransformation of endogenous molecules such as sterols, fatty acids, eicosanoids, and vitamins. Table 1.1 illustrates species comparison of CYP1, 2, and 3 found in human and rat (adapted from Lewis et al, 2002).

Table 1.1 *Species comparison of CYPs found in human and rat*

CYP subfamily	Human	Rat
1A	1A1, 1A2	1a1, 1a2
2A	2A6, 2A7, 2A13	2a1, 2a2, 2a3
2B	2B6	2b1, 2b2, 2b3, 2b12, 2b14, 2b15, 2b16
2C	2C8, 2C9, 2C19, 2C27, 2C28	2c6, 2c7, 2c11, 2c12, 2c13, 2c22, 2c23, 2c24
2D	2D6, 2D7, 2D8	2d1, 2d2, 2d3, 2d4, 2d5, 2d18
2E	2E1	2e1
2F	2F1	
2J	2J2	2j3
3A	3A4, 3A5, 3A7	3a1, 3a2, 3a9, 3a18, 3a23

1.2.1.1.2 Structure, Function, and Tissue Distribution of Cytochrome P450

The structure of CYP has been examined by spectroscopic methods. However, recent structural studies by x-ray crystallography have shed new light on structure-activity relationship. Since the first x-ray crystal structure of CYP [P450cam (CYP101)], 20 additional unique CYP structures have been solved and deposited in the Protein Data Bank. The unique CYP secondary foldings adapted for the heme-thiolate chemistry required for oxygen activation and the binding of the redox partner and substrate recognition are conserved (Lewis, 2001). In addition to a conserved O_2 activation region, as expected, the secondary structure elements that are closest to the heme group are the most highly conserved, whereas the region close to the substrate binding sites are the

most diverse. Compared to the prokaryotic CYP, most of eukaryotic CYPs contain an N-terminal membrane bound domain. However, for several mitochondrial CYPs, their transmembrane domain is cleaved during the transport process from the cytosol to the matrix side of the mitochondria (Robin et al., 2002). In contrast, the leading transmembrane domain is intact in the microsomal CYP. Although the proline-rich transmembrane domain itself does not serve a function, it is believed that the lipophilic N-terminus could promote transfer of lipophilic substrates to the nearby catalytic domain. There is evidence suggesting that mammalian metabolizing enzymes adapt conformationally in order to recognize structurally diverse substrates (Gerber and Sligar, 1994). Multiple binding sites are also common for the drug metabolizing enzymes. It is likely that either a substrate can fit into the active site in different orientations or a substrate can turn about inside of the binding pocket (Ortiz de Montellano and De Voss, 2002).

In essence, CYP catalyzed insertion of an oxygen molecule into a substrate results in a water molecule and a mono-oxygenated metabolite. The two reducing equivalents are supplied by NADH or NADPH. Depending on the type of CYP enzyme, other redox partners may include either an iron-sulphur redoxin, flavoprotein, or cytochrome b_5 (Lewis, 2001). As a result of CYP conversion, drug metabolites are often demethylated, hydroxylated, etc. Tissue distribution, subcellular localization, and typical reactions of members in the CYP1, 2, and 3 families are listed in Table 1.2 (Montellano, 2005).

1.2.1.1.3 Regulation and Polymorphism

Regulation of CYP involves two classes of nuclear receptors. The superfamily of nuclear hormone receptors (NHR) that includes constitutive androstane receptor (CAR), the pregnane X-receptor (PXR), and the peroxisome proliferator activated receptors (PPARs) are respectively involved in the regulation of CYP2, 3 and 4 families (Waxman, 1999). In the superfamily of PAS (**P**er-"period", regulator of circadian rhythms, **A**rnt-"Ah receptor nuclear translocator" and Sim-"single minded,"regulator of midline cell differentiation), only one member, aryl hydrocarbon receptor (AHR), is found to be involved in the regulation of CYP1 family members (Gu et al., 2000). In the resting stage, NHRs are bound to co-repressors that inhibit gene transcription by recruitment of histone deacetylase or other mechanisms. However, upon ligand binding, NHRs heterodimerize with retinoid X receptors (RXR) leading to the release of the co-repressors and recruitment of co-activators (SRC-1 and CBP) that result in an increased rate of transcription (Glass and Rosenfeld, 2000; McKenna and O'Malley, 2002). Once activated by ligand binding, AHR heterodimerizes with AHR nuclear translocator (ARNT) and binds to the dioxin response element (DRE) to initiate the transcription of CYP1 enzymes (Gu et al., 2000). The most important nuclear receptors that are implicated in drug-induced over expression of CYPs are CAR, PXR, and AHR. Clinically, drug-drug interactions occurring between CYP inducers and CYP substrates can lead to a significant decrease in plasma concentrations of CYP substrates and result in lack of efficacy.

Table 1.2 *Tissue distribution, subcellular localization and typical reactions of human cytochromes P450 after Ortiz de Montellano (2005)*

CYP	Tissue Sites	Subcellular Localization[a]	Typical reaction[b]
1A1	Lung, several extrahepatic sites, peripheral blood cells	ER	Benzo[a]pyrene 3-hydroxylation
1A2	Liver	ER	Caffeine N^3-demethylation
1B1	Many extrahepatic sites, including lung and kidney	ER	17β-Estradiol 4-hydroxylation
2A6	Liver, lung and several extrahepatic sites	ER	Coumarin 7-hydroxylation
2A7		ER	
2A13	Nasal tissue	ER	Activation of 4-(methylnitrosamino)-1-(3-pyridyl 1-butanone (NNK)
2B6	Liver, lung	ER	(*S*)-Mephenytoin 4'-hydroxylatrion
2C8	Liver	ER	Taxol 6α-hydroxylation
2C9	Liver	ER	Tobutamine methyl hydroxylation
2C18	Liver	ER	
2C19	Liver	ER	(*S*)-Mephenytoin 4'-hydroxylatrion
2D6	Liver	ER[c]	Debrisoquine 4-hydroxylation
2E1	Liver, lung, other tissues	ER	Chlorzoxazone 6-hydroxylation
2F1	Lung	ER	3-Methylindole activation
2J2	Lung	ER	Arachidonic acid oxidation
2R1			
2S1	Lung	ER	
2U1			
2W1			
3A4	Liver, small intestine	ER	Testosterone 6β-hydroxylation
3A5	Liver, lung	ER	Testosterone 6β-hydroxylation
3A7	Fetal liver	ER	Testosterone 6β-hydroxylation
3A43	mRNA detected in gonads	(ER)	

[a]ER = endoplasmic reticulum (microsomal)
[b] If known
[c] Mainly ER, some detected in mitochondria

Pharmacogenetic variations of CYPs were first demonstrated in terms of variability in drug responses. Although variation comes from physiological or environmental factors as well, genetic variation accounts for 15%- 30% of interindividual differences in drug metabolism and response. CYP3A4 has not been shown to be polymorphic. The most significant polymorphic CYPs are CYP2C9, CYP2C19, and CYP2D6 affecting 20%-30% of commonly prescribed drugs (Eichelbaum et al., 2006).

1.2.1.1.4 Clinical Significance and Drug Interactions

The majority of drug metabolizing enzymes are found in the hepatocytes that make the liver a major site of detoxification. Approximately 75% of metabolized drugs are oxidized by CYP3A4, 2D6, and 2C9 (Guengerich, 2005). Substrate specificity spans a wide variety of drug classes including HIV proteases, immunosuppressants, antibiotics, and calcium channel blockers. The most common drug-drug interactions are inhibition and induction of CYP enzymes that can lead to toxicity for narrow therapeutic index drugs or lack of efficacy, respectively. For example, co-administration of cyclosporine and ketoconazole (both CYP3A4 substrates) without dosing adjustment in post transplant patients would lead to serious renal toxicity (Foradori et al., 1998). For transplant recipients on concomitant protease inhibitor (CYP3A inducers) therapy, cyclosporine (CsA) area under the concentration-time curve (AUC) increased over time, requiring a progressive decrease in CsA dose to maintain CsA trough levels (Frassetto et al., 2005). Low bioavailability of CYP3A4 substrates are often observed clinically. In vitro and in vivo studies have shown that intestinal expression of CYP3A4 in conjunction with P-glycoprotein reduces plasma level of substrates (Cummins et al., 2003; Cummins et al.,

2004). As described previously, another source of variation in drug response is polymorphism of 2D6, 2C9, and 2C19. For 2D6, "poor", "intermediate", and "fast" metabolizers have been well documented in the clinic. This phenomenon is identified as gene duplication. Some "fast" metabolizers have as many as 13 copies of 2D6 in their genome (Guengerich, 2005)! In conclusion, CYP metabolism is a very important factor to consider when studying hepatic drug disposition and metabolism, as well as the pharmacokinetics of substrate compounds.

1.2.1.2 Other Phase I Enzymes

Flavin Monooxygenases (FMOs), just like CYP450, are N-terminally membrane bound to the endoplasmic reticulum. FMO typically catalyzes oxygen and NADPH dependent N- and S- oxidations (Ziegler, 1993). Of the five isoforms found in human, the predominant isoform found in the liver is FMO3. Mechanistically, FMOs are distinct from CYPs in that they react with oxygen and NADPH independent of substrate binding to form a 4 α-hydroperoxy flavin enzyme intermediate (Rettie, 1999). The substrate specificity is broader than any of the CYPs, which is likely due to the pre-existing active form of the enzyme intermediate as well as the fact that alignment or distortion of substrate molecules is not required for binding. Clinically, FMO is not as important as CYP, because most of the drugs in use today are not substrates for FMO.

Monoamine oxidases (MAO) are present in the outer membranes of mitochondria of various tissue types in the body. Two isoforms of MAO exist: MAO-A and MAO-B. MAO enzymes are responsible for the oxidative deamination of endogenous and

xenobiotic amines. MAO has been shown to be important in metabolism of β-adrenoceptor agonists and antagonists, prodrugs of dopamine, serotonin 5-HT_1-receptor agonists as well as primaquine, flurazepam and citalopram (Benedetti, 2001). Clinically, several MAO inhibitors, such as rasagiline and selegiline, have been introduced to treat neurological diseases, such as Parkinson's and Alzheimer's diseases (Youdim et al., 2005). Although potentially significant competitive interactions can occur for MAO substrates, very few have been reported.

A variety of epoxide hydrolases, esterases, carboxy- and amino- peptidases are also present in the liver. The relative abundance of these enzymes is low compared to CYPs. These enzymes are thought to serve more physiological functions rather than detoxification. Little is known about their clinical significance in drug disposition and metabolism. Collectively, phase I enzymes, other than CYPs, can and do play an important role in drug disposition and metabolism.

UCF LIBRARY

1.2.2 Conjugative Drug Metabolizing Enzymes (Phase II Enzymes)

Phase II enzymes are characterized by their ability to conjugate xenobiotics using small molecular weight endogenous molecules such as glutathione, UDP-glucuronic acid, or acetyl co-enzyme A. These reactions generally result in pharmacologically inactive metabolites that are often substrates for specific transport proteins. In most of the cases, conjugative reactions of drugs occur following the oxidative reactions. However, there are exceptions where phase I reactions are not required for conjugation. Phase II

enzymes have been shown to play an important role in drug disposition, metabolism, and pharmacokinetics.

1.2.2.1. UDP Glucuronotransferases (UGTs)

UGT is localized to the lumen of the endoplasmic reticulum (ER) with a C-terminal anchored in the ER membrane. UGTs catalyze glucuronidation of molecules containing hydroxyl, carboxyl, amino, imino and sulfyhydryl groups using UDP-glucuronic acid as a donor molecule. Substrate specificity of UGT isoforms overlaps greatly. There are at least 15 different UGT isoforms categorized into two UGT families (UGT1 and UGT2) expressed in various human tissues with liver levels of UGT being the most abundant (Fisher et al., 2001). Large inter-individual differences in UGT1A1 expression levels have contributed to differences in drug responses (Iyer et al., 1999; Fisher et al., 2000). Glucuronidation has been demonstrated to be the rate-limiting step for in vivo plasma clearance (Coffman et al., 1996). UGT can potentially limit bioavailability of orally administered drugs that are also substrates of P-gp and(or) MRP2 (Chang and Benet, 2005).

1.2.2.2. Glutathione Transferases (GSTs)

The major biological function of GST is thought to be removal of toxic electrophilic chemical species by conjugation of glutathione to electrophilic species. They are found in the cytosol as homodimers composed of subunits from one of the four classes, Alpha (α), Mu (μ), Pi (π), and Theta (θ) (Strange et al., 2001). GST A1-1 (α isoform) and GST M1-1 (μ isoform) are expressed in a few tissues including liver, intestine, kidney, and lung; whereas GST P1-1 (π isoform) is more widely distributed. Additionally, GST P1-1 is abundant in most types of tumor cells. GSTP1val^{105}/val^{105} genotype has been found to be significantly associated with the severity of airway dysfunction defined by bronchial hyper-responsiveness (Strange et al., 2001).

1.2.2.3. Sulfotransferase Enzymes (SULTs)

Sulfotransferase enzymes catalyze the conjugation of sulfate groups to a wide range of substrates such as hormones including 17β-estradiol, dehydroepiandrosterone, and catecholamines, and many drugs including acetaminophen and minoxidil. SULTs function as homodimers. Co-factor 3'-phosphoadenosine 5'-phosphsulfate (PAP) is required for activation of the enzymes. Two forms of SULTs are found in tissues: the cytosolic form, which is considered more important for drug metabolism, and the membrane bound form, which is involved in the sulfonation of glycosaminoglycans and glycoprotein. Ten SULTs have been found in humans, of which 5 are expressed in the liver (SULT1A1, SULT1A2, SULT1A3, SULT1E, and SULT2A1) (Blanchard et al.,

2004). Although sulfation generally results in the abolition of biological activity, in several cases, bioactivation of some drugs and many procarcinogens have been reported (Weinshilboum et al., 1997).

1.2.2.4. N-acetyltransferase Enzymes (NATs)

NATs convert aromatic amines and hydrazines to the respective amides and hydrazides using acetyl coenzyme A as a donor. They also mediate the biotransformation of O-acetylation of N-hydroxyaromatic amines to acetoxy esters. There are two isoforms of NATs found in human, NAT1 and NAT2. Tissue distribution of NAT1 is ubiquiteous, whereas NAT2 is expressed only in the liver. NAT polymorphism has been shown to play a role in the susceptibility to bladder and colon cancer for certain individuals, because NAT is involved in metabolism and bioactivation of heterocyclic aromatic amine carcinogens (Rodrigues-Lima et al., 2002) .

In conclusion, many significant drug-drug interactions involve inhibition, induction, or polymorphism of drug metabolizing enzymes. The consequences of drug-drug interactions range from dose adjustment to drug withdrawal from the market. However, not all drug interactions can be explained by enzymes alone. The discovery of membrane transporters that transport many of the endogenous and exogenous compounds adds a new dimension to the old problem of drug-drug interaction.

1.3 Hepatic Transporters

The liver is the most important site for drug metabolism. Approximately 80% of the cells found in the liver are hepatocytes. Hepatocytes are clustered into small functional groups called hepatic acini. Hepatocytes in each acinus are arbitrarily divided into 3 zones. Zone 1 cells are the best oxygenated because they are closest to the portal triad which consists of the portal vein, hepatic artery, bile duct, and lymph vessels.

In three dimensions, hepatocytes are polygonal in shape, and are highly polarized into a sinusoid (basolateral) domain which faces the blood and a canalicular (apical) domain that faces the common bile duct, as shown in Figure 1.1.

In order for a drug to gain access to drug metabolism enzymes, it must traverse polar bilayer of hepatocytes. For lipophilic drugs, passive diffusion is the primary mechanism. However, for many hydrophilic drugs, membrane transport proteins are necessary for the uptake into or efflux from the hepatocytes. Hepatic membrane proteins are roughly categorized into uptake and efflux transporters based on the direction of substrate transport. Uptake transporters are localized on the sinusoidal domain, whereas efflux transporters are present on both the sinusoidal and the canalicular domains. Hepatic transporters that are most important for drug disposition and metabolism are shown in Figure 1.2.

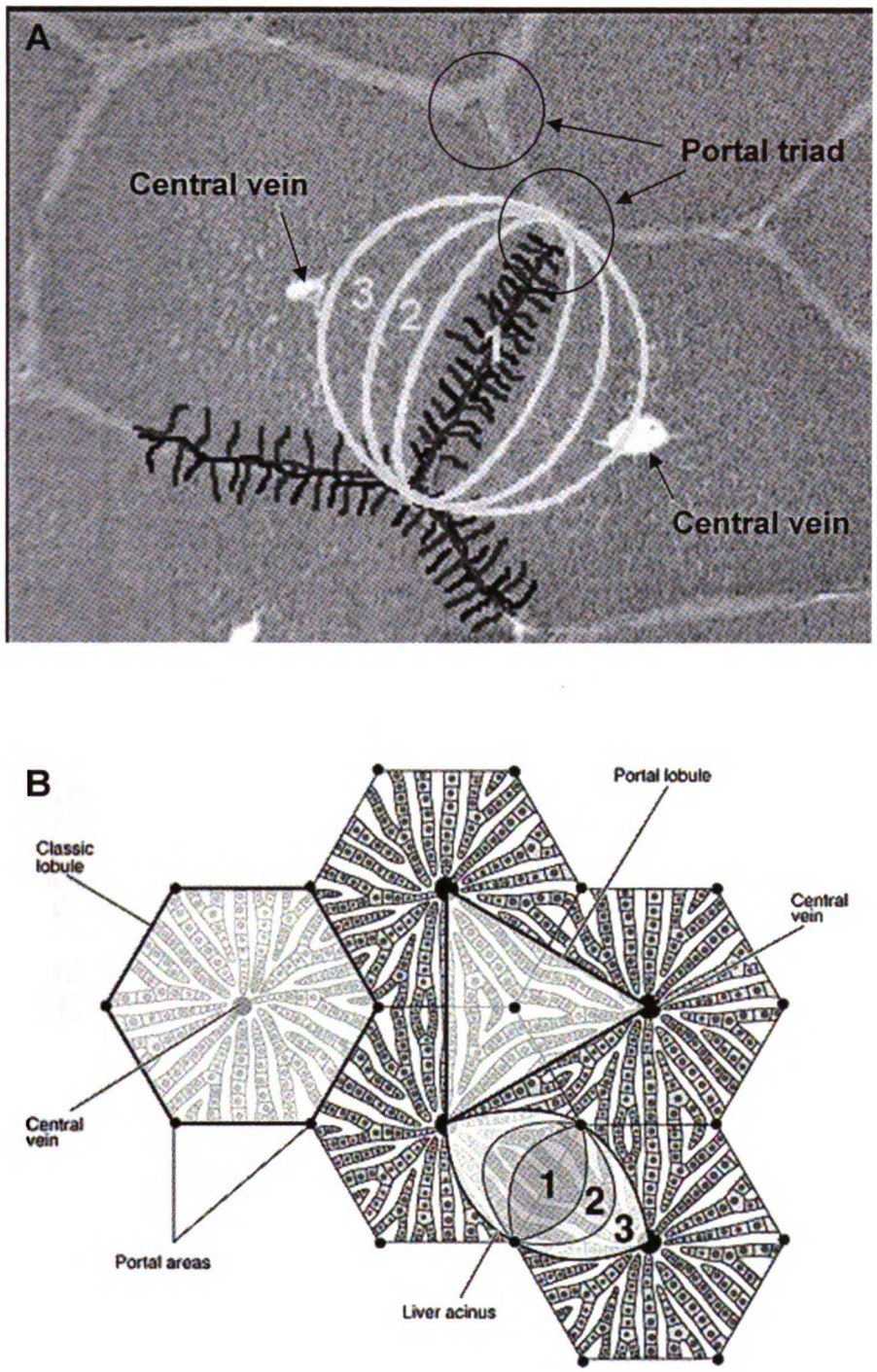

Figure 1.1 *Hepatic histology* (A) A micrograph of the arterial and venous blood supply emanating from one triad of porcine liver. (B) Cartoon depiction of (A). Adapted from http://arbl.cvmbs.colostate.edu/hbooks/pathphys/digestion/liver/histo_acinus.html

USF LIBRARY

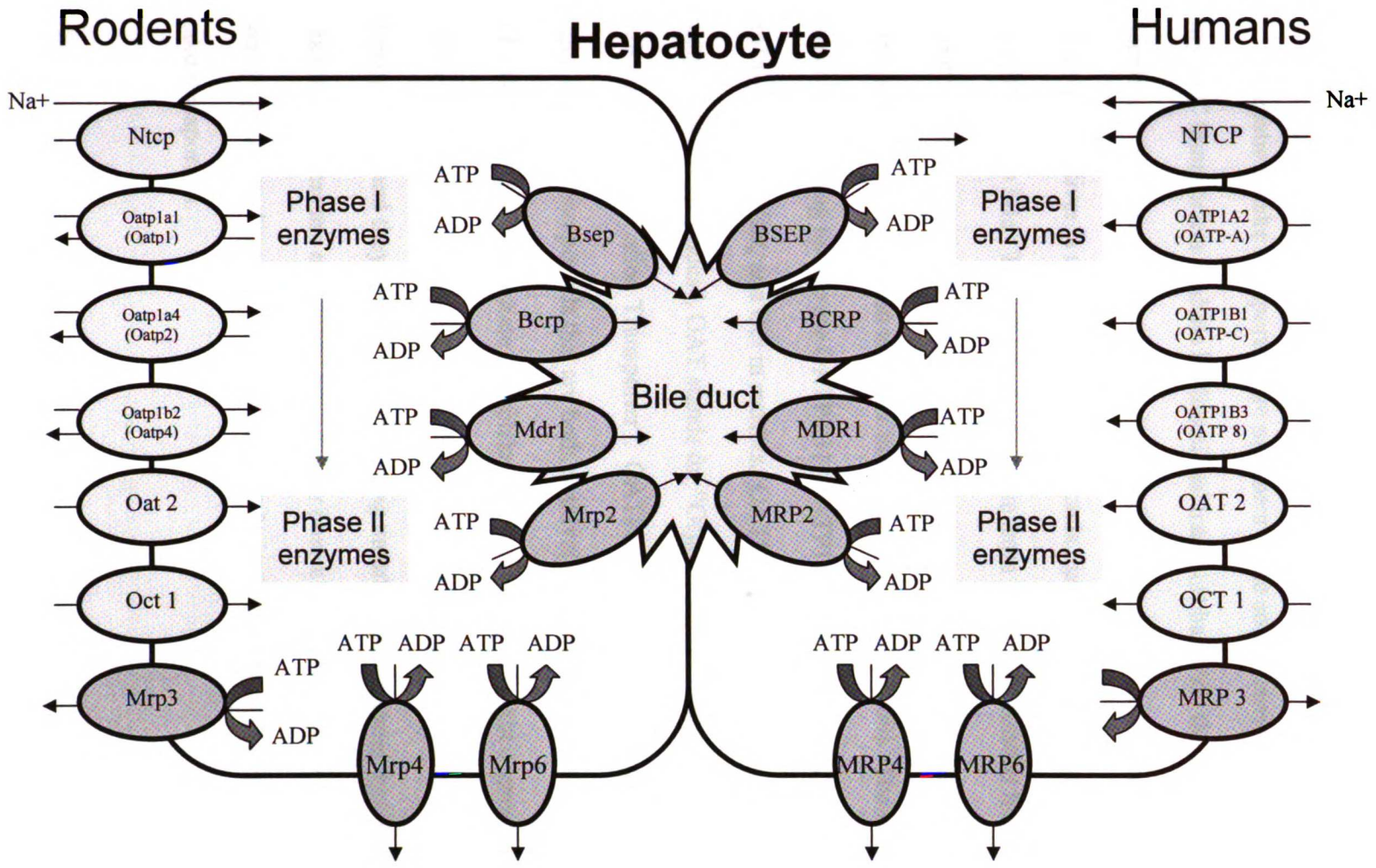

Figure 1.2 *Hepatic uptake and efflux transporters found in a rat or a human hepatocyte.*

UCSF LIBRARY

1.3.1 Hepatic Uptake Transporters

Hepatic uptake transporters are members of the solute carrier family (SLC). Many SLC transporters mediate bi-directional transport based on the substrate concentration gradient. The concentration gradient across the sinusoidal membrane from the blood to the liver is usually downhill, which is maintained by drug metabolism and active efflux into bile. This allows drug uptake from the blood. Results from in vitro cellular studies suggest that several SLC uptake transporters may also efflux drugs when the intracellular concentration is higher than outside (Li et al., 2000). The most important transporters for drug uptake are OATP1B1, OATP1B3, OAT, and OCT in human and Oatp1a4, Oatp1b2, Oat, and Oct in rodents. OATP stands for "**O**rganic **A**nion **T**ransporting **P**olypeptides", OAT stands for "**O**rganic **A**nion **T**ransporter", and OCT stands for "**O**rganic **C**ation **T**ransporter". OATPs/Oatps favor uptake of high molecular weight lipophilic compounds that are both positively and negatively charged, whereas OAT/Oat and OCT/Oct mediate the uptake of low molecular weight organic anions and cations, respectively. Substrates of the hepatic uptake transporters are both endogenous and exogenous, and they overlap widely among members of the same family. Since the uptake transporters are membrane bound, they pose a barrier to hepatic drug disposition. Several significant drug-drug interactions have been attributed in part to the hepatic uptake transporters.

UCSF

1.3.1.1 OATPs/Oatps

1.3.1.1.3 Background

Since the discovery of the first organic anion transporting polypeptides (Oatp1a1) in 1994, 13 additional members have been reported (Jacquemin et al., 1994; Mikkaichi et al., 2004). In general, the OATPs/Oatps mediate the uptake of high molecular weight (MW>400) compounds. Even though the name indicates uptake of anionic substrates, several studies have suggested that the OATPs/Oatps also uptake neutral as well as positively charged compounds. Substrate specificity overlaps significantly among the family members with a few exceptions that are isoform specific. Although the human and the rodent OATPs/Oatps are not real orthologues based on sequence, their substrate specificity overlaps considerably. Only a few OATPs/Oatps that are important for drug disposition have been characterized in detail in terms of structure, function, regulation, and polymorphism.

1.3.1.1.4 Structure, Function, and Tissue Distribution

Since it is difficult to purify membrane bound proteins without molecular manipulation, X-ray crystallography and NMR studies are almost impossible to carry out for OATPs/Oatps. Hydropathy analysis shows that OATP/Oatp family members all contain 12 transmembrane domains (TMD) (Jacquemin et al., 1994). Sequence alignment suggests that the "signature" of this transporter family is: (1) a large extracellular domain between TMs 9 and 10 that contains many conserved cysteine residues, (2) *N*-glycosylation sites in the extracellular loop between TMDs 2 and 3, and (3) the consensus

sequence, D-X-RW-(I,V)-GAWW-X-G-(F,L)-L, at the extracellular border of TMD 3 and 6 (Hagenbuch and Meier, 2003). OATP/Oatp related proteins are found in *B.taurus, R. erinacea, C. elegans and D. melanogaster* through blast search of GenBank database, however, none were found in either bacteria or yeast (Hagenbuch and Meier, 2003). The human OATPs are mapped to chromosomes 3, 8, 11, 12, 15, and 20. Interestingly, all of the drug transporting OATPs (OATP1A2, OATP1B1 and OATP1B3) are located on Chromosome 12 and clustered at 12p12 on a stretch of approximately 700,000 base pairs. This type of clustering indicates that these OATPs are results of gene duplications of an ancestral gene (Pizzagalli et al., 2002).

The substrates for subfamily OATP1A/Oatp1a and OATP1B/Oatp1b include amphipathic endogenous molecules and xenobiotics. A partial list of drug substrates is given in Table 1.3. Substrates that are commonly excreted through bile are often substrates for OATPs/Oatps. More studies are required to determine structural requirements for substrates. It is well accepted that the transport mechanism is Na^+ independent unlike NTCP/ntcp (Walters et al., 2000). Detailed studies are still needed to determine the exact mechanism of transport for human OATPs. Preliminary studies done on rat Oatp1a1 and Oatp1a4 suggest that the bi-directional transport is sensitive to intracellular concentration of glutathione (GSH) in addition to the concentration gradient of the substrate. For Oatp1a1, the mechanism appeared to be taurocholate/HCO_3 exchange and GSH in-to-out gradient dependent, whereas, for Oatp1a4, the taurocholate mediated uptake is only sensitive to intracellular concentration of GSH (Shi et al., 1995; Satlin et al., 1997; Li et al., 2000).

OATPs/Oatps involved in drug uptake and detoxification are abundant in the liver. OATP1B1 and OATP1B3 are expressed exclusively in the liver. Other OATPs/Oatps are detected in almost every tissue type investigated, which suggests their involvement in housekeeping functions. Tissue distribution of drug transporting OATPs/Oatps is listed in Table 1.3.

1.3.1.1.5 Regulation and Polymorphism

Transcriptional regulation and polymorphism has only been studied for a few OATPs/Oatps. PXR regulates multiple CYPs and the hepatic efflux transporter P-glycoprotein that have been shown to function synergistically to eliminate xenobiotics. Whether any of the human OATPs can be regulated by PXR remains to be tested. So far, only the Oatp1a4 promoter region has been shown to contain a PXR response element (Staudinger et al., 2003). All other OATPs/Oatps are regulated through different isoforms of hepatic nuclear transcription factor (HNF), as shown in Table 1.3.

Polymorphism research of OATP is in its infancy with only a few studies concentrating on OATP1B1. More than 22 SNPs have been mapped in the coding regions. Clinically relevant SNPs are V174A, N130D, and G-11187A (found in the promoter region). All three SNPs lead to decreased transport activity. The allelic frequency of OATP1B1*5 (V174A) is 14% in European-American, while only 0.7% in Japanese (Tirona et al., 2001; Nozawa et al., 2002). Unique to the Japanese population, allelic frequency of OATP1B1 *15 (N130D, V174A) is 3% (Nozawa et al., 2002). Cell surface biotinylation experiments indicated that the decreased transport activity of

Table 1.3 *Tissue expression, transcriptional regulator, drug substrate and references for hepatic uptake transporters*

Protein name (Alias)	Tissue expression	Transcriptional regulation	Drug substrates	References
OATP1B1 (OATP-C)	LIVER	HNF-1α	Benzylpenicillin, methotrexate, rifampin, pravastatin	(Jung et al., 2001; Hagenbuch and Meier, 2003)
OATP1B3 (OATP 8)	LIVER	HNF-3β	Digoxin, methotrexate, rifampin, pitivastatin	(Hagenbuch and Meier, 2003; Vavricka et al., 2004)
Oatp1a1 (Oatp1)	LIVER, kidney	HNF-1α	Enalapril, fexofenadine, pravastatin, ouabain, dexamethasone	(Jung et al., 2001; Hagenbuch and Meier, 2003)
Oatp1a4 (Oatp2)	LIVER, retina brain	PXR/RXR	Digoxin, atorvastatin, erythromycin, rifampin, pravastatin	(Guo et al., 2002; Hagenbuch and Meier, 2003)
Oatp1b2 (Oatp4)	LIVER, retina	HNF-1α	Erythromycin, pravastatin	(Jung et al., 2001; Fujino et al., 2004; Lam JL, 2006)
NTCP/ Ntcp	LIVER	RAR/RXR/ HNF-1α		(Karpen et al., 1996; Shih et al., 2001)
OCT1/Oct1	LIVER, kidney	HNF-4α/ PPAR α & γ	Cimetidine, dopamine, acyclovir, metformin, zidovudine	(Nie et al., 2005; Shitara et al., 2005; Saborowski et al., 2006)
OAT2/Oat2	LIVER, kidney intestine, muscle, heart	unknown	Methotrexate, zidovudine, NSAIDs	(Shitara et al., 2005)

OATP1B1*5 and *15 is due, in part, to decreased plasma membrane expression (Tirona et al., 2001). OATP*17 (N130D, V174A, G-11187A) is found in all races and is responsible for impaired uptake functions (Niemi et al., 2005b).

1.3.1.1.6 *Clinical Significance and Drug Interactions*

The inhibition of hepatic uptake transporters contributes to several clinical drug interactions. OATP1B1 mediated uptake of cerivastatin is inhibited by cyclosporine at a low concentration (Ki ~ 0.3-0.7 μM). This clinically relevant drug interaction is primarily caused by competitive inhibition of OATP1B1 in addition to inhibition of CYP3A4 (Ki ~ 50 μM) by cyclosporine (Shitara et al., 2003). Plasma concentrations of other "statins", such as pravastatin, pitavastatin and atorvastatin, were reported to be higher with co-administration of cyclosporine than without (Regazzi et al., 1993; Asberg et al., 2001; Hasunuma T, 2003). Gemfibrozil also interacts with a wide range of statins, especially with cerivastatin, which leads to severe side effects, such as mitotoxicity. In extreme cases, some patients suffered lethal rhabdomyolysis. As a result, cerivastatin was withdrawn from the market (Backman et al., 2000; Backman et al., 2002). Gemfibrozil and its major metabolite inhibit OATP1B1 mediated uptake of multiple statins, and together with inhibition of CYP2C9 and MRP2 (possibly BCRP) is likely the cause of increased plasma levels of statins (Sasaki et al., 2002; Shitara et al., 2005).

Several clinical studies have indicated that polymorphic OATP1B1 plays an important role in drug disposition. Reduced plasma concentrations of pravastatin were observed in Japanese subjects with homozygous OATP1B1 *15 compared to subjects that are heterozygous (Nishizato et al., 2003). In heterozygous carriers of OATP1B1

*15, the mean AUC_{0-12} (area under the curve of concentration-time plot from 0-12 hour) was 93% higher than the reference group. Furthermore, heterozygous carriers of OATP1B1 *17 exhibited 130% increase compared to the noncarriers (Niemi et al., 2004). Decreased cholesterol lowering effects of pravastatin were observed in heterozygous carriers of OATP1B1 *17 (Niemi et al., 2005b). Another clinical study showed that OATP1B1 is important in disposition of repaglinide by examining effects of transporter polymorphism on pharmacokinetics. Compared to that of the V174 reference genotype, A174 subjects exhibited a 152% increase in AUC and a 188% increase in C_{max}. Moreover, OATP1B1 (G-11187A) SNP was associated with an increased glucose-lowering effect of repaglinide (Niemi et al., 2005a).

1.3.1.2 Other Hepatic Uptake Transporters

Some other important uptake transporters expressed in the liver are OAT/Oat, OCT/Oct, NTCP/ntcp, PEPT1/Pept1, and prostaglandin transporters (PGT/rPGT). NTCP/ntcp, PEPT1/Pept1, and PGT/rPGT primarily mediate the uptake of endogenous molecules such as bile acid by NTCP and peptides by PEPT1/Pept1. OATs/Oats and OCTs/Octs have been shown to play an important role in drug disposition in the kidney, however, less is known about the roles of OAT2 and OCT1 in the liver. Some important drug substrates for OAT2/Oat2 are methotrexate, zidovudine, and NSAIDs; while important subrates for OCT1/Oct1 include cimetidine, dopamine, acyclovir, metformin, and zidovudine. The transport mechanism of OAT2/Oat2 is sodium-independent and not driven by an out-wardly directed glutarate gradient (Sekine et al., 1998). In contrast,

OCT1/Oct1 is sensitive to membrane potential and the substrate gradient (Zhang et al., 1997). To date, very little is known about the regulation and polymorphism of OAT2 and OCT1. Clinically significant drug-drug interactions involving OATs include: (1) cephalosporin antibiotics with probenecid (Brown, 1993), (2) methotrexate with penicillin, probenecid, and NSAIDs (Tracy et al., 1992; Furst, 1995; Kremer and Hamilton, 1995). It is not clear how much OAT2 contributes to the overall disposition of these drugs. Evidence from several studies suggest that kidney OATs may play a more important role in these drug-drug interactions (Shitara et al., 2005). Currently, no drug-drug interaction due to OCT1 has been reported.

1.3.2 Hepatic Efflux Transporters

Hepatic efflux transporters are members of the ATP binding cassette (ABC) superfamily. ABC transporters utilize energy derived from ATP hydrolysis to drive the transport of a wide variety of substances across the plasma membrane as well as intracellular membranes of the endoplasmic reticulum, peroxisomes, and mitochondria (Higgins, 1992; Strautnieks et al., 1998; Dean et al., 2001). Functional ABC transporters have three distinctive features in that they: (1) contain two nucleotide binding domains (NBD) that include ATP-binding sites and the Walker A and B domains; (2) contain at least two sets of transmembrane domains (TMD), typically consisting of six membrane spanning α-helices; and (3) contain a signature C-terminal consensus sequence (Hyde et al., 1990). ABC transporters are present either as full transporters containing at least two

TMDs and two NBDs or as half transporters containing one TMD and one NBD. The half transporters assemble as either homodimers or heterodimers to create functional full transporters (Hyde et al., 1990). Currently, the human ABC transporter superfamily consists of 49 members and is categorized into 7 subfamilies based on sequence homology. Table 1.4 lists the tissue distribution, function and major drug substrates of ABC transporters that are expressed in the liver.

1.3.2.1 P-glycoprotein (MDR1)

1.3.2.1.3 Background

In the 1970's, clinicians noticed that tumors became resistant to chemo-therapeutic agents during the course of therapy. Several research groups reported that tumor cell lines exhibiting drug resistant properties over expressed a 170 kDa glycosylated protein (Ling and Thompson, 1974; See et al., 1974). P-glycoprotein, also known as multi-drug resistant protein (MDR1), was named after its effects on drug permeability in tumor cells. Three groups cloned P-gp from hamster (Gerlach et al., 1986), mouse (Gros et al., 1988), and human (Roninson et al., 1986) cell lines. In contrast to human P-gp, rodent p-gp is encoded by 2 different genes (mdr1a and mdr1b) that have tissue specific expression and different substrate specificities. To address P-gp's physiological functions, md1ra&b (-/-) knock out mice were generated (Schinkel et al., 1997). These knock out mice were viable and fertile with no obvious abnormal phenotypes. However, the brain concentration of the anthelmintic drug ivermectin was 90 fold higher in the knock out mice than in the wildtype mice due to high expression of

Table 1.4 *Expression, function and substrates of human hepatic efflux transporters*

Symbol	Alias	Expression	Function	Substrates (Schinkel et al., 1997; Lage, 2003)
ABCA6		Liver		
ABCB1	PGY1, MDR1	Liver, intestine, adrenal, kidney, BBB[a], testis, ovary, placenta	Drug resistance	verapamil, digoxin, Rhodamine 123, FK506
ABCB4	PGY3	Liver	Phosphatidyl-choline transport	paclitaxel, vinca alkaloids
ABCB11	SPGP	Liver	Bile salt transport	
ABCC1	MRP1	Liver, lung, intestine, PBMC[a],choroid plexus, testis	Drug resistance	anthracyclines, vinca alkaloids, methotrexate
ABCC2	MRP2	Liver, intestine, kidney, brain, placenta	Organic anion efflux	methotrexate, anthracyclines, glucuronides, gluta-thiones, platin-drugs camptothecins,
ABCC3	MRP3	Liver, kidney, lung, intestine, adrenal gland, gallbladder	Drug resistance	methotrexate, bile salts, E217G, vinca alkaloids, epipodophyllotoxins
ABCC4	MRP4	Liver, prostate, lung, kidney, pancreas, spleen, testis, ovary, thymus, intestine	Nucleoside transport	nucleotide analogues, methotrexate
ABCC6	MRP6	Kidney, liver		
ABCG2	ABCdP, MXR, BCRP	Liver, placenta, intestine, kidney	Toxin efflux, drug resistance	prazosin, mitoxantrone, anthracyclines, camptothecins, topotecan
ABCG5	White3	Liver, intestine	Sterol transport	
ABCG8		Liver, intestine	Sterol transport	

a : BBB: blood brain barrier,
PBMC: Peripheral blood mononuclear cells

P-gp in the brain of wild-type mice (Schinkel et al., 1994). This brought the attention of pharmaceutical scientists to the importance of transporter effects on drug disposition.

1.3.2.1.4 Structure, Function and Tissue Distribution

The human P-gp has 1280 amino acids (140 kDa) that are arranged in two homologous halves connected by a linker region, as shown in Figure 1.3 (Loo and Clarke, 2005). Each half includes six transmembrane domains, an ATP binding site and a nucleotide binding domain (NBD). The extracellular loop between TMD 1 and 2 contains several glycosylated amino acids leading to its observed molecular weight, 170 kDa. Since it is very difficult to purify membrane bound protein for x-ray crystallography, the only structural data available for ABC transporters are bacterial transporters that are not membrane bound. In addition to bacterial structural data, electron microscopic studies and 2D crystals have provided low resolution structural information for P-gp (Borges-Walmsley et al., 2003). These studies suggest a hexagonal ring of protein with a central asymmetrical pore of approximate dimension of 30Å × 5-10 Å. Each six TMD helices form a channel open to the membrane, as shown in Figure 1.3.

P-gp mediates efflux of substrates from intracellular to extracellular space using energy derived from ATP hydrolysis, thus allowing transport against steep substrate gradients. Extensive mutagenesis studies and quantitative structure-activity relationship (QSAR) studies lead to the three following proposed mechanisms of P-gp transport, shown in Figure 1.4. The classic transport model involves direct movement of drug molecules from inside of the cell to outside of the cell through the hydrophilic pore following substrate recognition. The hydrophobic vacuum cleaner model requires

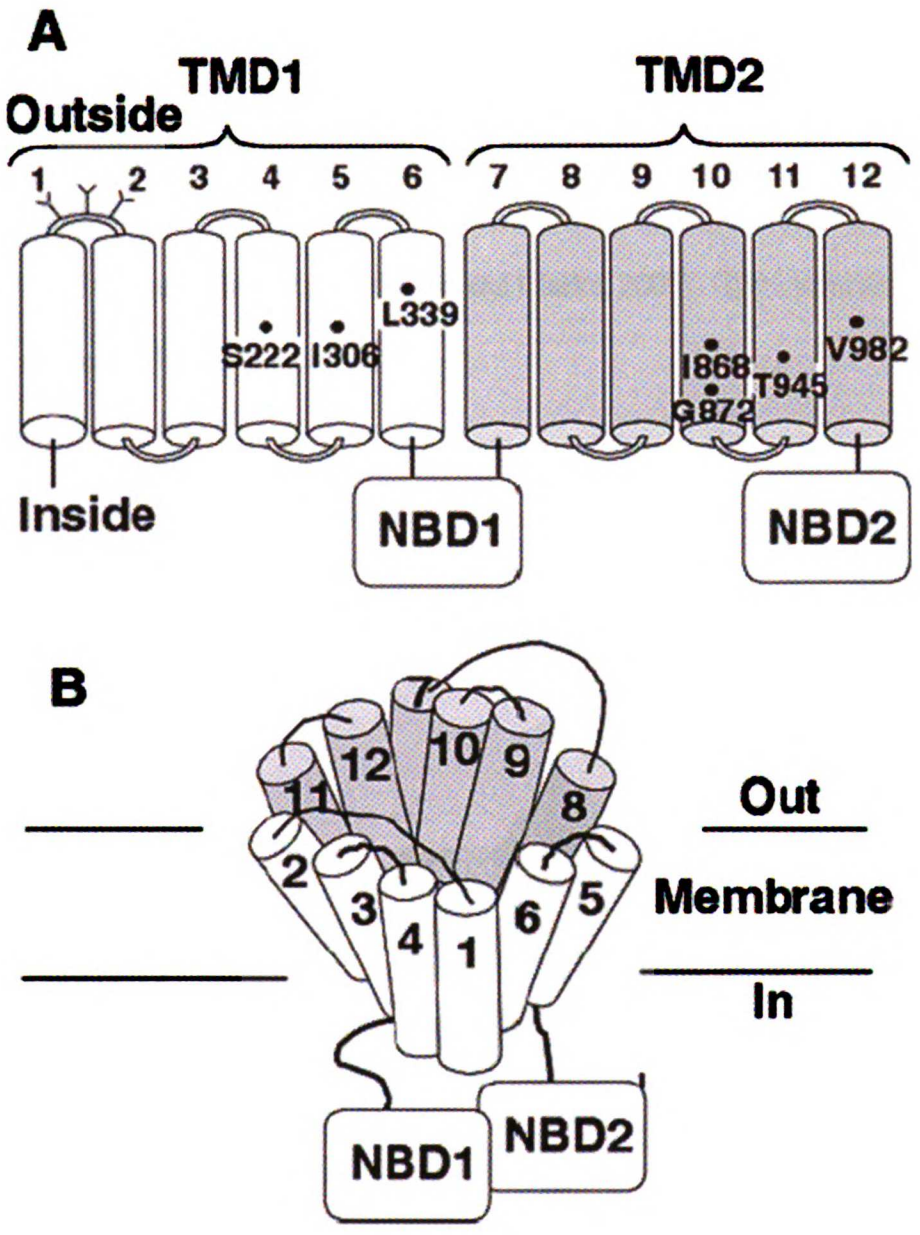

Figure 1.3 *Schematic models of P-gp* (A) The white cylinders represent the TM segments in TMD1, while the grey cylinders represent TM segments within TMD2. The branched lines between TMD 1 and 2 represent glycosylation sites and the rounded rectangles represent the NBDs. The residues shown in the TM segments are predicted to be part of the drug-binding pocket because cysteines introduced at these positions in TMD1 can be cross-linked to cysteines introduced at the indicated positions in TMD2 with MXM cross-linkers that are substrates of P-gp (Loo & Clarke, 2001c). (B) Model of the organization of the TM segments based on cross-linking and cysteine scanning mutagenesis studies. The common drug-binding pocket is at the interface between the TMDs. Adapted from Loo and Clarke (2005).

UCSF LIBRARY

substrate to enter the bilayer first before moving into the hydrophilic pore and eventually being pumped out from the pore. The flippase model suggests that drug molecules flip from the inner leaflet (intracellular side of bilayer) to the outer leaflet through the hydrophilic pore of P-gp. Recent studies using labeled P-gp protein favor the hydrophobic vacuum cleaner model (Loo and Clarke, 2005). The mechanism of P-gp transport remains highly controversial.

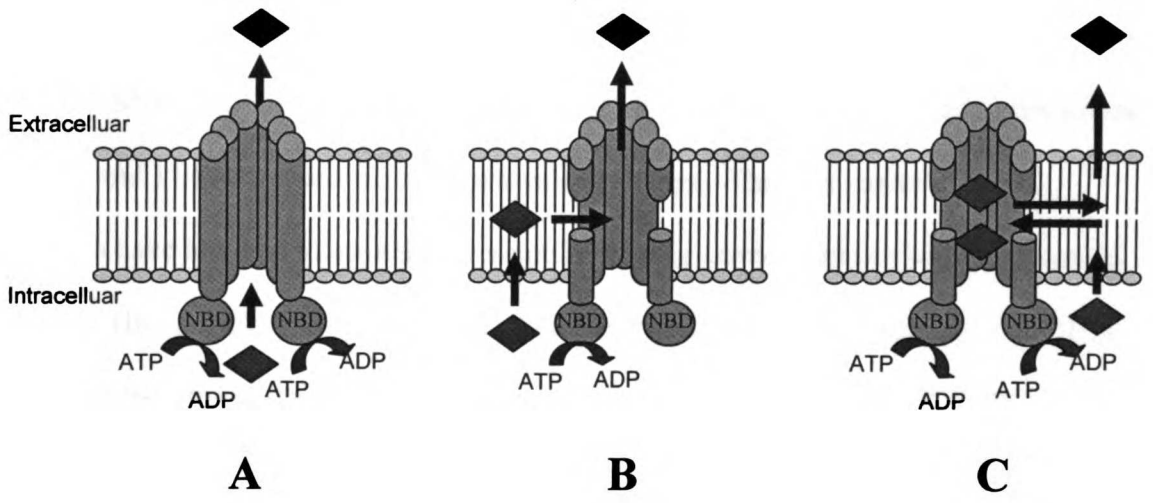

Figure 1.4 *The proposed models for P-gp transport mechanism:* (A) classical transport model, (B) hydrophobic vacuum cleaner model, and (C) flippase model.

P-gp was first cloned from tumor cell lines, but it is also highly expressed in a number of normal tissues that are important for drug disposition, such as liver, intestine, kidney, brain, testis, ovaries, and placenta. Function and localization of P-gp suggest this transporter physiologically functions as a protective barrier against foreign toxins.

1.3.2.1.5 Regulation and Polymorphism

A number of ligand-activated nuclear receptors are key transcriptional regulators of P-gp, but only pregnane X receptor [PXR; steroid and xenobiotic receptor (SXR) in humans], has been shown to regulate p-glycoprotein expression (Staudinger et al., 2003; Bauer et al., 2004). Just as for CYP3A4, upon ligand binding, PXR heterodimerized with RXR to initiate transcription. The human MDR1 gene is encoded by 28 exons. To date, 29 SNPs have been identified in the MDR1 gene, 19 SNPs are located in the exonic region, and 11 SNPs result in non-synonymous change. The first variant found to have lowered intestinal expression of P-gp is a synonymous change at exon 26, C3435T (Ile) (Hoffmeyer et al., 2000). Another important SNP on exon 26,G2677T/A, results in two distinctive amino acid changes, Ala 893 Ser and Ala 893 Thr. G2677T/A and T129C are likely associated with altered transport activity and expression of P-gp (Kim et al., 2001; Tanabe et al., 2001). Studies have shown a linkage disequilibrium between C3435T and G2677T/A suggesting that functional differences in P-gp attributed to C3435T may be a result of associated G2677T/A (Horinouchi et al., 2002). Recently, it has been shown that a synonymous SNP in exon 12 (C1236T) is linked to C3435T and G2677T/A (Marzolini et al., 2004).

1.3.2.1.6 ***Clinical Significance and Drug Interactions***

Expressed on the luminal surface of the brain microvascular endothelium and in isolated brain capillary endothelial cells, P-gp limits brain tissue exposure of drugs from the systemic blood. Studies using transgenic mice (*mdr1a/1b* -/-) demonstrated brain accumulation of several P-gp substrates, including digoxin, cyclosporine, and ivermectin, suggesting that the brain is more sensitive to alteration of P-gp function than other organs that also express P-gp (Schinkel et al., 1994; Schinkel et al., 1997). The central opioid effects observed from co-administration of loperamide and the P-gp inhibitor quinidine indicate inhibition of P-gp at the BBB (Sadeque et al., 2000). The pharmaceutical industry now routinely screens new chemical entities for being P-gp substrates or inhibitors that may cause significant drug interactions with other P-gp inhibitors or substrates and lead to neurotoxicity.

P-gp plays a significant role in intestinal metabolism. In the intestine, P-gp is expressed on the apical membrane of the enterocytes facing the lumen. After a fraction of intracellular drug molecules is effluxed out to the lumen by P-gp, it is ready for reabsorption and re-efflux. This cycling of drug molecules prolongs the drug transit time in the intestine, which gives intestinal enzymes the opportunity to metabolize the drug and potentially lead to decreased oral bioavaibility (Cummins et al., 2002; Cummins et al., 2003; Cummins et al., 2004). In a clinical study, an inhibitory effect of verapamil on intestinal secretion rate of talinolol was reported. This P-gp mediated interaction resulted in a decrease in i.v. infused talinolol intestinal secretion rate from 4.0 ug/min to 2.0ug/min after administering verapamil orally (Gramatte and Oertel, 1999).

The role of P-gp in hepatic drug disposition and metabolism is less well understood. In hepatocytes, P-gp is expressed on the bile canalicular domain and is actively involved in excretion. In an isolated prefused rat liver study, when tacrolimus was co-administered with GG918 (a potent P-gp inhibitor), the AUC decreased significantly compared to that without the inhibitor. This finding suggests increased metabolism of tacrolimus as a result of P-gp inhibition (Wu and Benet, 2003). An in vivo study showed that compared to that of wildtype mice, metabolism of i.v. administered [^{14}C]-erythromycin increased more than 2-fold in mdr1a/1b (-/-) mice indicating the significance of P-gp in hepatic drug disposition and metabolism (Lan et al., 2000).

It is worth mentioning that the MDR1 gene and CYP3A4 gene are located in close proximity on the same chromosome 7q22.1 and 7q21.1, respectively (Wacher et al., 1995). Expression of both genes is under the regulation of PXR. Substrates and inhibitors for CYP3A4 and P-gp overlap considerably. Since both genes are highly expressed in the intestine and liver, they work together to eliminate foreign toxins from the body.

1.3.2.2 Multidrug Resistance Proteins (MRPs/Mrps)

The MRP family consists of 9 efflux transporters, 5 of which are expressed in the liver. MRP2 is localized on the bile canalicular domain, whereas MRP1, 3, 4, and 6 are found on the basolateral domain of hepatocytes (Kruh and Belinsky, 2003). MRP2 is the best studied member of this family, because the majority of its expression is in the liver. Unlike P-gp which mediates the extrusion of neutral and slightly positively charged

exogenous compounds, MPRs favors endogenous and exogenous anions such as bile acids, glutathions, and glucuronide conjugates (Akita et al., 2001). Dubin-Johnson syndrome is associated with defective MRP2 (Paulusma et al., 1997). A major manifestation of Dubin-Johnson syndrome is jaundice resulting from impaired excretion of bilirubin glucuronide. Together with OATPs, MRP2 has been shown to eliminiate organic anions such as the "statins" from the blood (Ito et al., 2005). Expression of MRP1 and 3 are low in the liver compared to MRP2. However under cholestatic conditions when canalicular excretion is impaired, MRP3 expression is up-regulated (Soroka et al., 2001). This could explain elevated blood levels of bile acid under cholestatic conditions since MRP3 substrate specificity overlaps with MRP2. Mrp3 (-/-) knock out mice are healthy suggesting that Mrp3 is a backup system for Mrp2 (Belinsky et al., 2005). Recently, MRP4 and 6 have been found to be expressed on the sinusoidal domain of hepatocytes. They are also anion transporters, and their role in drug efflux is not entirely clear.

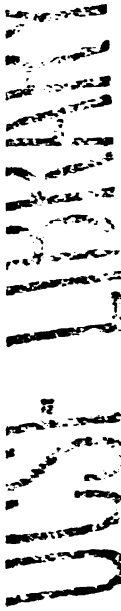

1.3.2.3 Other Efflux Transporters

BCRP (breast cancer resistance protein) was first cloned from breast cancer cells and human placenta. Its expression is high in placenta, but relatively low in breast, ovary, small intestine, and liver. Compared to P-gp, BCRP is a "half" transporter consisting of only 6 transmembrane domains and one ATP binding site. BCRPs homo-dimerize to form a functional transporter. Its substrates including doxorubicin, methotrexate, and topotecan overlap with those of P-gp. Several groups have shown the

significance of BCRP in limiting bioavailability in the intestine; however, its role in liver requires further investigation (Sarkadi et al., 2004).

BSEP (bile salt export pump) is predominantly found in the liver, on the apical domain of hepatocytes. The physiological function of BSEP became apparent when mutations in BSEP were found to cause type 2 progressive familial intrahepataic cholestasis, a condition that interrupts bile salt flow (Strautnieks et al., 1998). Physiological functions of BSEP include: (1) limiting intracellular bile acid concentration and (2) maintaining the enterohepatic circulation of bile acids. BSEP mediates the efflux of both primary and secondary bile salts with high affinity, however, its role in drug disposition is very limited, if any (Gerloff et al., 1998).

MDR3 (Mdr2 in rodents) is identified as canalicular phospholipid flippase (Smith et al., 1994). Type 3 progressive familial intrahepataic cholestasis, a disease causing defective biliary phospholipid excretion, results from mutations in MDR3 (de Vree et al., 1998). MDR3 is capable of transporting a few drugs namely digoxin, vinblastine, and paclitaxel in vitro (Smith et al., 2000). Its role in hepatic drug disposition has yet to be demonstrated.

In conclusion, the hepatic transporters play an important role in the disposition and metabolism of endogenous molecules and xenobiotics. Inhibition and induction of the hepatic transporters could lead to significant drug-drug interactions. The contribution of the hepatic transporters to drug metabolism is unclear and will require further investigation.

1.4 Interplay Between Hepatic Enzymes and Transporters

1.4.1 Overlapping Substrate Specificity, Tissue Distribution and Regulation

In addition to Phase I and II enzymes, transporters play an important role in drug disposition, distribution, and elimination. Wacher et al.(1995) first recognized that substrates and inhibitors of CYP3A overlap with those of P-gp. Since then, our lab and others have demonstrated that P-gp and CYP3A4 work together in the intestine and the liver to modulate drug disposition and metabolism.

The recently discovered hepatic uptake transporters add another barrier to hepatic drug disposition and metabolism. Because of their strategic location on the sinusoidal membrane where the uptake transporters are expressed, a drug substrate would meet the uptake transporters before subsequently finding its way to the metabolizing enzymes and(or) efflux transporters. Although the list of substrates for the uptake transporters is small compared to the substrates for CYP3A4 and P-gp, the overlapping substrate specificity indicates the significance of uptake transporters in drug disposition and metabolism. In addition, Oatp1a4, cyp3a and p-gp are under the regulation of PXR. This synchronized regulation suggests that the hepatic uptake and efflux transporters and enzymes operate together to eliminate foreign toxins from the body serving a protective function.

The proposed mechanism of action is shown in Figure 1.5. Drug molecules can enter a rat hepatocyte from the blood either through passive diffusion or via active uptake by Oatp1a4 (Oatp2) and/or Oatp1b2 (Oatp4). Once the drug molecules enter the cell, they are subject to the metabolizing enzymes. The parent molecules and the metabolites can exit the cells through active efflux by either basolateral or apical efflux transporters or by passive diffusion. Rifampin (an excellent uptake tranporter inhibitor) and GG918 (a potent p-gp inhibitor) were co-administered with drug molecules to determine the effect of the uptake or the effect of the efflux transporters on drug metabolism, respectively. We expect that when the uptake transporters are inhibited, less drug enters the hepatocytes and less metabolites will form. In contrast, when the efflux transporters are blocked, more drug will accumulate in the cells, leading to increased metabolism.

1.4.2 Working Hypothesis

The goal of this thesis is to evaluate the relative effects of hepatic uptake and efflux transporters on drug metabolism. We hypothesize: (1) hepatic microsome studies are insufficient to characterize *in vivo* hepatic metabolic clearance and metabolic drug-drug interactions; rather, primary hepatocyte studies should be conducted because intact hepatic uptake and efflux transporters, which are not found in microsomes, modulate drug disposition and metabolism; (2) metabolic drug-drug interactions at the hepatic uptake or efflux transporter level, independent of enzymatic activity, alter metabolism and pharmacokinetics of substrate compounds. Two model compounds will be used to test the hypothesis, digoxin and erythromycin.

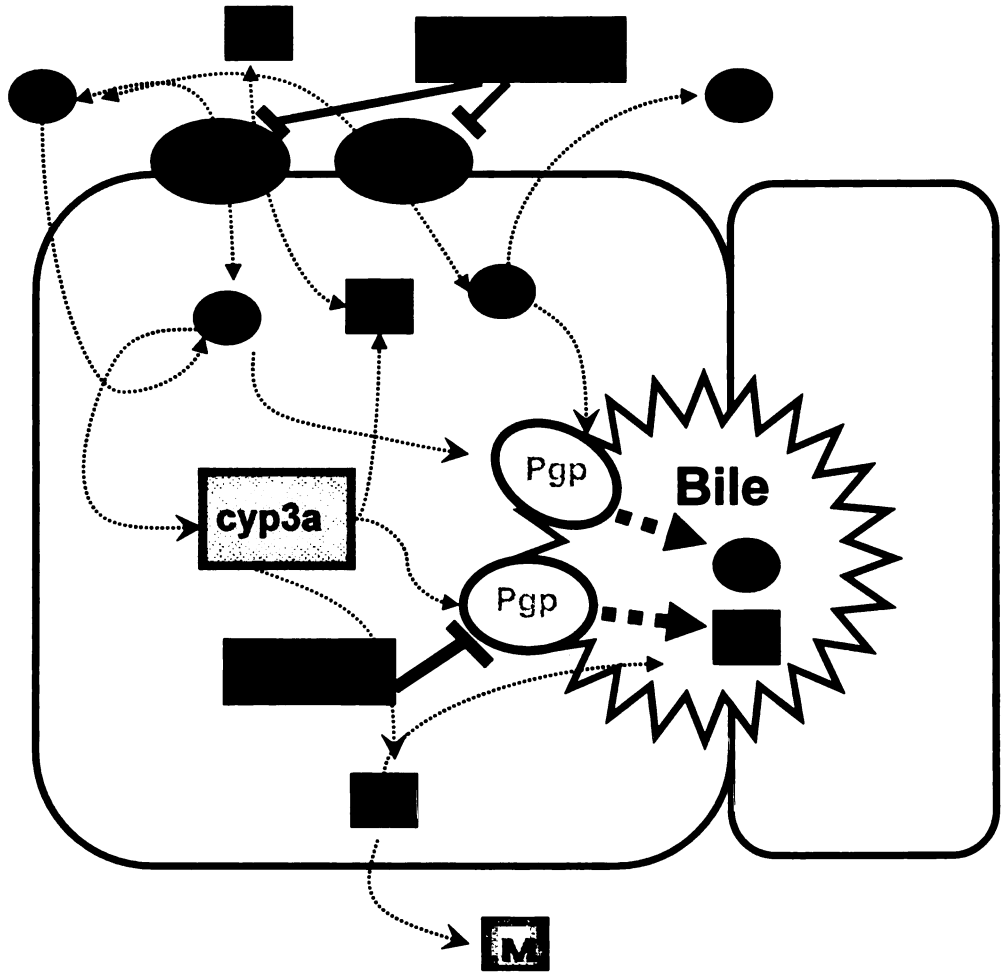

Figure 1.5 *Proposed mechanism of action in rat hepatocyte as described in the text.*

● represents drug. M represents metabolites.

UVA LIBRARY

1.4.3 Specific Aims

1. Correlate intrinsic clearances and hepatic metabolic clearances calculated from microsome incubations and from hepatocyte incubations to that from *in vivo* data in rats. Use transporter inhibitors to evaluate the effects of uptake or efflux transporters on drug metabolism

2. Study whether drug-drug interactions at the transporter level may alter metabolic clearance of a compound *in vitro and in vivo* in rats.

3. Study the effects of final day dosing of rifampin on hepatic drug disposition and metabolism in induction studies *in vitro and in vivo* in rats.

Chapter 2

Examine the Interplay of Hepatic Transporters and Enzymes In Vitro: Studies Using Rat Liver Microsomes versus Freshly Isolated Hepatocytes[1]

UBC Library

2.1 Introduction

The liver is a major site of metabolism of many endogenous compounds and xenobiotics, since hepatocytes (which comprise 80% of the liver cells) contain large amounts of smooth endoplasmic reticulum, where many metabolizing enzymes reside. These metabolizing enzymes are primarily involved in two major types of processes: redox reactions catalyzed by P450 mono-oxygenases (phase I) and conjugation with endogenous molecules (phase II) as reviewed in chapter 1. In recent years, much effort in drug discovery and development has focused on defining the metabolic profile and the

[1] A portion of this chapter was published in a manuscript entitled "Hepatic microsome studies are insufficient to characterize *in vivo* hepatic metabolic clearances and metabolic drug-drug interactions: studies of digoxin metabolism in primary rat hepatocytes vs. microsomes" Lam J.L. and Benet L.Z., Drug Metab. Dispos. (2004) 32:1311-6.

pharmacokinetics of new chemical entities. A major portion of preclinical development involves characterizing the liver enzymes affecting drug disposition and elimination.

Liver microsome incubations are routinely carried out to survey the metabolism of potential drugs by pharmaceutical companies. Microsomes are vesicles derived from the smooth endoplasmic reticulum that contain an array of phase I and a few phase II enzymes. They are easy to prepare and store; furthermore, the enzymatic activity is relatively reproducible from one experiment to the next within a couple of months of isolation. Intrinsic clearances (V_{max}/K_m) of compounds are often calculated using microsome incubations in an effort to predict *in vivo* hepatic clearances. While *in vitro* microsome studies are able to predict *in vivo* hepatic clearances for some compounds, numerous failed attempts have been reported (Naritomi et al., 2001). We hypothesize that hepatic transporters present in hepatocytes, but not in microsomes, are often the missing link explaining such discrepancies between microsome data and *in vivo* profiles.

As reviewed in chapter 1, hepatic transporters are roughly categorized into two groups: efflux transporters that are localized on the canalicular (apical) membrane and the more recently discovered uptake transporters that are found on the sinusoidal (basolateral) membrane. Many of the well-studied efflux transporters, such as P-glycoprotein (P-gp), MRP2 and BCRP are members of the ATP binding cassette (ABC) transporter superfamily. P-gp favors the transport of large hydrophobic molecules that are either neutral or positively charged (Ambudkar et al., 1999). BCRP appears to transport a smaller subset of similar compounds (Allen and Schinkel, 2002). MRP2 is known to mediate the extrusion of some negatively charged compounds, but primarily

conjugated compounds such as glutathione, glucuronide and sulfate conjugates (Renes et al., 2000).

The uptake transporters are members of the solute carrier (Slc) family and are generally categorized into three sub-families: the organic anion transporting peptides (OATP in humans/Oatp in rodents), the organic anion transporters (OAT/Oat), and the organic cation transporters (OCT/Oct). Oatp1 (gene symbol: *Slc21a1*), Oatp2 (*Slc21a5*), Oatp4 (*Slc21a10*), Oat2 (*Slc22a7*), Oat3 (*Slc22a8*), and Oct1 (*Slc22a1*) have been demonstrated to be expressed in the liver and localized in the basolateral membrane (Zhang et al., 1997; Shitara et al., 2002) of hepatocytes. Of all the hepatic uptake transporters, the OATP family is the most extensively studied. While OATs transport mainly low molecular weight compounds, OATPs mediate the uptake of much larger and structurally diverse substrates such as digoxin (Noe et al., 1997; Kullak-Ublick et al., 2001) and bilirubin (Cui et al., 2001). Coincidentally, many compounds that are substrates for the uptake and the efflux transporters are substrates for the metabolizing enzymes as well. Our hypothesis is that microsomes alone are insufficient to estimate drug metabolic clearance, because hepatic transporter effects are not taken into account. Instead, freshly isolated hepatocytes will provide a better model to assess drug metabolic clearance and to predict correlations between *in vitro* and *in vivo* data.

Digoxin, a cardiac glycoside used clinically for more than 200 years (Antman and Smith, 1985; Heller, 1990), is excreted in humans mainly unchanged by the kidney; however, in the rat, it is extensively metabolized by cyp3a (Salphati and Benet, 1999). Biotransformation of digoxin involves a stepwise hydrolysis of digitoxosides to form digoxigenin bis- and mono-digitoxoside and the aglycone digoxigenin before conjugation

and elimination (Harrison and Gibaldi, 1976). The chemical structure of digoxin and its metabolites are shown in Figure 2.1. Tanigawara et al.(1992) have shown that digoxin is

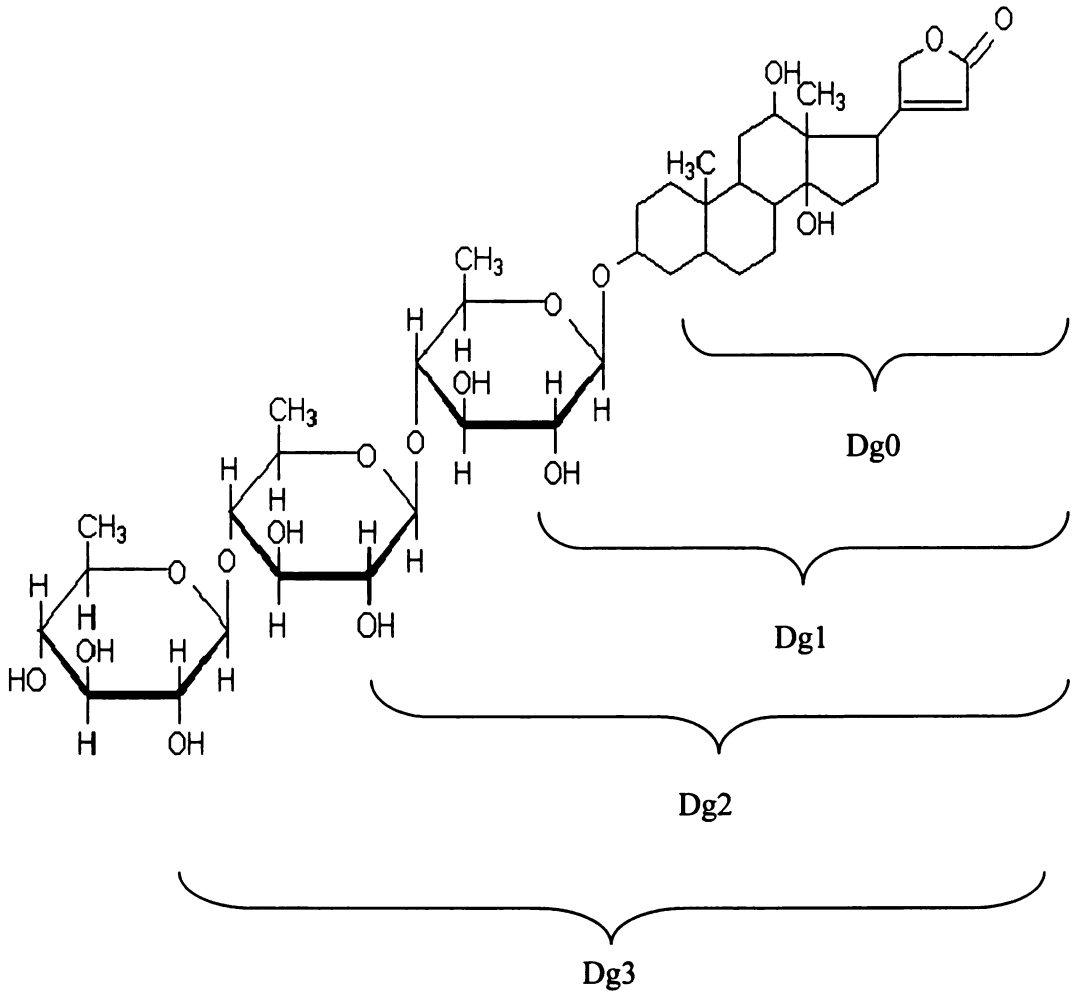

Figure 2.1 *Chemical structure of digoxin and its metabolites.* Digoxigenin (Dg0), digoxigenin mono-digitoxoside (Dg1), digoxigenin bis-digitoxoside (Dg2) and digoxin (Dg3).

a good substrate for P-gp. Recently, it has been demonstrated that digoxin is a substrate for Oatp2 with a K_m value of 240 nM (Shitara et al., 2002; Hagenbuch and Meier, 2003). In this study, we investigated the influence of hepatic transporter on digoxin metabolism in hepatocytes versus microsomes by comparing incubations containing inhibitors of hepatic uptake and efflux transporters versus control digoxin incubations. We also addressed the lack of specificity of many inhibitors. For example, rifampin, used here to inhibit the uptake transporter Oatp2 (Shitara et al., 2002), has recently been suggested to also inhibit P-gp (Zong and Pollack, 2003). We show here that the potent P-gp inhibitor, GG918, at higher concentrations is an effective uptake inhibitor.

2.2 Materials and Methods

2.2.1 Materials

Digoxin, digoxigenin (dg0), rifampin, corticosterone and NADPH were purchased from Sigma-Aldrich (St Louis, MO). Digoxigenin bis-digitoxoside (dg2) and digoxigenin mono-digitoxoside (dg1) were kind gifts from Professor Emil Lin, UCSF. [^{3}H] digoxin (37 Ci/mmol) was obtained from Perkin Elmer Life Sciences (Boston, MA). GG918 (GF120918; GlaxoSmithKline, Research Triangle Park, NC) was graciously supplied by the manufacturer. HPLC grade methanol and *tert*-butyl-methyl-ether (MTBE) were purchased from Sigma-Aldrich (St Louis, MO). Male Wistar rats (200-

300 g, Bantin and Kingman, San Leandro CA) were housed in the UCSF animal care facility with a 12 hour light/dark cycle and allowed free access to water and food. Approval of the described studies reported here was obtained from the Committee on Animal Research, UCSF.

2.2.2 Microsome Preparation

Rat liver microsomes were isolated as previously described (Salphati and Benet, 1999). Protein concentrations were determined using the Bio-Rad protein assay kit (Hercules, CA) with BSA standards. P450 content was measured using a dual-beam spectrophotometer SLM-AMINCO (DW-2000, UV-VIS, Aminco, Rochester, NY).

2.2.3 Hepatocyte Preparation

Rat hepatocytes were prepared using a modified collagenase perfusion method as described previously (Seglen, 1976). In brief, anesthesia was induced by intraperitoneal injection with a 1 ml/kg dose of ketamine/xylazine (80 mg/ml, 12 mg/ml) prior to surgery. The portal vein was cannulated with an IV catheter (catalog number 2007-04, Becton Dickinson, Sandy, UT) and perfused with oxygenated liver perfusion buffer (Invitrogen, Carlsbad, CA) for 5 minutes at 30 ml/min followed by perfusion with an oxygenated hepatocyte washing buffer (Invitrogen, Carlsbad, CA) modified with 2 mM

of L-glutamine, 10 mM Hepes, and 1.2 U/ml collagenase (Sigma-Aldrich, St. Louis, MO) for 5 minutes at 20 ml/min. At the end of the perfusion, Glisson's capsule of the digested liver was excised with scissors. The liver tissue was broken down in ice cold buffer by gentle tapping with a glass stirring rod. The hepatocytes were washed twice with an ice cold hepatocyte wash buffer containing 2 mM of L-glutamine and 10 mM Hepes and were centrifuged at 50 x g for 2-3 minutes. Cell viability was determined using the trypan blue exclusion method. Cells with viability of greater than 90% were used for further studies.

2.2.4 Microsome Incubations

Incubation conditions were as previously described (Salphati and Benet, 1999). In brief, each reaction contained 0.5 mg/ml microsomes, 1mM NADPH, 10 μM digoxin, various concentrations of inhibitors and 0.1M phosphate buffer (pH 7.4). The DMSO concentration, used to solublize substrates and inhibitors, was less than 1%. The total reaction volume was 250 μl, and the incubation period was 15 minutes, a time period shown previously to be in the linear region of the metabolite formation (Salphati and Benet, 1999). For each sample, the reaction was stopped by protein precipitation through addition of an equal volume of methanol containing 5 μg/ml of the internal standard, corticosterone. The supernatants were stored in -80°C prior to LCMS analysis.

2.2.5 *Hepatocyte Incubations*

Hepatocyte incubations were carried out immediately following cell isolation. For Michaelis-Menten studies, two million hepatocytes in Kreb-Henseleit buffer (pH 7.4) containing 0.21 g/L of sodium bicarbonate and supplemented with 1% BSA and 10 mM glucose were used in each incubation in an uncapped 20 ml glass vial. Reactions were carried out at 37°C in a water bath at a constant shaking speed of 100 rpm for 30 minutes. At the end of 30 minutes, an aliquot of hepatocytes were removed from the incubations containing highest drug concentrations to determine drug effects on cell viability using the trypan blue exclusion method. Incubations were stopped by quick freezing samples in a methanol/dry ice bath and stored at -80°C. Stored samples were frozen and thawed three times to lyse the cells. Twice the sample volume of MTBE containing 5 µg/ml of corticosterone was added to each sample and vortexed. The sample mixtures were then centrifuged at 2000 x g for 10 minutes. After quick freezing the aqueous layer in a methanol/dry ice bath, the organic layer was poured into a new tube and evaporated under nitrogen gas. Each sample was reconstituted with 300 µl of methanol for LCMS analysis.

2.2.6 *Hepatocyte Uptake Studies*

Prior to each incubation, 2 million hepatocytes were pre-warmed in Kreb-Henseleit buffer (pH7.4) containing 0.21 g/L of sodium bicarbonate and supplemented with 1% BSA and 10 mM glucose for 5 minutes. For incubation studies [^{3}H] digoxin (100nM) with and without 100 μM rifampin, 1 μM GG918 or 25 μM GG918 were added to the cells. To determine kinetic parameters of digoxin hepatocyte uptake, unlabeled digoxin (0-500 μM) was added to the incubations. After 2 minutes, the reactions were terminated by transferring 1 million hepatocytes into a centrifuge tube containing 150 μl of 2 N NaOH under a layer of a 500 μl of mixture of silicone oil and mineral oil (Shitara et al., 2003) and centrifuged at 13,000 x g for 10 seconds. The spun down cell pellets were left at 65°C overnight to ensure complete lysis. For the inhibition studies, after removing the oil layer, 150 μl of 2 N HCl and scintillation cocktail were added to each sample and radioactivity was measured using a scintillation counter (LS6000TA, Beckman Coulter, Fullerton, CA). For the kinetic parameter studies, after removing the oil layer, the cell pellets were re-suspended in water and sonicated for 30 minutes. Two hundred micro-liters of methanol containing internal standard were added to each sample and centrifuged for 15 minutes at 13,000 rpm. The supernatants were transferred to HPLC vials for LCMS analysis

2.2.7 *Time Course Studies*

Incubations were carried out in 50 ml round-bottom flasks with continuous rotation while gassed with 95% O_2/5% CO_2 at 37°C (Li et al., 2002). Aliquots of two million hepatocytes in Kreb-Henseleit buffer (pH7.4) containing 2.73 g/L of sodium bicarbonate and supplemented with 1% BSA and 10 mM glucose were taken at 5, 10, 15, 20, 30, 45 and 60 minute time points. At the end of 60 minutes, an aliquot of hepatocytes was removed from each incubation to determine drug effects on cell viability using the trypan blue exclusion method. Each aliquot was quick frozen in a methanol/dry ice bath to stop the reaction and stored at -80°C. Sample preparation was the same as described earlier for hepatocyte incubations.

2.2.8 *Assay of Digoxin and Its Metabolites*

Samples were analyzed on a liquid chromatography-mass selective detector system (Hewlett Packard) consisting of the 1100 HPLC components HPLCI and HPLCII as described previously (Christians et al., 2000). The two HPLC systems were connected via a 7240 Rheodyne six-port switching valve mounted on a step motor (Rheodyne, Cotati, CA). The system was controlled and data were processed using ChemStation Software revision A.06.01 (Hewlett Packard). Samples (100 µl) were injected onto a 10 x 6-mm extraction column (Keystone Scientific, Bellefonte, PA) filled with Hypersil ODS-1 of 5-

μm particle size (Shandon, Chadwick, UK). Samples were washed with a mobile phase of 20% methanol and 80% 0.1% formic acid supplemented with 1 mM sodium acetate. The flow was 2 ml/min, and the temperature for the extraction column was set to 65°C. After 0.75 min, the switching valve was activated, and the analytes were eluted in the backflush mode from the extraction column onto a 100 x 4.6-mm C_8, 3.5-μm analytical column (Zorbax XDB, C_8; Hewlett Packard). The mobile phase consisted of methanol and 0.1% formic acid supplemented with 1 mM sodium acetate:ACN (80:20, v:v). The following gradient was run: time 0 min, 40% methanol; 6 min, 90% methanol. The flow rate was 0.7 ml/min. The analytical column was also maintained at 65°C. Two minutes after sample injection, the mass-selective detector was activated. The detection limits were 50 ng/ml, 5 ng/ml, 10 ng/ml, 10 ng/ml and 100 ng/ml for digoxin, dg2, dg1, dg0 and rifampin, respectively. A representative LCMS chromatogram is shown in Figure 2.2.

2.2.9 *Clearance Calculations and Data Analysis*

Microsomal and hepatocyte digoxin metabolite formation rates as a function of digoxin concentration were fitted using the Hill equation from which values for V_{max}, K_{50} and the Hill coefficient were determined. For the microsomal studies, V_{max} was converted from the measured nmol/min/mg protein to per kg body weight using the standard scaling factors of 44.8 microsomal protein/g liver and a liver weight of 40g/kg body weight (Naritomi et al., 2001). For the hepatocyte studies, scaling on the basis of

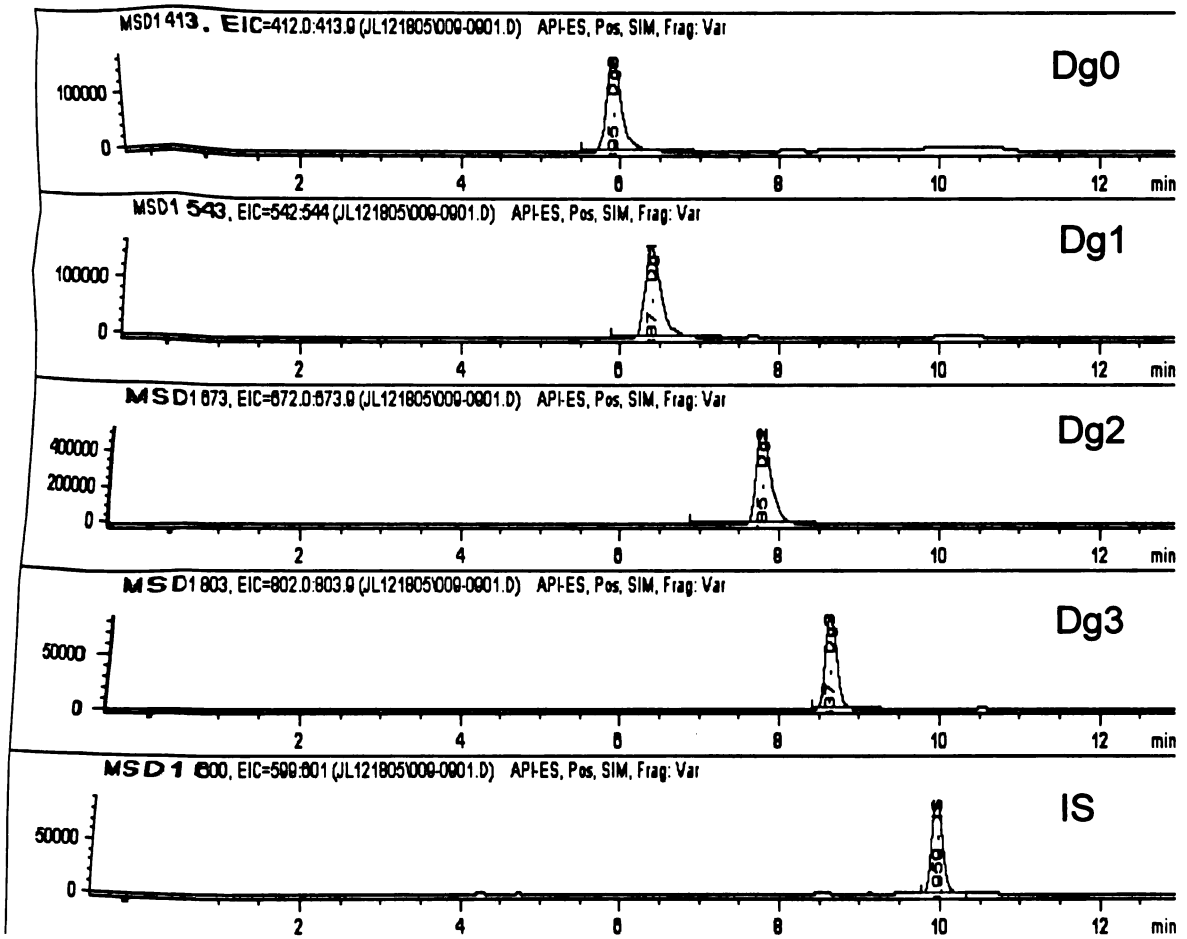

Figure 2-2 *A sample chromatogram of digoxin, its metabolites and the internal standard*

120×10^6 hepatocytes/g liver (Bayliss et al., 1999) was used. For the hepatocyte uptake studies, the rates of uptake (v) at different substrate (S) concentrations were fitted to the equation $v = [V_{max} \cdot S/(K_m + S)] + P_{dif} \cdot S$ where P_{dif} is the passive permeability value. *In vivo* blood metabolic clearance values were predicted from both microsome and hepatocyte Michaelis-Menten values using the well-stirred model with a hepatic blood

flow of 55.2 ml/min/kg (Naritomi et al., 2001) and a fraction unbound of 0.75 (Harrison and Gibaldi, 1976). Since (Hinderling, 1984) found *in vivo* blood cell to plasma partition coefficients to be 0.943 ± 0.154, the total blood to plasma ratio would not differ by more than 3% from 1.0, and no correction was utilized. *P*-values were computed using two-tailed Student t-tests.

2.3 Results

2.3.1 Michaelis-Menten Study of Digoxin Using Rat Microsomes and Hepatocytes

Results of the Michaelis-Menten studies of digoxin using both rat microsomes and hepatocytes are shown in Figure 2.3 P450 content was determined by the carbon monoxide (CO) spectrum assay (Omura and Sato, 1964) and found to be 27.4 nmol/mg microsome (data not shown). Metabolites dg2, dg1 and dg0 were monitored, but since the amounts of dg1 and dg0 contributed less than 5% of the total metabolites observed, only dg2 profiles were used for all further calculations. From the microsome studies (n=3), V_{max} and K_{50} of digoxin were calculated using non-linear regression (WinNonlin) of the Hill equation to be 1.12 ± 0.33 nmol/min/mg protein and 310 ± 123 μM (mean ± SD), respectively, with a Hill coefficient not significantly different than unity (1.03 ±

A.

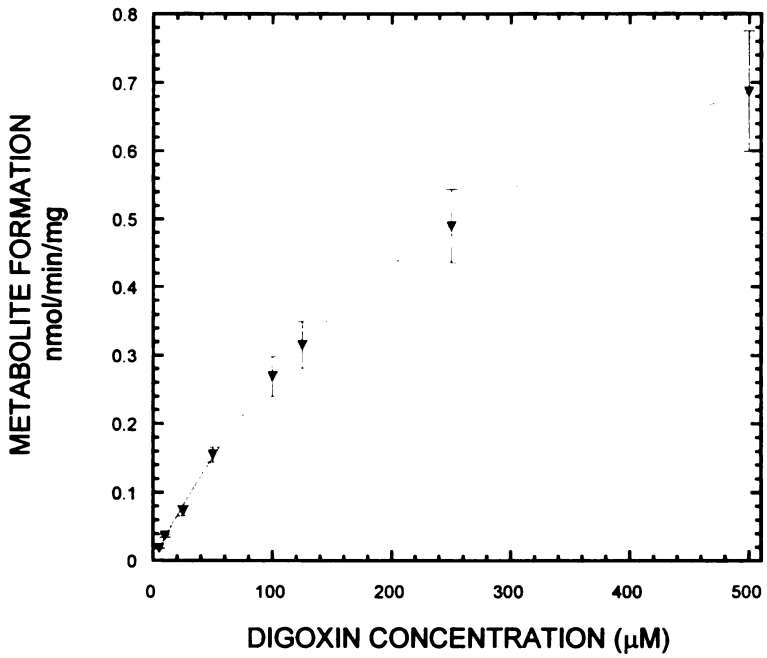

B.

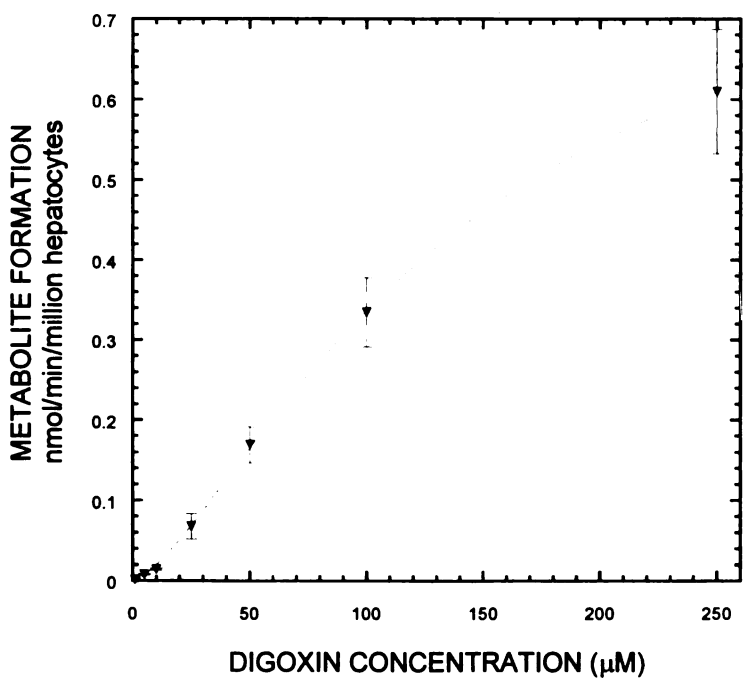

Figure 2.3 *Michaelis-Menten study of digoxin.* (A) Microsome incubations of digoxin and (B) Hepatocyte incubations of digoxin. Each curve is fitted using the Hill equation. Data are depicted as the mean ± SD, n=3.

0.03). Intrinsic clearance (V_{max}/K_{50}) was 3.73 ± 0.56 µl/ml/mg protein. Using the well-stirred model, the standard scaling factors of 44.8 microsomal protein/gram liver, liver weight of 40 g/kg body weight, liver blood flow of 55.2 ml/min/kg (Naritomi *et al.*, 2001) and fraction unbound of 0.75 (Harrison and Gibaldi, 1976), the hepatic metabolic clearance based on the microsome results was estimated to be 4.59 ± 0.69 ml/min/kg. Comparable data for hepatocytes (n=3) were 0.94 ± 0.34 nmole/min/10^6 cells for V_{max}, 159 ± 83 µM for K_{50}, with a Hill coefficient of 1.47 ± 0.25. Here a value of 6.21 ± 1.16 µl/min/10^6 cells was calculated for apparent intrinsic clearance. Scaling on the basis of 120 x 10^6 hepatocytes/gram liver (Bayliss et al., 1999) and the parameters listed above provided an estimated apparent hepatic metabolic clearance of 15.9 ± 3.0 ml/min/kg; a 3.5-fold higher value than that derived from the microsomal data.

2.3.2 *Effects of Rifampin and GG918 on Digoxin Metabolism in the Microsome System*

To determine whether rifampin or GG918 inhibit CYP3A activity, microsome incubations with each inhibitor were carried out, as shown in Figure 2.4. Compared to control, both inhibitors (rifampin and GG918) exerted no statistically significant effects on digoxin metabolism over 15 minutes.

2.3.3 *Effects of Rifampin and GG918 on Digoxin Metabolism in the Hepatocyte System*

To determine the effects of hepatic uptake and efflux transporters on digoxin metabolism, rifampin (an Oatp and Oat inhibitor) and GG918 (a very potent P-gp inhibitor) were co-administered in the hepatocyte systems. Rifampin markedly reduced digoxin metabolism in the hepatocyte incubations (Fig. 2.5A). Interestingly, with GG918, a biphasic response was noted; at concentrations at or below 1 μM, digoxin metabolism was increased and at concentrations above 1 μM of GG918 digoxin metabolism was decreased (Fig. 2.5B). An IC_{50} value was estimated using non-linear regression (WinNonlin). The Ki value was estimated by $IC_{50}/[1+S/K_{50}]$. The apparent IC_{50} and K_i values of rifampin were 478 ± 53 μM and 451 ± 50 μM. The apparent IC_{50} and K_i values of GG918 (at concentrations above 1 μM) were 4.64 ± 0.49 μM and 4.38 ± 0.46 μM. Cell viability determined at the end of incubations was above 90%.

2.3.4 *Uptake of Digoxin in Hepatocytes*

The uptake of digoxin in hepatocytes is shown in Figure 2.6. The values for V_{max}, K_m, and P_{dif} were 162 ± 10 pmol/min/million cells, 36.2 ± 8.7 μM, and 1.99 ± 0.03 μl/min/million cells, respectively. At digoxin concentrations much less than Km, the estimated transporter mediated uptake is 70%.

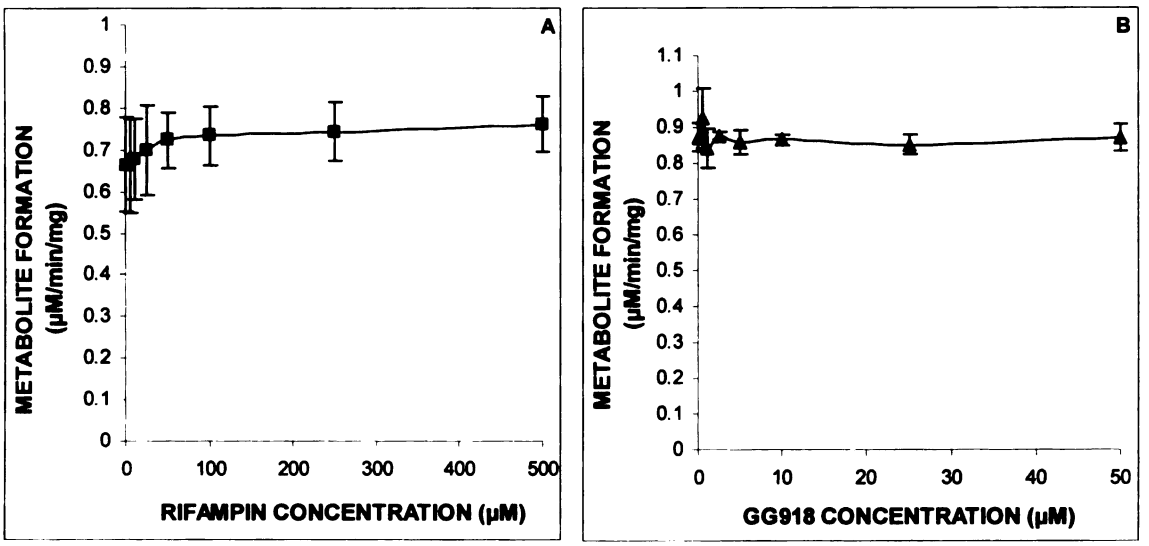

Figure 2.4 *Microsome incubations of digoxin with inhibitors.* Inhibition study of rifampin and GG918 on digoxin metabolism to dg2 in the microsome system. Digoxin concentration used was 10 µM. (A) rifampin and (B) GG918. Lines are drawn point-to-point. Data are depicted as the mean ± SD, n=3.

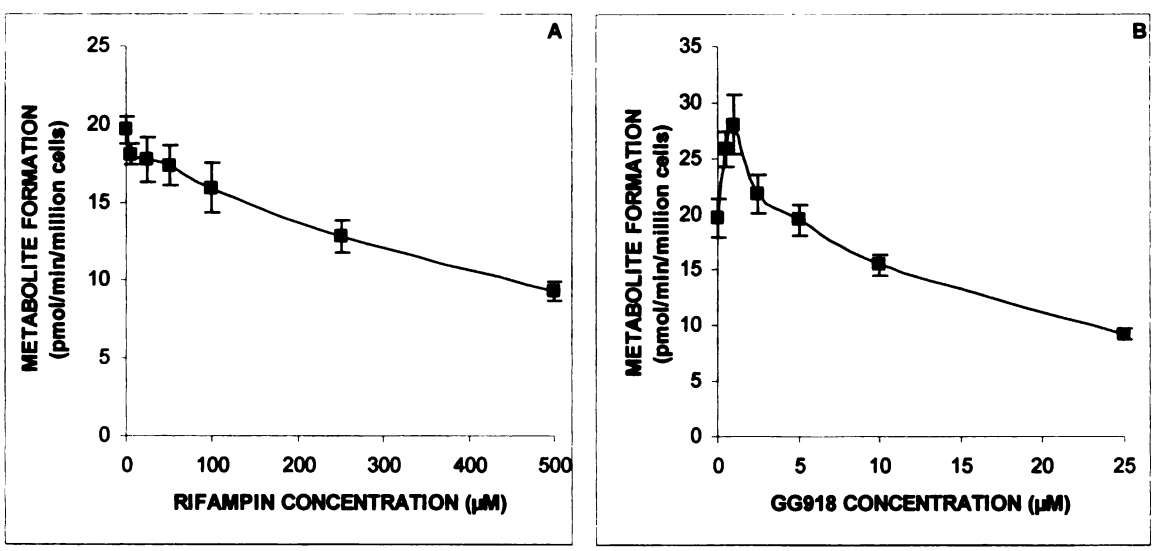

Figure 2.5 *Hepatocyte incubations of digoxin with inhibitors.* Inhibition study of rifampin and GG918 on digoxin metabolism to dg2 by hepatocytes. Digoxin concentration used was 10µM. (A) rifampin and (B) GG918. Lines are drawn point-to-point. Data are depicted as the mean ± SD, n=3.

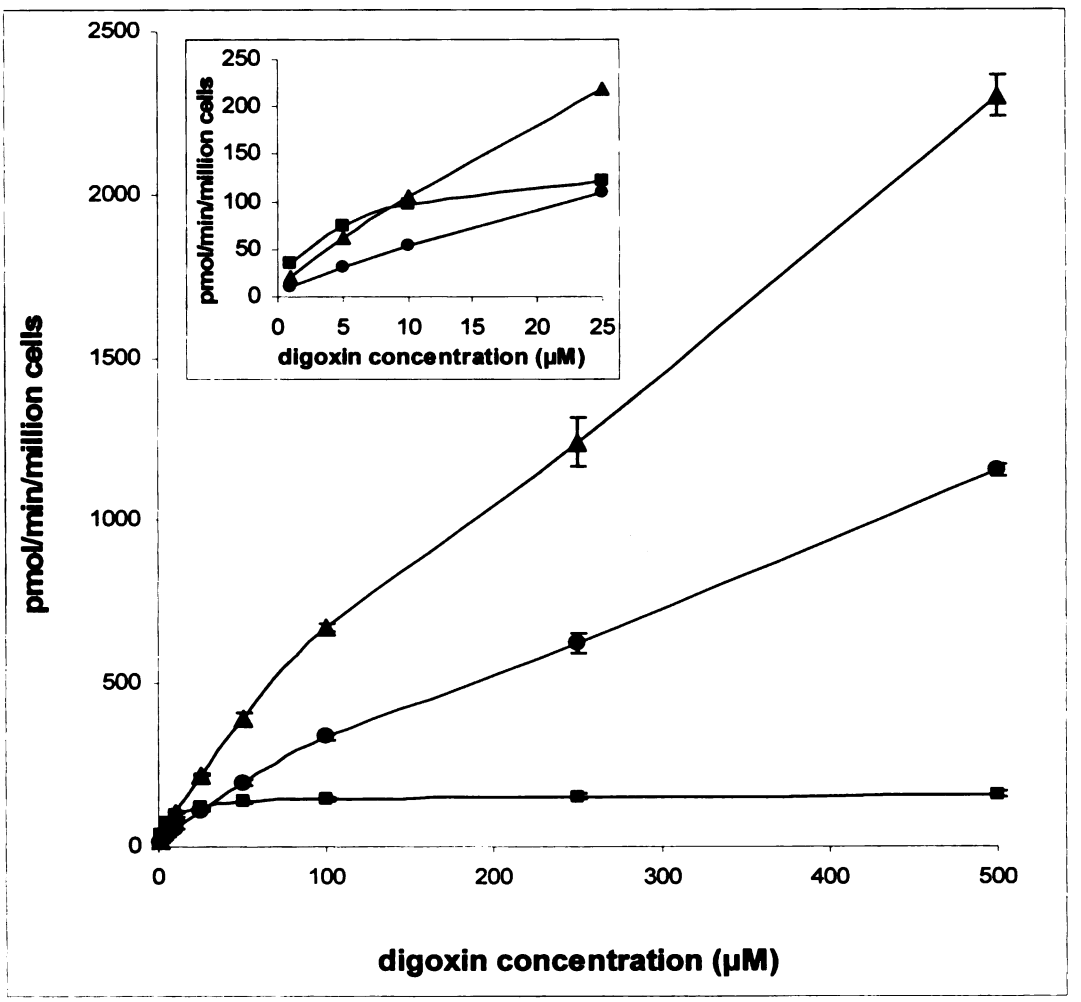

Figure 2.6 *Uptake kinetics of digoxin was studies in freshly isolated rat hepatocytes.* Inset shows the uptake of digoxin at lower concentrations. Triangles (▲) represent overall uptake, squares (■) represent transporter-mediated uptake, and circles (●) represent passive diffusion. Data are depicted as the mean ± SD, n=3.

2.3.5 *Effects of Rifampin and GG918 on Uptake of [^{3}H] Digoxin in Hepatocytes*

The effects of rifampin and GG918 on digoxin uptake in the freshly isolated rat hepatocytes are shown in Figure 2.7. Compared to the digoxin only control, co-administration of 100 μM rifampin significantly reduced uptake to 23 ± 6.5 % of the control, $p<0.0005$. Co-administration of 1 μM GG918 slightly increased digoxin uptake to 104 ± 4 %. However, co-administration of 25 μM GG918 inhibited uptake to 42.2 ± 12.2 %, $p<0.005$.

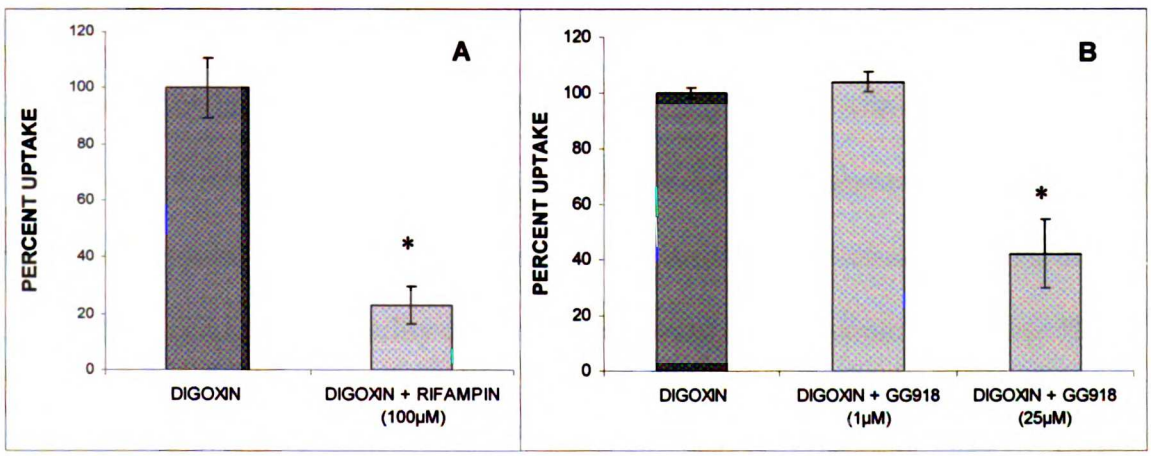

Figure 2.7 *Uptake study of digoxin in hepatocytes.* Hepatocytes (2 x 10^6) were incubated for 2 min with 100nM of [^{3}H] digoxin in the absence and presence of (A) 100μM of rifampin (B) 1μM and 25μM of GG918. Data are depicted as the mean ± SD, n=3. *, $p< 0.05$.

UvaT HDIVAN

2.3.6 *Time Course Studies of the Effects of Rifampin and GG918 on Digoxin Metabolism*

Time course studies over 60 minutes were carried out to investigate the effects of rifampin and GG918 on digoxin metabolism (hepatocyte and supernatant) as illustrated in Figure 2.8. The parent compound profile showed that co-administration of 100 μM of rifampin with 200 nM of digoxin resulted in a significant increase in digoxin concentration and a significant decrease in metabolite formation compared to the control without addition of rifampin. In contrast, co-administering 0.5 μM GG918 with digoxin significantly reduced parent drug concentration and increased metabolism compared to the control without GG918. Using the parent compound profile, the area under the curve (AUC) over 60 minutes of digoxin alone, digoxin with rifampin, and digoxin with GG918 were calculated to be 15.6 ± 0.1 μM•min, 20.1 ± 0.5 μM•min (p<0.005), and 14.1 ± 0.1 μM•min (p<0.01), respectively, an increase of 28.8 % with rifampin and a reduction of 9.6 % with GG918. At 60 minutes, the dg2 concentration in the presence of rifampin decreased 56.0 % relative to the control versus 9.5 % increase relative to the control for GG918. Cell viability determined at the end of incubations was above 90%.

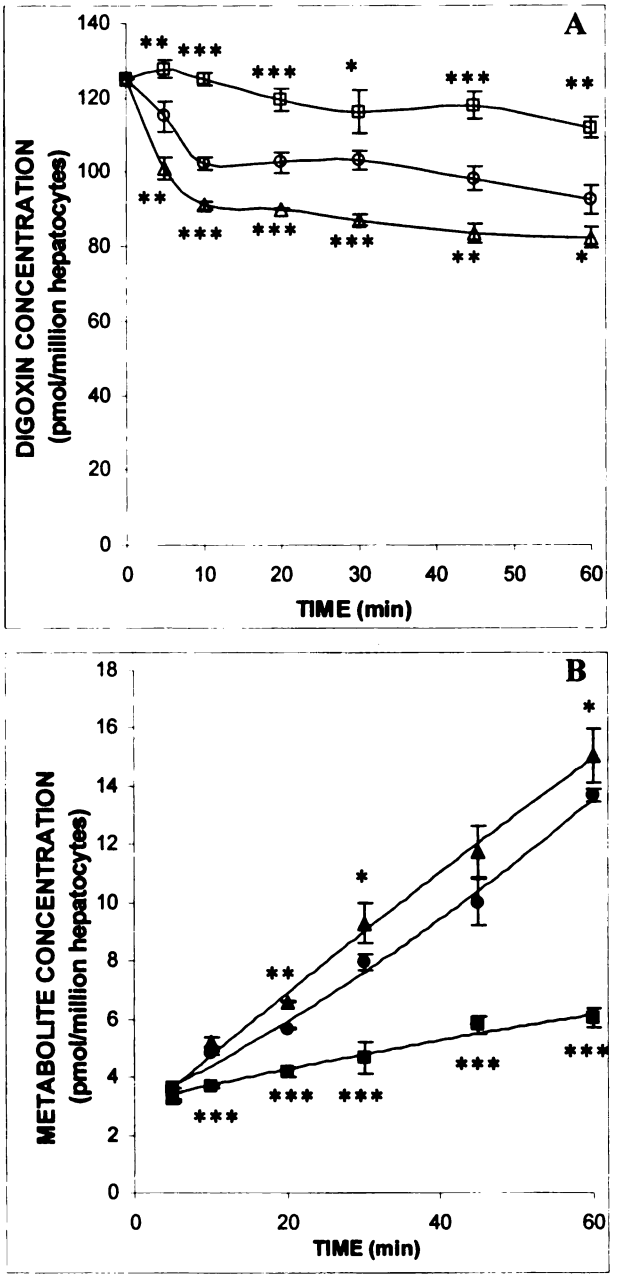

Figure 2.8 *Time course studies of digoxin with and without inhibitors.* A time course study of digoxin metabolism with and without transporter inhibitors in rat hepatocytes. (A) Profile of the parent compound; ○, digoxin alone; □, co-administration of digoxin and rifampin; Δ, co-adminstration of digoxin and GG918. (B) Profile of metabolite (dg2); ●, digoxin alone; ■, co-administration of digoxin and rifampin; ▲, co-administration of digoxin and GG918. Data are depicted as the mean ± SD, n=3. *, p <0.05; **, p<0.01; ***, p<0.001,

2.4 Discussion

With increasing awareness of the effects of hepatic transporters on drug disposition, our laboratory has investigated their role and importance in the overall drug metabolism process. Based on a model cellular system containing human P-gp and CYP3A4 (Cummins et al., 2001), we showed that inhibiting P-gp, with no effect on CYP3A activity, reduces CYP3A metabolism in the apical to basolateral direction mimicking the gut, but increases CYP3A metabolism in the basolateral to apical direction mimicking the liver (Cummins et al., 2002a; Benet et al., 2003; Cummins et al., 2004). We suggested that this inverse orientation (i.e. the drug encounters the enzyme CYP3A prior to the efflux transporter P-gp in the liver, which is reversed in the intestine) could explain the increased metabolic clearance observed for CYP3A/P-gp dual substrates in women versus men (Cummins et al., 2002b). In that paper, we reviewed the seminal studies of Lan et al., (2000) who showed that in P-gp knock-out mice, CYP3A metabolism of erythromycin was increased when P-gp was absent; and we reported that increased hepatic metabolism was also observed for paclitaxel, vinblastine, and doxorubicin in knock mice versus controls. More recently, using the isolated perfused rat intestine (Cummins et al., 2003) and isolated perfused rat liver (IPRL) (Wu and Benet, 2003), we confirmed the results hypothesized from the cellular system described above. The increased metabolism of digoxin in the IPRL during P-gp inhibition and the decrease of digoxin metabolism in the IPRL during Oatp2 inhibition (Lau et al., 2004) were confirmed.

The results reported here demonstrate that the conventional way of defining liver intrinsic clearance using a microsome incubation profile is not sufficient. Here we demonstrate that the freshly isolated hepatocytes that maintain uptake and efflux transporters should be a better model for defining intrinsic clearance. A pharmacokinetic study conducted in our laboratory (Salphati and Benet, 1998) measured total clearance of digoxin to be 37 ± 11 ml/min/kg. An earlier study of Harrison and Gibaldi (1975) reported a total digoxin clearance to 28.0 ml/min/kg, with a metabolic clearance of 12.9 ml/min/kg. The apparent metabolic clearance predicted using hepatocytes (15.9 ± 3.0 ml/min/kg) in the present study appears to be much better approximation of the measured *in vivo* values. This hepatocyte value is 3.5-fold greater than the metabolic clearance calculated using microsomes (4.59 ± 0.69 ml/min/kg), which is a counter-intuitive finding since it would be expected that drug access to the metabolizing enzymes would be enhanced in microsomes.

To demonstrate the effects of hepatic uptake and efflux transporters on digoxin metabolism, rifampin, an inhibitor of Oat/Oatp, and GG918, a well established P-gp inhibitor, were administered. The results of the digoxin uptake study using freshly isolated hepatocytes showed that 100 μM of rifampin effectively inhibited the uptake of [^{3}H] digoxin by more than 75 %. The remaining 25 % of digoxin that is found intracellularly is probably due to passive diffusion or uptake mediated by other transporters. Figure 2.5A demonstrates that increasing the concentration of rifampin decreased digoxin metabolism in hepatocytes, whereas no effect of rifampin was observed in microsomes (Fig. 2.4A). GG918 also had no effect on digoxin metabolism in microsomes (Fig. 2.4B), while in hepatocytes GG918 concentrations up to 1 μM

increased digoxin metabolism, but higher concentrations caused decreased metabolism (Fig. 2.5B). Many studies have documented GG918's potent inhibition of the efflux transporter P-gp with a $K_i < 0.5$ μM (Annaert et al., 2001; Luo et al., 2002; Savolainen et al., 2002; Wu and Benet, 2003), but the results here suggest that GG918 may also effectively ($K_i = 4.38 \pm 0.46$ μM) inhibit Oatp2, or another hepatic uptake transporter for digoxin. This lack of specificity of transporter inhibition does not appear to be unique to GG918, and this study should provide a caution to investigators to test alternate inhibitory (and activating) potential effects beyond that being investigated. Here, we chose to utilize 0.5 μM GG918 in the time course studies as our efflux inhibitory example, but we recognize that some Oatp2 inhibition may occur. The determination of apparent IC_{50} and K_i values validate that the metabolism differences observed between microsome and hepatocyte incubations are due to uptake and efflux transporters that are present in hepatocytes but not in microsomes.

Time course studies demonstrated that over 60 minutes, metabolism was impaired by 100 μM of rifampin and enhanced by 0.5 μM of GG918 (Fig. 2.8). Since rifampin limits the amount of digoxin entering the hepatocytes, we expect that less drug would be available for metabolism and more parent drug would be found in the cell suspension compared to the control without addition of rifampin. Conversely, we expected that inhibition of P-gp by GG918 would result in an accumulation of digoxin intracellularly, thus increasing its exposure to the metabolizing enzyme and leading to an increase in metabolite formation and a decrease in parent drug concentration compared to that of digoxin alone control. We see that 100 μM rifampin does decrease hepatic uptake markedly at 2 minutes (Fig. 2.7A) consistent with the decreased metabolism of digoxin

over the 60 minutes time course (Fig. 2.8). A slight but non-significant increase in digoxin hepatic uptake is noted with 1 μM GG918 at 2 minutes (Fig. 2.7B). This lack of a significant increase is not surprising due to the relative small overall change found for digoxin and dg2 (~9.5 %) over 60 minutes, and the fact that the intracellular increase is counteracted by the increased metabolism. However, the recognition that GG918 also possess hepatic uptake inhibitory properties (Figs. 2.5 and 2.7) further complicates the analysis.

The total AUC (hepatocytes plus supernatant) for co-administration of rifampin with digoxin is significantly (p<0.005) higher (20.1 ± 0.5 μM) than that of digoxin alone (15.6 ± 0.1 μM). The AUC for co-administration of GG918 with digoxin is significantly (p <0.01) lower (14.1 ± 0.1 μM) than that of the control (15.6 ± 0.1 μM). These directional AUC changes for parent digoxin and the inverse findings for the dg2 metabolite are consistent with the results from *ex situ* perfused rat liver studies of our laboratory (Lau et al., 2004). These results strongly support our hypothesis that the hepatic uptake and efflux transporters, Oatp 2 and P-gp, are responsible for the altered digoxin metabolism.

In conclusion, hepatic uptake and efflux transporters play important roles in drug disposition and metabolism. Hepatic intrinsic clearance may be better defined by using hepatocytes (or other methodology that preserves the transporter/enzyme architecture of the liver) rather than microsomes so that transporter effects are taken into account. Uptake and efflux transporters, such as Oatp 2 and P-gp, may modulate a compound's metabolism by altering its accessibility to the metabolizing enzymes. Furthermore, inhibitors of an efflux transporter may also affect uptake. The interplay of transporters

and enzymes must be considered in defining the intrinsic metabolic clearance of the liver (and other organs such as intestine and kidney) and in evaluating potential drug-drug interactions.

Chapter 3

In Vitro and *In Vivo* Correlation of Hepatic Transporter Effects on Erythromycin Metabolism: Characterizing the Importance of Transporter-Enzyme Interplay

3.1 Introduction

The liver is a major site of metabolism of many xenobiotics and endogenous molecules. The process of metabolism starts with the uptake of the molecules via passive diffusion and (or) active transport. Hepatic uptake transporters are localized on the sinusoidal membrane of the hepatocytes and are members of the solute carrier (SLC) family (Meier et al., 1997). The uptake of xenobiotics is predominantly mediated by the isoforms of organic anion transporting polypeptides (OATP in human/Oatp in rats), organic anion transporter 2 (OAT2/Oat2), and organic cation transporter 1 (OCT1/oct1)

[1] A portion of this chapter was published in a manuscript entitled "*In Vitro* and *In Vivo* Correlation of Hepatic Transporter Effects on Erythromycin Metabolism: Characterizing the Importance of Transporter-Enzyme Interplay" Lam J.L., Okochi H., Huang Y., Benet L.Z. (2006) Drug Metab. Dispos. **[Fast Forwad May 12]**

(Meier et al., 1997; van Montfoort et al., 2003; Hagenbuch and Meier, 2004). Once a substrate enters the cell, it is subject to metabolism by phase I and (or) phase II enzymes. These enzymes are responsible for the conversion of non-polar lipophilic compounds to their more polar hydrophilic metabolites before excretion. Phase I enzymes, such as cytochrome P450s, are involved in oxidation and reduction reactions, whereas, phase II enzymes such as UDP-glucuronosyltransferase and glutathione S-transferase are involved in bi-molecular conjugation reactions. The substrate and its metabolites can either exit back to the blood via diffusion and (or) basolateral efflux transporters or exit to the bile through diffusion and (or) canalicular efflux transporters such as P-glycoprotein (P-GP/P-gp) and MRP2/Mrp2 (Ambudkar et al., 1999; Konig et al., 1999). The canalicular efflux transporters are members of the ATP-binding cassette superfamily; essentially, they mediate the extrusion of substrates that are neutral, positively or negatively charged from inside of the cell to the bile (Ambudkar et al., 1999). Uptake and (or) efflux transporters facilitate the hepatic metabolism of substrate compounds.

Altered pharmacokinetics due to hepatic enzyme based drug-drug interactions have been extensively described in the literature; however, less is known about interactions associated with hepatic transporters. Recently, several significant drug-drug interactions, such as cyclosporin A with bosentan (Treiber et al., 2004), cyclosporine with cerivastatin (Shitara et al., 2003; 2004a), and gemfibrozil with cerivastatin (Shitara et al., 2004b) have been attributed in part to inhibition of hepatic uptake transporters. Sun et al. (2004) reported that uremic toxins accumulated in the circulation of late stage renal failure patients also inhibit hepatic uptake transporters leading to an increase in systemic exposure of several drugs. Recently, we have shown that the interplay of membrane

transporters and metabolizing enzymes are important in drug disposition and metabolism (Benet et al., 2003; 2004). In the intestine, CYP3A and P-gp function synergistically to limit substrates entering the blood from the lumen (Cummins et al., 2002; 2003; 2004).

Previously, we have shown that hepatic transporters play important roles in drug disposition and metabolism in freshly isolated rat hepatocytes and in the isolated perfused rat liver system where the integrity of hepatic transporters are intact as compared to rat liver microsomes where the transporters are absent (Chapter 2; Lam and Benet, 2004; Lau et al., 2004; Sun et al., 2004). In addition, rifampin (an inhibitor of Oatp's and Oat) significantly decreased and GG918 (a P-gp inhibitor) significantly increased the metabolism of digoxin in hepatocytes, respectively, while exhibiting little effect on metabolism in microsomes (Chapter 2; Lam and Benet, 2004). Based on these previous results, we further hypothesize that metabolic drug-drug interactions at the hepatic uptake or efflux transporter level, independent of enzymatic activity, alter metabolism and pharmacokinetics (PK) of substrate compounds. In this study, our hypothesis was tested in vitro and, for the first time, in vivo in rats.

The model compound chosen to examine the hypothesis was erythromycin (ERY), an antibiotic effective against infections caused by both gram positive and gram negative bacteria. In humans, ERY is partially metabolized by CYP3A4 to its major metabolite, N-demethyl-ERY, but ERY is excreted primarily unchanged in the bile. Chemical structures of ERY and its major metabolite N-demethyl-ERY are shown in Figure 3.1. Eighty percent of ERY is bound to plasma protein, and the total clearance of ERY in human is 9.1 ml/min/kg (Chambers, 2001). It is well demonstrated that ERY and N-demethyl-ERY are excellent substrates of P-gp (Schuetz et al., 1998; Sun et al., 2004).

Recently, ERY has been shown to be a good substrate of Oatp1a4, and the estimated saturable component of the total uptake in rat hepatocytes is approximately 56% (Sun et al., 2004) at concentrations much less than Km (72 μM). In the present study, the relative contributions of hepatic uptake and efflux transporters to the metabolism and the pharmacokinetics of ERY were evaluated. We examined trends observed from in vitro studies with that from in vivo studies in rats.

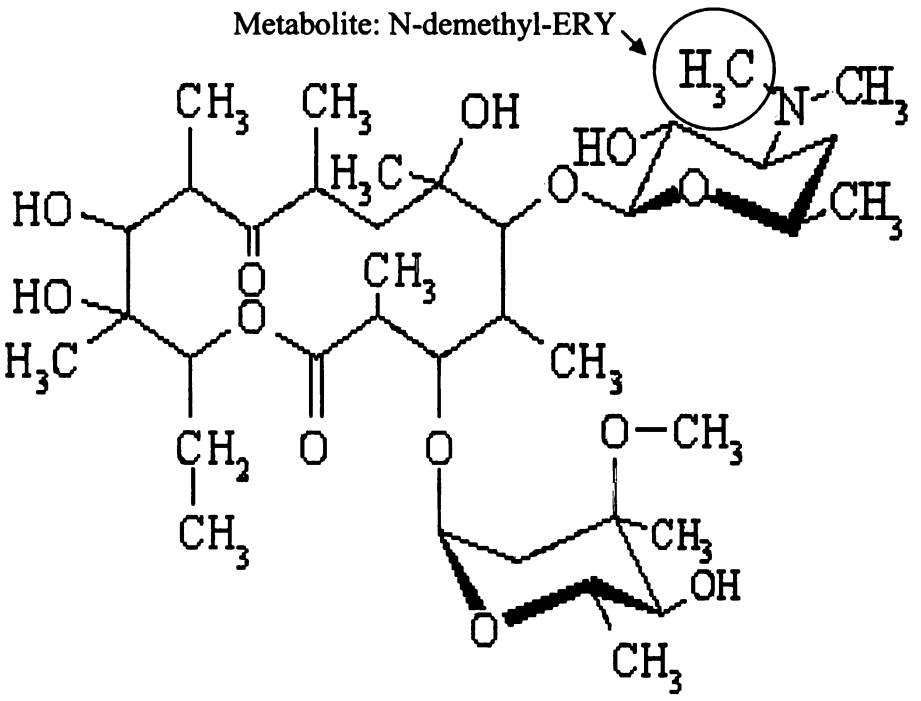

Figure 3.1 *Chemical structure of ERY and its major metabolite N-demethyl-ERY.*

3.2 Materials and Methods

3.2.1 Materials

ERY, oleandromycin, rifampin, digoxin, [Try(SO_3H)^{27}]-cholecystokinin amide fragment 26-33 (CCK8), and quinidine as well as HPLC grade dimethyl-sulfoxide, *tert*-butyl-methyl-ether (MTBE) and acetonitrile (ACN) were purchased from Sigma-Aldrich (St. Louis, MO). Erythrocin lactobionate- I.V. (Abbott laboratories, N. Chicago, IL) and rifampin (Bedford laboratories, Bedford, OH) for i.v. infusion were purchased from the UCSF pharmacy for research use only. N-demethyl-ERY standard was purchased from U.S. Pharmacopeia (Rockville, MD). GG918 (GF120918) was graciously supplied by GlaxoSmithKline (Research Triangle Park, NC). Pooled male Wistar rat liver microsomes were acquired from Xenotech (Lenexa, KS). Male Wistar rats (200-350 g) from Charles-River Laboratories (Wilmington, MA) were housed in the UCSF animal care facility with a 12 hour light/dark cycle and allowed free access to water and food. Approval of the described studies reported here was obtained from the Committee on Animal Research, UCSF.

3.2.2 Microsome Incubations

The incubation conditions were as previously described (Salphati and Benet, 1999). In brief, each reaction mixture contained 0.5 mg/ml microsomes, 1mM NADPH, various concentrations of inhibitors, 2 μM ERY, and phosphate buffer. The total DMSO concentration used to solublize ERY and all inhibitors was less than 1% for all in vitro studies. The total reaction volume was 250 μl. The reaction period was 5 minutes at 37°C. For each sample, the reaction was stopped via protein precipitation by addition of an equal volume of ACN containing 1 μg/ml of the internal standard (IS), oleandromycin. The supernatants were stored at -80°C for LC-MS analysis.

3.2.3 Hepatocyte Isolation

Anesthesia was induced by intraperitoneal injection with a 1 ml/kg dose of ketamine/xylazine (80 mg/ml, 12 mg/ml) prior to surgery. The portal vein was cannulated with an IV catheter (catalog number 2007-04, Becton Dickinson, Sandy, UT) and perfused with oxygenated liver perfusion buffer (Invitrogen, Carlsbad, CA) for 5 minutes at 30 ml/min followed by perfusion with an oxygenated hepatocyte washing buffer (Invitrogen, Carlsbad, CA) modified with 2 mM L-glutamine, 10 mM HEPES, and 1.2 U/ml collagenase (Sigma-Aldrich, St. Louis, MO) for 5 minutes at 20 ml/min. The digested liver was excised and broken down. Hepatocytes were then washed twice with an ice cold hepatocyte wash buffer containing 2 mM L-glutamine and 10 mM HEPES

and were centrifuged at 50 x g for 2-3 minutes. Cell viability was determined using the trypan blue exclusion method. Cells with viability of greater than 90% were used for further studies.

3.2.4 Hepatocyte Incubations

Hepatocyte incubations were carried out immediately following cell isolation. Cells were resuspended and diluted to 2 million per ml in Kreb-Henseleit buffer (pH7.4) containing 0.21 g/L of sodium bicarbonate and supplemented with 1% BSA and 10 mM glucose. Cell suspensions for all hepatocyte incubations were pre-warmed for 5 minutes in a 37°C shaking water bath prior to initiation of incubations.

For the uptake studies, ERY (2 μM) or N-demethyl-ERY (2 μM) with and without 50 μM rifampin, 50 μM digoxin, 30 μM CCK8, 50 μM quinidine or 0.5 μM GG918 were added to the cell suspensions that were shaking in a 37°C water bath. At 2 minutes, the reactions were terminated by transferring 1 million hepatocytes into a centrifuge tube containing 700 μl of a mixture of silicone oil and mineral oil (Shitara et al., 2003) and centrifuged at 13,000 x g for 10 seconds. After removing the buffer layer and the oil layer, each cell pellet was re-suspended in 100 μl of water and sonicated for 15 minute to ensure a thorough cell lysis. This was followed by adding 200 μl of ACN containing IS and spinning at 13,000 x g for 15 minutes to precipitate protein. The supernatant was then transferred into a HPLC vial (Hewlett Packard, Palo Alto, CA) for LC-MS analysis.

For evaluating transporter inhibition on metabolism, ERY (2 μM) and various concentrations of rifampin or GG918 were co-incubated for 5 minutes in a 37°C shaking water bath. The reaction was stopped by transferring 1 ml of cells to a fresh glass tube containing MTBE and IS followed by vortexing. All samples were spun down at 2000 g for 10 minutes. After quick-freezing the aqueous layer in a methanol/dry ice bath, the organic layer was poured into a new tube and evaporated under nitrogen gas. Each sample was reconstituted with 300 μl of ACN:water (50:50, v:v) for LC-MS analysis.

For the time course studies, 15 ml of hepatocytes (2 million/ml) were warmed in a 50 ml flask shaking in a 37°C water bath for 5 minutes. Each study was initiated by concomitantly adding ERY (2 μM) with DMSO (control), 2.5 μM rifampin or 0.5μM GG918. At 5, 10, 15, 20, 30, and 45 minutes, 0.5 ml of cells were transferred into a centrifuge tube containing 700 μl of a mixture of silicone oil and mineral oil and centrifuged at 13,000 x g for 10 seconds to stop the reaction. Ten seconds later, 1 ml of cells was transferred into a glass tube containing MTBE and IS followed by vortexing to stop the reaction. Sample preparation for the intracellular measurement of ERY metabolism was the same as for the uptake studies. Sample preparation for the measurement of ERY metabolism was the same as that for the inhibition studies.

3.2.5 Surgery and Pharmacokinetic Study In Vivo in Rats

To determine the influence of rifampin and GG918 on ERY metabolism, 24 rats were divided equally into 4 groups. Since rifampin (25 mg/ml) was dissolved in saline

and GG918 (0.25 mg/ml) was dissolved in 10% DMSO, 3% BSA in saline, two sets of vehicle controls were needed for each treatment group. Male Wistar rats (300g-350g) were under anesthesia induced by intraperitoneal injection with a 1 ml/kg dose of ketamine/xylazine (80 mg/ml/12 mg/ml, Sigma-Aldrich, St. Louis, MO) prior to surgery and several times during the 4 hour study to ensure complete anesthetization. The femoral vein and the femoral artery were cannulated using a 10 cm PE-10 tube (I.D. 0.28 mm, O.D. 0.61 mm, BD Intramedic, Sparks, MD) and a 10 cm SP-35 tube (I.D. 0.5 mm, O.D. 0.9 mm, Natume Co., Tokyo, Japan), respectively. The lines were washed immediately with saline containing 10 unit/ml heparin to prevent clotting. The bile duct was cannulated with a 15 cm PE-10 tube, with average bile flow rate of 0.4 ml per 15 minutes. ERY (10 mg/kg) with vehicle control or with either rifampin (2.5 mg/kg) or GG918 (0.25 mg/kg) were co-administered through the femoral vein. Blood (150 µl) samples were collected at time points 3, 5, 10, 15, 30, 60, 90, 120, 180 and 240 minutes via femoral artery and stored in K_2EDTA-pretreated microtainer tubes (Becton-Dickinson, Franklin Lakes, NJ). Results from preliminary studies showed that extrapolated AUC's were less than 20% of the total AUC over 4 hours; thus in vivo studies were stopped at 240 minutes. Bile samples were collected at 15 minute intervals until 120 minutes, then every 30 minutes. Urine was also collected for the duration of the PK study, and the bladder was emptied at the end of the study. Rat livers were excised and weighed at 240 min. To each 100 µl of blood, bile, urine and liver homogenate sample, 200 µl of ACN containing IS were added, and samples were centrifuged for 15 minute at 10,000 × g. The supernatants were transferred into HPLC vials and assayed using LC-MS.

3.2.6 *Measurement of ERY, N-demethyl-ERY, Rifampin and GG918*

All samples were analyzed on a LC/LC coupled with a mass selective detector system (Hewlett Packard) that consists of 1100 HPLC components HPLC I and HPLC II as described previously (Christians et al., 2000). A representative LC-MS chromatogram is shown in Figure 3.2. The two HPLC systems were connected by a 7240 Rheodyne six-port switching valve mounted on a step motor (Rheodyne, Cotati, CA). The LC/LC-MS system was controlled, and the data were integrated by ChemStation

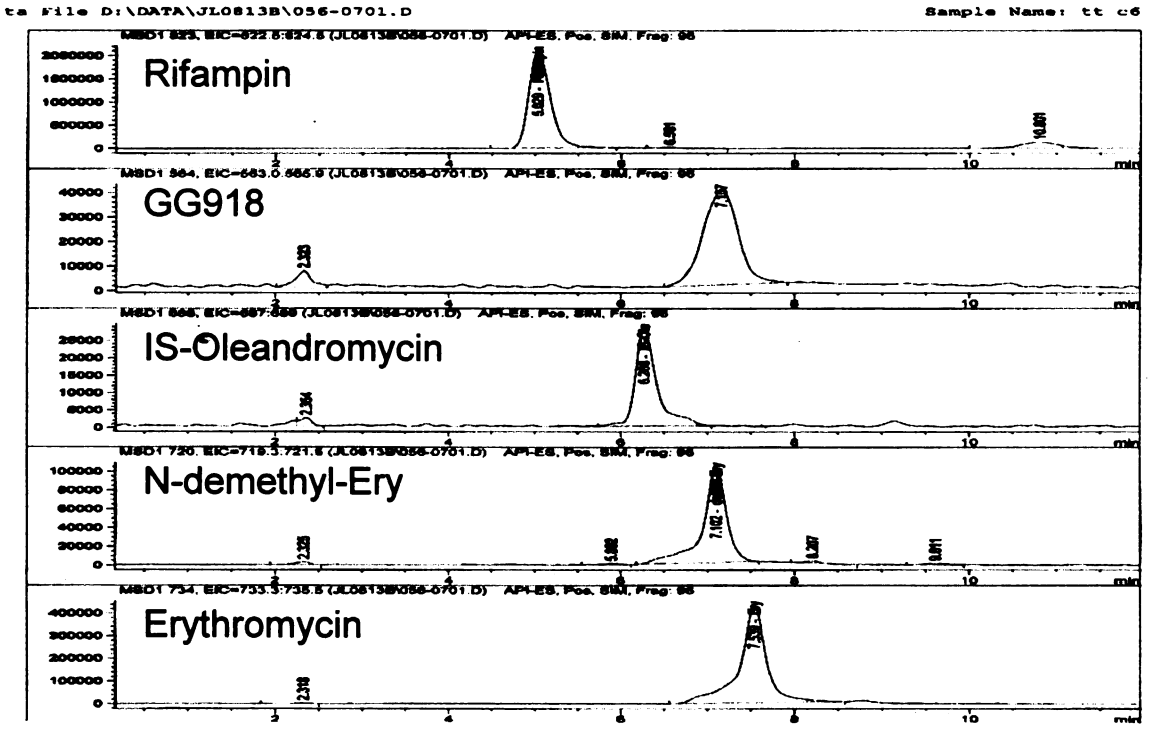

Figure 3.2 *A representative chromatogram of ERY, N-demethyl-ERY, rifampin, GG918 and the internal standard olenandromycin.*

software version A.06.01 (Hewlett Parkard). Samples (100 µl) were first injected into a 10 x 5 mm Hypersil ODS-1 5 µm extraction column (Thermo Hypersil-Keystone, Shelton, CT) at a flow rate of 2 ml/min followed by washing with 2 mM ammonium acetate. After 1 minute, the switching valve was activated, and the analytes were eluted with ACN in the back-flush mode from the extraction column into a 4.6 mm x 150 mm C18 XTerra MS 5 µm analytical column (Waters, Milford, MA). For the detection of ERY, N-demethyl-ERY and IS, the analytes were separated isocratically with 60 % 2 mM ammonium acetate (pH 9) and 40% ACN at a flow rate of 1.5 ml/min and at 50 °C. For the detection of rifampin and GG918, all column and HPLC setups were identical to that in the ERY method; however, the extraction column was washed with water containing 0.1% formic acid and the inhibitors were eluted isocratically with 70% water containing 0.1% formic acid and 30% ACN.

3.2.7 Data Analysis

The kinetic parameters for the uptake of N-demethyl-ERY were estimated using fitting of the following equation: $v = (V_{max} \times S)/(K_m + S) + P_{diff} \times S$, where v is rate of uptake (pmol/min/million cells), S is the substrate concentration (µM), K_m is the Michaelis-Menten constant (µM), and P_{diff} is the non-saturable diffusion constant (µl/min/million cells). For the pharmacokinetic studies, terminal half-life ($T_{1/2}$) was determined from the log linear regression of the last three concentration measurements. Area under the curve (AUC), calculated by the trapezoid rule, was extrapolated to infinite

time by the additions of $C_{blood,\ last} \cdot T_{1/2} / 0.693$. Clearance (CL) was calculated by dose/AUC(0-inf). Biliary and renal clearances [CL(biliary) and CL(renal)] were respectively determined by dividing amount of ERY excreted into the bile and urine over 240 minutes by the AUC over that time interval. Renal clearance of the metabolite [CL(renal,met)] was calculated using the 240 minute blood and urine measurements of the N-demethyl-ERY. CL(other) was calculated as CL – CL(biliary) – CL(renal) for ERY measurements. Volume of distribution at steady-state (Vss) and mean resident time (MRT) were calculated using moments (Benet and Galeazzi, 1979). Student's *t* test was used to analyze differences between two groups such as in the in vivo studies. Analysis of variance was used to analyze differences among more than two groups, such as in the in vitro studies. The significance between two means in these groups was evaluated using Bonferroni's multiple comparison test. The *p*-value for statistical significance was set at < 0.05.

3.3 Results

3.3.1 Uptake of ERY and Its Major Metabolite N-demethyl-ERY by Freshly Isolated Rat Hepatocytes

The estimated saturable portion of the ERY uptake in the freshly isolated rat hepatocytes has been previously described by Sun et al. (2004) to be 55%. In this study,

we examined the uptake kinetics for N-demethyl-ERY. Various concentrations of N-demethyl-ERY were incubated with hepatocytes for 2 minutes. Both saturable and non-saturable components were observed (Figure 3.3). The fitted kinetic parameters were 25.0 ± 1.0 pmol/min/million cells for V_{max}, 31.7 ± 4.6 μM for K_m, and 0.696 ± 0.014 μl/min/million cells for P_{diff}. The estimated transporter mediated uptake for N-demethyl-ERY (V_{max} / K_m) is 53% of the total uptake at the relevant in vitro and in vivo concentrations.

To determine which major isoforms of the hepatic uptake transporters are responsible for the uptake of ERY and its metabolite, 2μM of ERY and N-demethyl-ERY were co-incubated with various concentrations of transporter inhibitors for 2 minutes. The substrate concentration (2 μM) was in the linear range of uptake without saturating the uptake transporters (data not shown). Rifampin is a general inhibitor of Oatps and Oats, whereas digoxin and CCK8 differentially inhibit Oatp1a4 and Oatp1b2, respectively (Ismair et al., 2001; Shitara et al., 2002). Quinidine inhibits both Oatp1 and P-gp (Shitara et al., 2002). We have previously shown that GG918 is also an inhibitor of Oatp1a4, but this could only be clearly seen at concentrations much higher than 0.5 μM (Chapter 2; Lam and Benet, 2004). The results are depicted in Figure 3.4. At a concentration of 50μM, rifampin respectively reduced the intracellular concentration of ERY and N-demethyl-ERY to 54.4 ± 2.7 % and 38.8 ± 5.6 % of the controls. Digoxin (50μM) and CCK8 (30μM) significantly decreased the uptake of ERY and N-demethyl-ERY to 84.7 ± 9.5 %, 75.4 ± 0.6 %, and 63.5 ± 7.3 %, 77.3 ± 3.2 %, respectively.

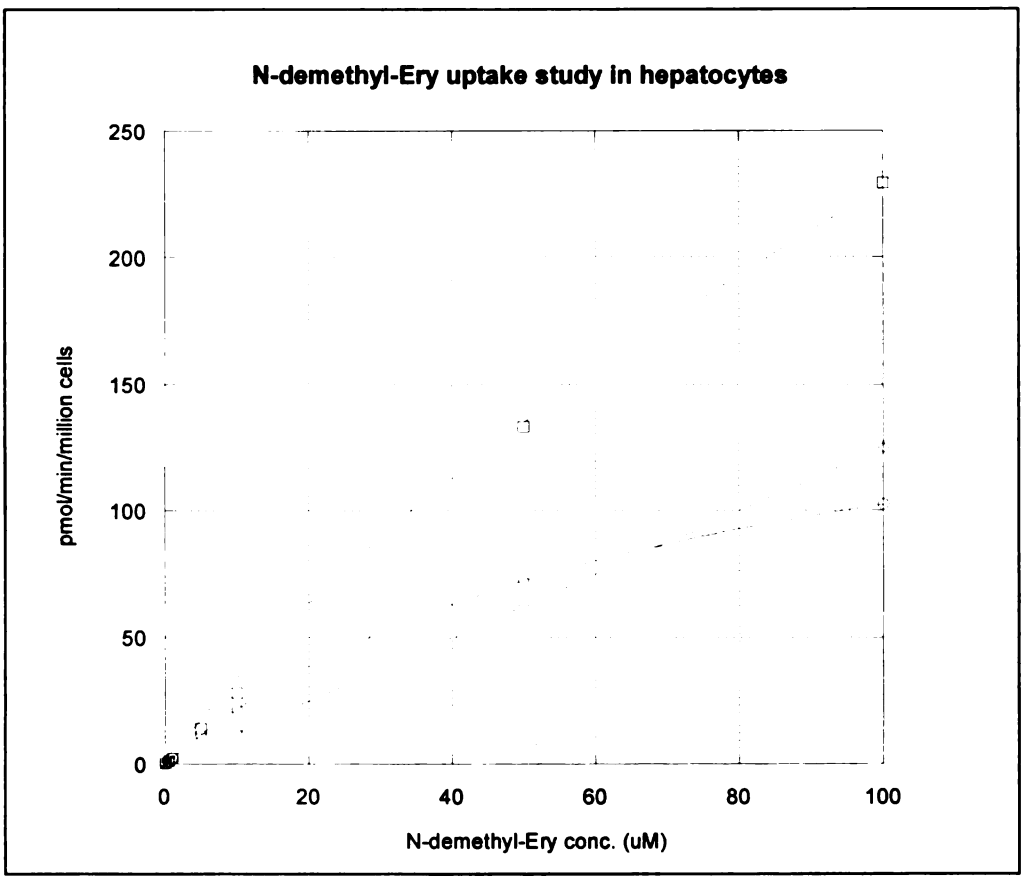

Figure 3.3 *Uptake kinetics of N-demethyl-ERY.* Squares (□) represent the total uptake; diamonds (◊) represent the non-saturable process; Circles (○)represent the saturable process; n=3. Lines are drawn by fitting data points with the uptake kinetic equation listed in Section 3.2.7 Data Analysis.

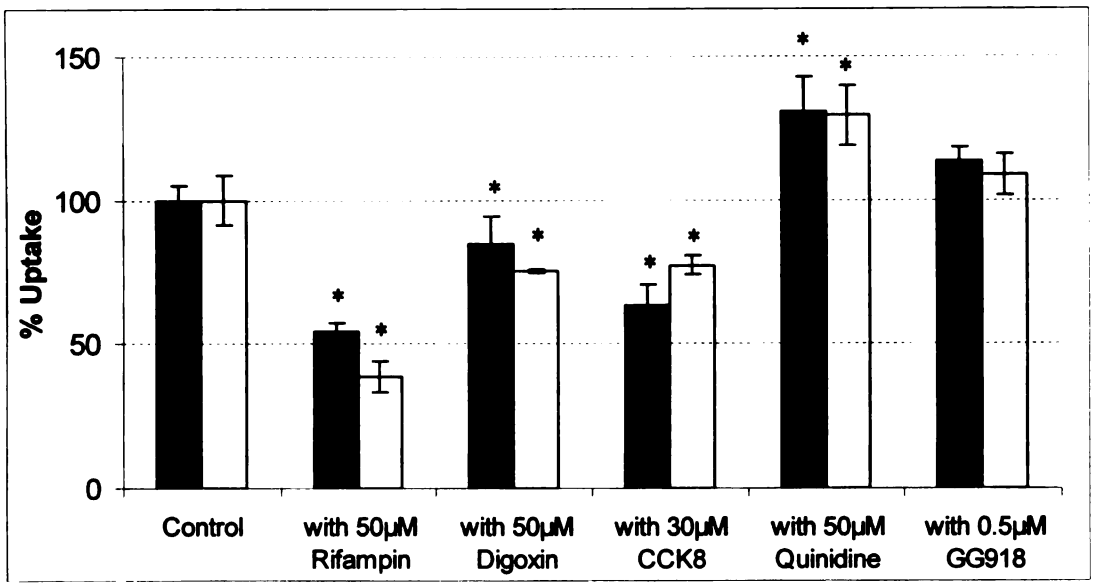

Figure 3.4 *Uptake study of ERY and N-demethyl-ERY in hepatocytes.* Two μM ERY (black bars) and 2 μM N-demethyl-ERY (white bars) were incubated for 2 minutes with various concentrations of transporter inhibitors. Data are depicted as the mean ± S.D., n=3. *, $p<0.05$, significantly different from control (ERY only).

Sun et al. (2004) also showed significant uptake inhibition at 100 μM digoxin. Quinidine (50μM) did not reduce the uptake of ERY and its metabolite but increased their intracellular concentrations by 130 ± 12 %, 130 ± 10 %, as might be expected if cellular efflux was inhibited. GG918 (0.5μM) had no significant effects on the uptake of ERY and N-demethyl-ERY,113 ± 5 %, 108 ± 7 %, respectively, which indicates a possible increase due to efflux inhibition countered by possible uptake inhibition. This inhibition profile suggests that ERY and N-demethyl-ERY are substrates of Oatp1a4 (Oatp2) and Oatp1b2 (Oatp4) but not Oatp1a1 (Oatp1) in rats.

3.3.2 *Effects of Rifampin and GG918 on ERY Metabolism in Rat Liver Microsomes and in Freshly Isolated Hepatocytes*

Various concentrations of rifampin (Figure 3.5 A) and GG918 (Figure 3.5 B) were co-incubated with ERY in microsomes and in hepatocytes. Concentrations of rifampin less than 25μM did not show a significant effect on ERY metabolism in microsomes (Figure 3.5A, black bars); however, at concentrations of 0.5μM or higher, rifampin exhibited a significant dose-dependent inhibition of ERY metabolism in the hepatocytes (Figure 3.5A, white bars). At concentrations of GG918 less than 5μM, ERY metabolism was not affected in microsomes (Figure 3.5B, black bars). In contrast, a significant increase in ERY metabolism was observed in a dose-dependent manner up to 0.5μM GG918 in hepatocytes (Figure 3.5B, white bars), even though no increase in intracellular concentrations was observed at this 0.5μM GG918 concentration (Figure 3.4). However, at GG918 concentrations higher than 0.5μM, there was a decrease in metabolism in hepatocytes which suggests inhibition of Oatp1a4 at higher GG918 concentrations, as we have shown previously (Chapter 2; Lam and Benet, 2004).

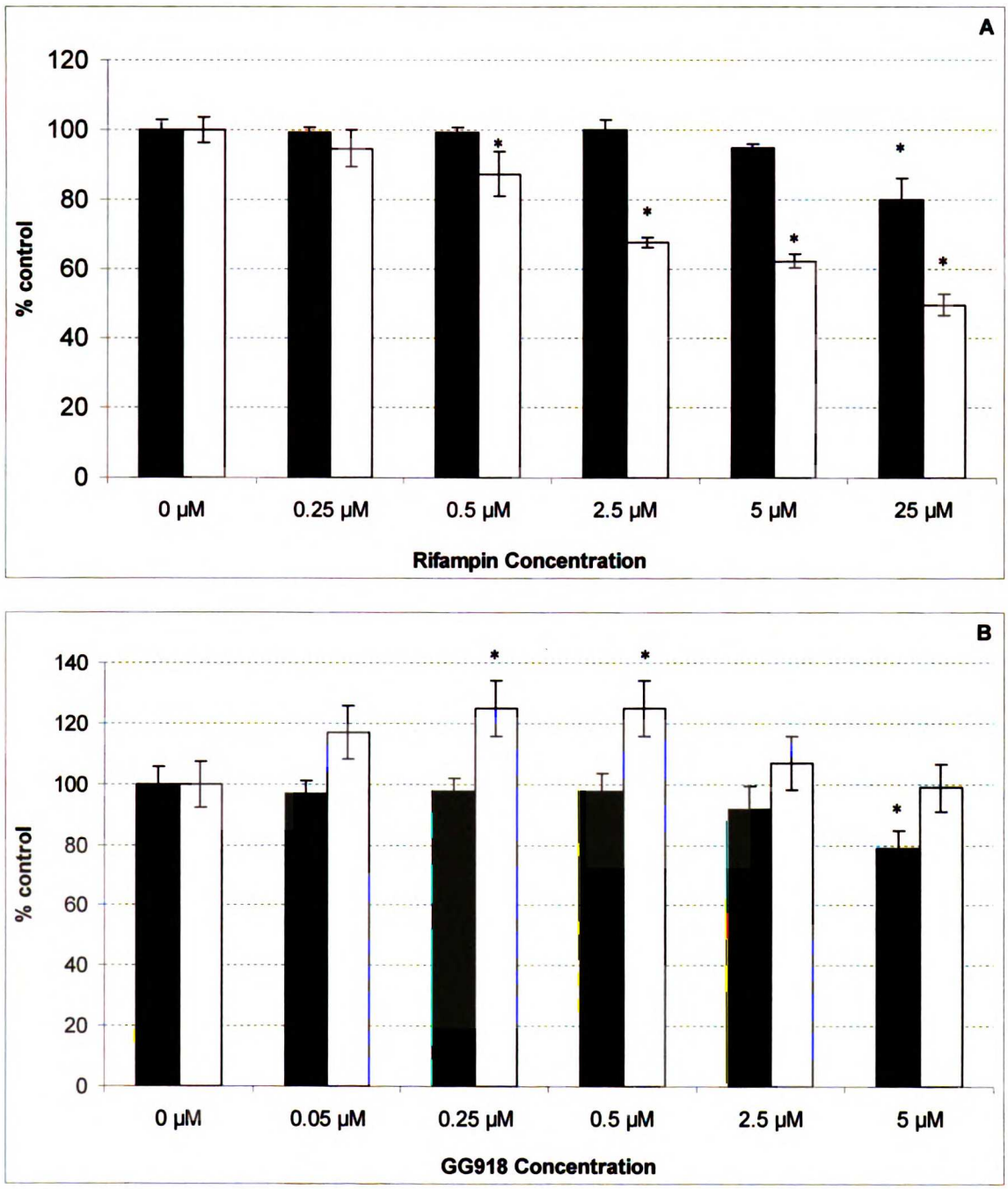

Figure 3.5 *Microsome (black bars) and hepatocyte (white bars) incubations of ERY with inhibitors.* Inhibition of N-demethyl-ERY formation by rifampin (A) and GG918 (B). ERY concentration used was 2 µM. Data are depicted as the mean ± S.D., n=3. *, $p<0.05$, for significantly different from control.

3.3.3 *Time Course Studies of Effects of Rifampin and GG918 on ERY Metabolism in Hepatocyte Suspension*

For the time course studies, 2.5μM of rifampin and 0.5μM of GG918 were used based on the results from Figure 3.5, which showed that these two concentrations had no effect on microsome metabolism but a significant effect on hepatocyte metabolism. When 2.5μM of rifampin was co-incubated with 2μM of ERY over 45 minutes, a non-significant increase in ERY concentration (cell and media) (Figure 3.6A) but a significant decrease in metabolite formation compared to that of ERY only control (Figure 3.6B) were observed. In contrast, when 0.5μM GG918 was co-incubated with ERY, a non-significant decrease in ERY concentration (Figure 3.6A) but a significant increase in N-demethyl-ERY formation were observed compared to controls (Figure 3.6B). AUC's of ERY and N-demethyl-ERY were calculated (Table 3.1). Mass balance was also determined (Table 3.1). Compared to the control (100 ± 5%), the mass balance was 101 ± 4% for the rifampin treatment group and 99.3 ± 3.5% for the GG918 treatment group, which indicates that N-demethyl-ERY is the major metabolite formed in the hepatocyte system, and no other metabolites needed to be monitored.

Changes in AUC became significant when the intracellular concentrations of ERY and N-demethyl-ERY were measured (Figure 3.7). Inhibition of uptake transporters by rifampin led to a reduction in intracellular concentration of ERY (Figure 3.7A) and resulted in a decreased metabolism in comparison with the controls (Figure 3.7B). Conversely, when the efflux transporters were inhibited by GG918, an accumulation of ERY resulted, and an increase in metabolism was observed compared to the controls

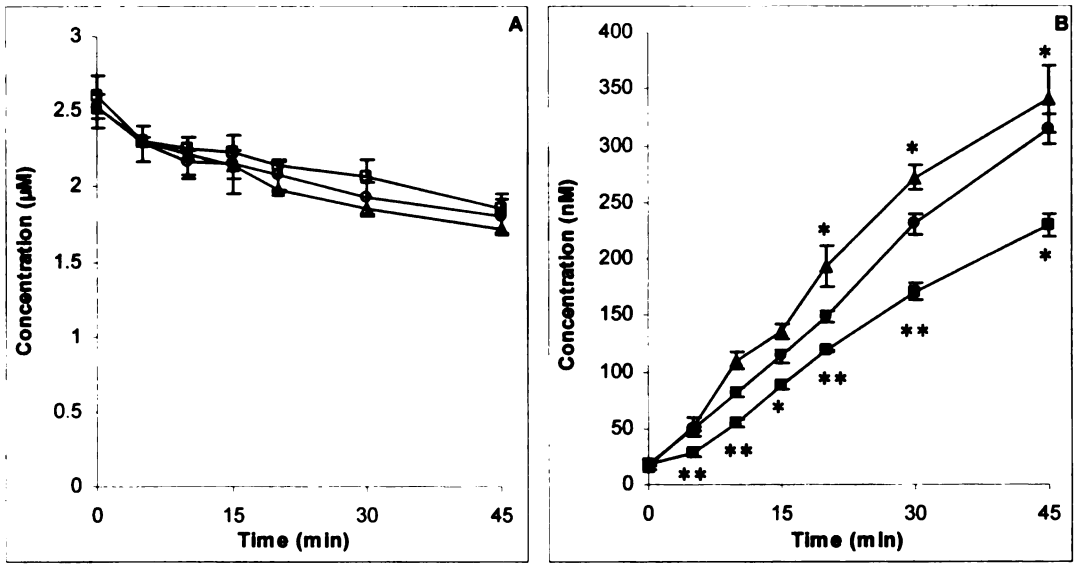

Figure 3.6 *Concentrations of ERY (A) and N-demethyl-ERY (B) in the cells and media over 45 minutes.* Circles (○, ●) represent the ERY control group; squares (□, ■) represent the co-administration of ERY and rifampin group; triangles (Δ, ▲) represent the co-administration of ERY and GG918 group, n=3. *, $p<0.05$, **, $p<0.01$, significantly different from control. Lines are drawn point-to-point.

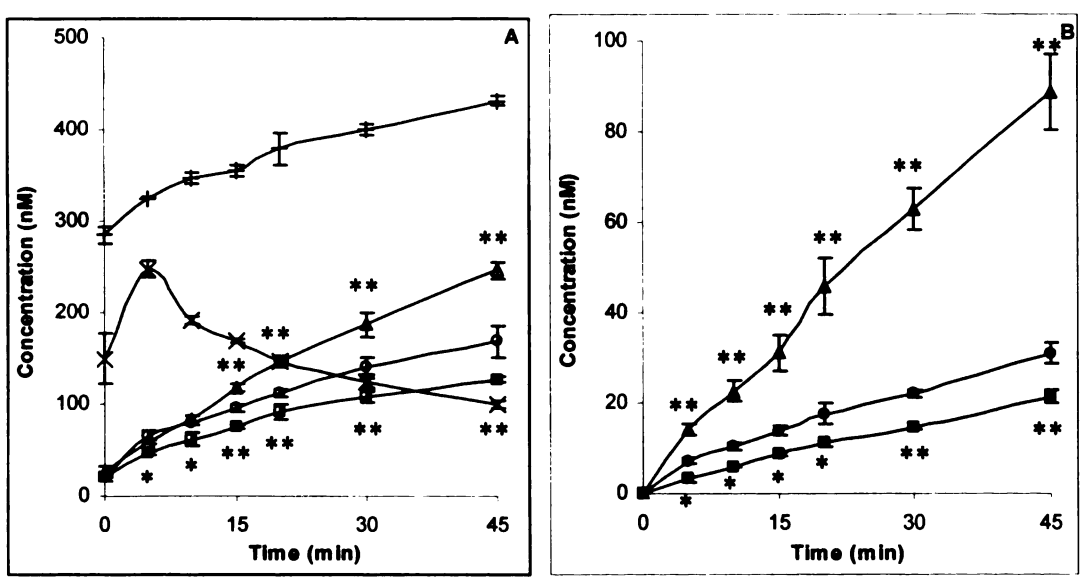

Figure 3.7 *Intracellular concentrations of ERY (A, open symbols) and N-demethyl-ERY (B, closed symbols) over 45 minutes.* Circles (○, ●) represent the ERY control group; squares (□, ■) represent the co-administration of ERY and rifampin group; triangles (Δ, ▲) represent the co-administration of ERY and GG918 group; plus signs (+) represent the concentrations of rifampin; crosses (x) represent concentrations of GG918; n=3. *, $p<0.05$, **, $p<0.01$, rifampin and GG918 group concentrations significantly different from control. Lines are drawn point-to-point.

(Figures 3.7A and 3.7B). Intracellular rifampin and GG918 concentrations were also measured. For rifampin, there was a slight increase in concentrations over time, whereas for GG918, a brief increase followed by a steady decrease in concentrations was observed. AUCs and AUC ratios of ERY and N-demethyl-ERY were calculated (Table 1). Co-incubation of GG918 with ERY significantly increased the metabolite to parent AUC ratio from 0.155 (control group) to 0.320. In contrast, no significant change in the metabolite to parent ratio was observed when rifampin was coincubated with ERY.

Total Measurement (cell and media) of ERY and N-demethyl-ERY			
AUC (μM•min)	ERY only	ERY + rifampin	ERY + GG918
ERY	92.5 ± 4.6	96.2 ± 3.7	90.4 ± 3.3
N-demethyl-ERY	7.63 ± 0.31	5.65 ± 0.24 *	8.92 ± 0.62 *
Mass balance (%)	100 ± 5	101 ± 4	99.3 ± 3.5
Intracellular Measurement of ERY and N-demethyl-ERY (Met)			
AUC (μM•min)	ERY only	ERY + rifampin	ERY + GG918
ERY	5.13 ± 0.33	3.96 ± 0.22 *	6.67 ± 0.30 *
N-demethyl-ERY	0.795 ± 0.057	0.513 ± 0.028 *	2.14 ± 0.21 **
Met/ERY ratio	0.155 ± 0.021	0.129 ± 0.025	0.320 ± 0.035 *

Table 3.1 *Rat hepatocyte incubations:* area under the curves (AUC) over 45 minutes of total measurements (intracellular and incubation media) of ERY and N-demethyl-ERY, as well as intracellular measurements of ERY and N-demethyl-ERY, were calculated for 1) the ERY control group, 2) the ERY with 2.5μM rifampin group and 3) the ERY with 0.5μM of GG918 group, n=3. Mass balances were determined. AUC ratios of N-demethyl-ERY to ERY were also calculated. *, $p<0.05$, **, $p<0.01$, significantly different from ERY only.

3.3.4 *Effects of Rifampin and GG918 on the Pharmacokinetics of ERY in Rats*

To determine the pharmacokinetics of ERY and N-demethyl-ERY with and without transporter inhibitors, i.v. bolus studies were carried out in Wistar rats. The blood concentrations of drugs were measured to obviate correction of plasma values since the blood to plasma concentration ratio is 1.3 for ERY (data not shown). For the rifampin treatment group, the concentration-time profile showed that in the presence of rifampin, there is an increase in AUC of ERY (Figure 3.8A) and N-demethyl-ERY (Figure 3.8B) compared to that without rifampin. The blood concentrations of rifampin were also measured (Figure 3.8A). For the GG918 treatment group, when GG918 was co-administered, there was an increase in AUC of ERY (Figure 3.9A) and N-demethyl-ERY (Figure 3.9B) compared to that of the controls. Levels of GG918 in the blood were below the detection limit of 250 nM.

Pharmacokinetic parameters, $T_{1/2}$, $AUC_{(0\text{-inf})}$, CL, MRT and Vss, were calculated (Table 3.2). No significant differences were found between the two control groups for $T_{1/2}$, $CL_{(blood)}$ and $CL_{(other)}$. However, significant differences were observed for Vss, MRT, $CL_{(renal)}$ and $CL_{(biliary)}$, suggesting that the addition of DMSO and BSA to the GG918 dosing solution did not alter overall ERY kinetics but may have affected certain eliminating organs. Compared to their respective controls, $T_{1/2}$ and MRT were significantly prolonged with either rifampin or GG918 co-administration. The $AUC_{(0\text{-inf})}$ of both treatment groups were also increased significantly, which resulted in significant decreases of total clearances relative to the controls (Table 3.2).

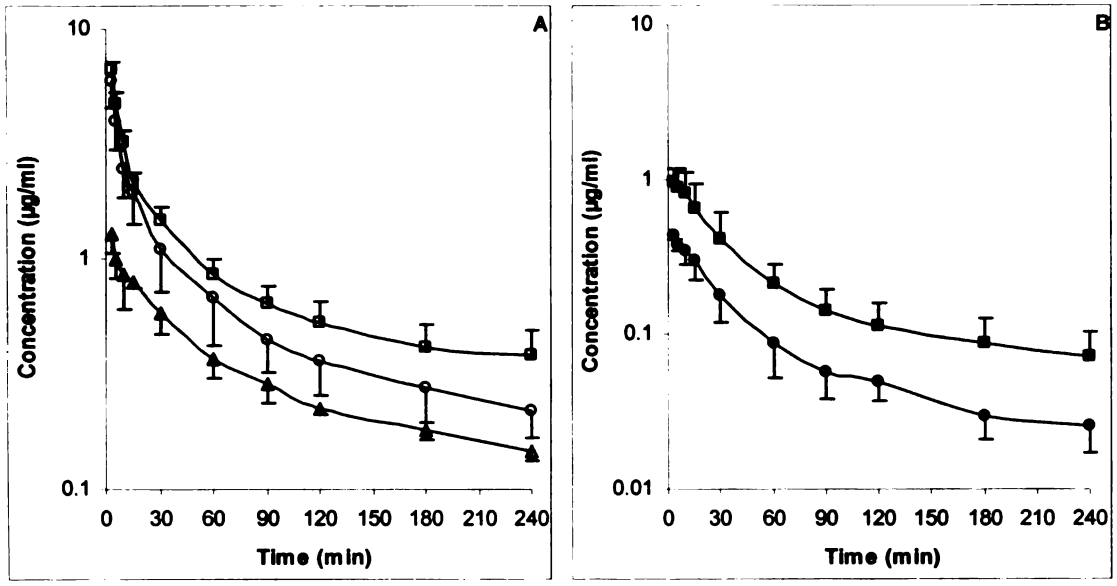

Figure 3.8 *Concentrations of ERY (A, open symbols) and N-demethyl-ERY (B, closed symbols) in the blood over 240 minutes.* Circles (○, ●) represent the ERY control group; squares (□, ■) represent the co-administration of ERY and rifampin group; triangles (Δ) represent the concentrations of rifampin, n=6. Lines are drawn point-to-point.

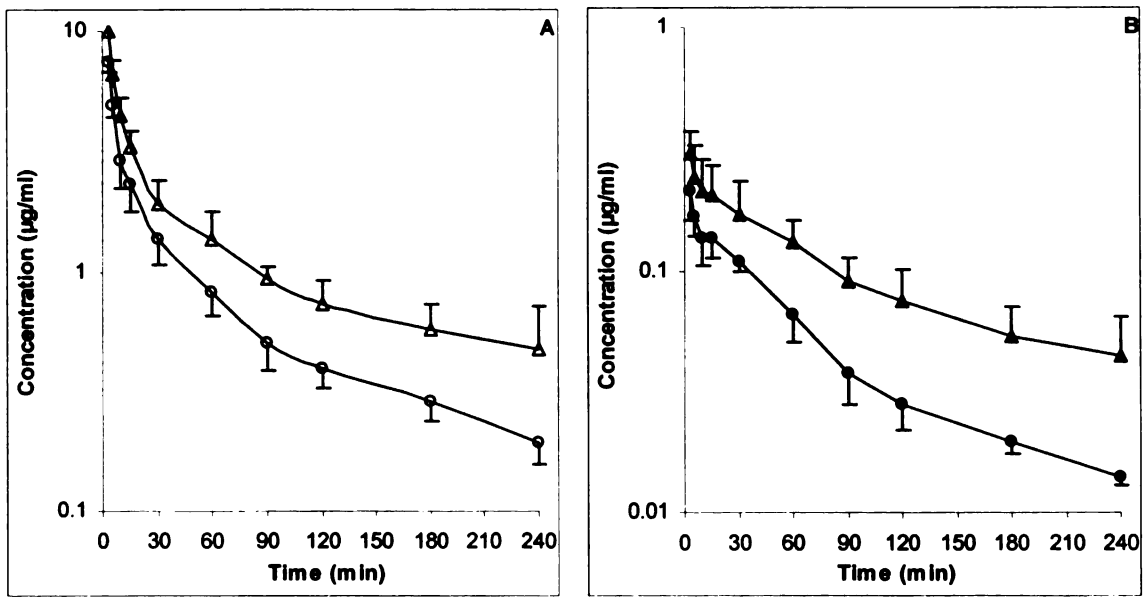

Figure 3.9 *Concentrations of ERY (A, open symbols) and N-demethyl-ERY (B, closed symbols) in the blood over 240 minutes.* Circles (○, ●) represent the ERY control group; triangles (Δ, ▲) represent the co-administration of ERY and GG918 group, n=6. Lines are drawn point-to-point.

PK Parameters	Rifampin group		GG918 group	
	ERY only	w/Rifampin	ERY only	w/GG918
$T_{1/2}$ (term) min	151 ± 27	219 ± 47 *	124 ± 33	250 ± 77 *
$AUC_{(0\text{-inf})}$ µg/ml•min	224 ± 55	348 ± 73 **	240 ± 29	537 ± 221 **
$CL_{(blood)}$ ml/min/kg	47.2 ± 12.5	29.8 ± 6.1 *	42.1 ± 5.7	21.7 ± 9.0 **
MRT min	147 ± 27	237 ± 66 *	109 ± 28	242 ± 135 *
Vss l/kg	6.30 ± 1.12	6.80 ± 1.11	4.51 ± 0.98	3.94 ± 1.28
CL(biliary) ml/min/kg	15.5 ± 2.9	7.23 ± 1.46 ***	11.2 ± 2.0	3.50 ± 1.16 ***
CL(other) ml/min/kg	25.4 ± 9.0	15.3 ± 6.7 †	26.9 ± 5.8	17.0 ± 8.5 *
CL(renal) ml/min/kg	6.26 ± 2.18	7.21 ± 2.44	4.02 ± 0.93	1.18 ± 0.61 ***
CL(renal,met) ml/min/kg	0.644 ± 0.127	0.691 ± 0.090	0.691 ± 0.192	0.421 ± 0.183 *

Table 3.2 *Pharmacokinetic parameters of ERY* in rats after i.v. dosing with and without rifampin or GG918 co-administration, n=6. †, p =0.05, *, p<0.05, **, p<0.01, ***, p<0.001, significantly different from control.

Concentrations of ERY and N-demethyl-ERY were measured in the bile (Figures 3.10 and 3.11). Rifampin and GG918 both reduced bile concentrations of ERY and N-demethyl-ERY compared to controls. In the presence of GG918, there was a delay in C_{max} of ERY and its metabolite relative to the controls, as would be expected when biliary efflux is inhibited rather than hepatic uptake. Biliary clearances were significantly reduced when rifampin or GG918 were co-dosed (Table 3.2). Renal clearances were also determined. For the rifampin group, there was no significant change in the renal clearances of ERY or N-demethyl-ERY, whereas, a significant decrease in renal clearances were observed for both parent drug and metabolite when GG918 was co-administered with ERY (Table 3.2). Liver concentrations of ERY, N-demethyl-ERY, rifampin, and GG918 were measured at 240 minutes (Figure 3.12). Parent drug to metabolite concentration ratios were also calculated. For the rifampin group, compared to controls, ERY and N-demethyl-ERY concentrations decreased significantly; however, their ratios were unchanged. For the GG918 group, significant increases of ERY and N-demethyl-ERY concentrations were observed, and their ratios increased in comparison with that of the controls (Figure 3.12).

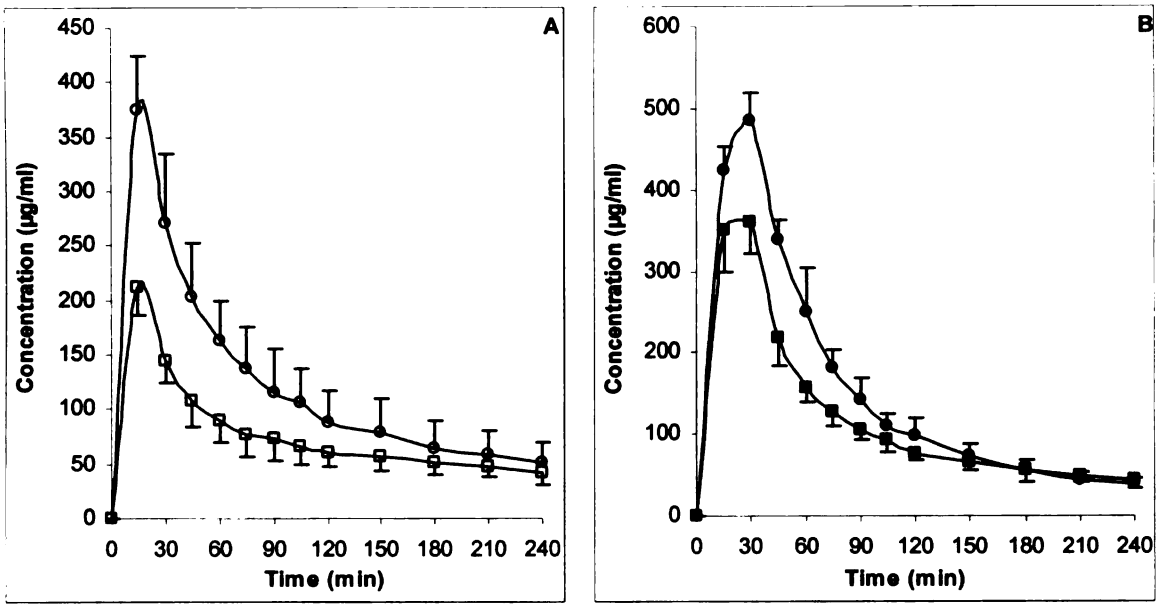

Figure 3.10 *Concentrations of ERY (A, open symbols) and N-demethyl-ERY (B, closed symbols) in the bile over 240 minutes with and without rifampin co-administration.* Circles (○, ●) represent the ERY control group; squares (□, ■) represent the co-administration of ERY and rifampin group, n=6. Lines are drawn point-to-point.

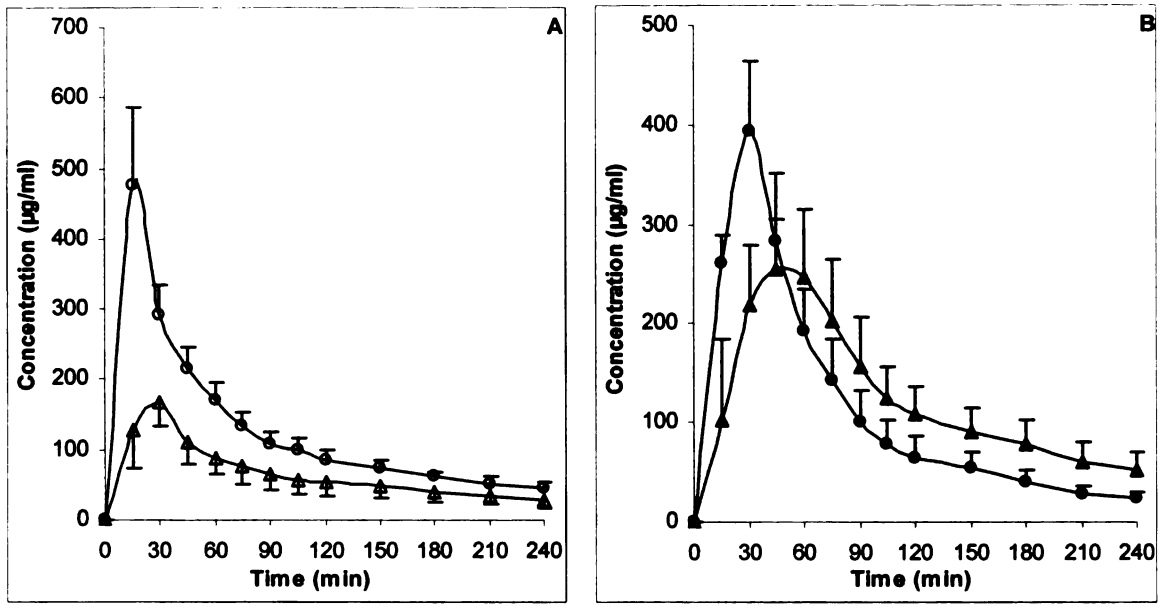

Figure 3.11 *Concentrations of ERY (A, open symbols) and N-demethyl-ERY (B, closed symbols) in the bile over 240 minutes with and without GG918 co-administration.* Circles (○, ●) represent the ERY control group; triangles (Δ, ▲) represent the co-administration of ERY and GG918 group, n=6. Lines are drawn point-to-point.

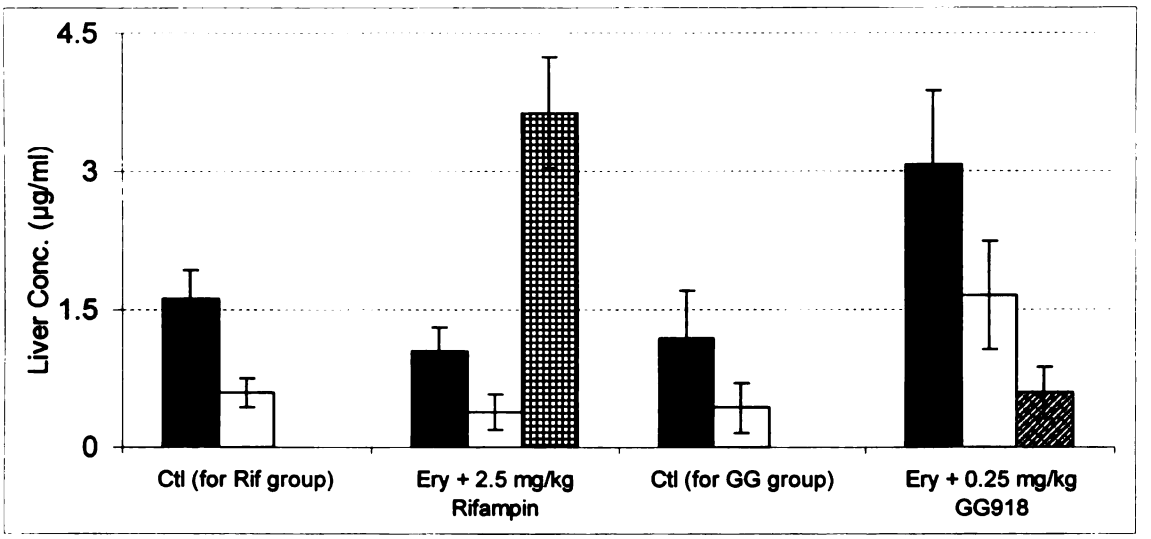

Figure 3.12 *Measurement of drugs in liver.* Liver concentrations of ERY (black bars), N-demethyl-ERY (white bars), rifampin (grid bar) and GG918 (stripe bar) were measured at 240 minutes, n=6. *, $p = 0.05$; ** $p < 0.01$; *** $p < 0.001$, significantly different from control. M/P represents the concentration ratio of N-demethyl-ERY/ERY.

3.4 Discussion

We previously reported that hepatic drug metabolism involves the interplay of Oatps, P-gp and metabolizing enzymes (Chapter 2; Lam and Benet, 2004; Lau et al., 2004). Here, we compared results from in vitro microsome studies, hepatocyte studies, and rat in vivo pharmacokinetic studies with erythromycin and its primary metabolite to further investigate the significance of transporter-enzyme interplay.

Results from the hepatocyte uptake study here (Figure 3.4) and our previous work (Sun et al., 2004) suggests that ERY and N-demethyl-ERY are likely substrates of

Oatp1a4, Oatp1b2 and P-gp. Instead of limiting the uptake of ERY's, quinidine, a good inhibitor of Oatp1a1 and P-gp (Shitara et al., 2002), caused a significant increase in intracellular concentrations of substrates. This is most likely due to quinidine inhibiting efflux transporters. If that were true, it might be expected that GG918 would also increase intracellular concentrations; however, we suspect that no significant increase was observed since GG918 is also an inhibitor of hepatic uptake (Chapter 2; Lam and Benet, 2004). At higher concentrations, GG918 has been shown to inhibit BCRP, but ERY and its metabolite are not substrates for BCRP (data not shown).

Results from the hepatocyte inhibition studies show that rifampin and GG918 cause a significant dose-dependent decrease and increase in ERY metabolism, respectively (Figure 3.5). In contrast, both inhibitors exerted little effect on ERY metabolism in microsomes at the concentrations that caused transporter inhibition. When ERY was incubated with concentrations of GG918 higher than 0.5μM, a decreased ERY metabolism was noted in hepatocytes, most likely due to inhibition of Oatp1a4 in rats by GG918. This agrees with our previous observation using digoxin as a substrate (Chapter 2; Lam and Benet, 2004). In the microsome incubations, at rifampin concentrations of 25μM and higher and at GG918 concentrations of 5μM and higher, ERY metabolism decreased significantly. When surveying metabolic drug-drug interactions, hepatocyte incubations should be conducted in addition to microsome incubations. Drug interactions at the transporter level can't be detected using microsome incubations.

Time course studies demonstrated that over 45 min, ERY metabolism was reduced by rifampin and enhanced by GG918. These results indicate that when uptake transporters were inhibited by 2.5μM rifampin, less ERY entered the cells (Figure 3.7A),

less metabolites were formed (Figures 3.6B, 3.7B), and more parent drug remained in the cell and in the media (Figure 3.6A). In contrast, inhibition of P-gp by 0.5μM GG918 resulted in an accumulation of ERY intracellularly (Figure 3.7A) that led to increased metabolite formation (Figures 3.6B, 3.7B) and less parent drug remained in the cell and in the media (Figure 3.6A). AUC ratios of ERY and N-demethyl-ERY were also determined (Table 3.1). No change in AUC ratio compared to the control when rifampin was present suggests that the metabolic process was not inhibited, only that the drug available to be metabolized was decreased. In contrast, an increase in the AUC ratio relative to control suggests an increase in access of the drug available to be metabolized when GG918 was incubated, as both ERY and metabolite intracellular concentrations increased significantly versus control. Note the increase in intracellular drug and metabolite concentrations in the presence of GG918 at 45 min contrasts with the lack of change noted in the 2 min uptake studies (Figure 3.4). Intracellular levels of rifampin and GG918 did not reach concentrations where cyp3a activities would be inhibited as seen with microsome studies (Figures 3.5, 3.6).

For the in vivo studies, the amounts of ERY, rifampin, and GG918 administered were carefully chosen so that levels of N-demethyl-ERY were detectable in the blood and cyp3a activity was not inhibited in any case. ERY serum clearance in rats has been reported to be 73ml/min/kg using an HPLC method (Duthu, 1985). Since the ERY partition coefficient of blood to plasma is 1.3, our ERY clearance is reasonably consistent with this previous result. For the rifampin co-administered group, the blood concentration-time profile showed that, compared to the control, an increase in AUC was observed leading to a significant (1.5-fold) decrease in total clearance (Figure 3.8A). A

similar trend in AUC was observed in hepatocytes (Figure 3.6A), but it is obvious that in vivo changes in ERY were markedly greater than seen in hepatocytes over 45 min. As expected, since less compound entered the liver as a result of inhibition of Oatps by rifampin, more ERY remained in the blood. This increase in blood AUC cannot be attributed to inhibition of cyp3a since the range of rifampin blood concentrations (1.56μM at 2 min to 0.17μM at 240 min) should not affect enzymatic activity based on our in vitro inhibition studies. There was an increase in blood concentration of N-demethyl-ERY when rifampin was present (Figure 3.8B). We speculate that after the metabolite exits the liver through either passive diffusion or basolateral efflux, it cannot be effectively re-absorbed back into the liver due to the inhibition of the uptake transporters by rifampin since N-demethyl-ERY is also a substrate for Oatp1a4 and Oatp1b2 (Figure 3.4). Ex situ and in vivo increases in metabolites subject to Oatp uptake in the presence of rifampin were also observed by Lau et al. (2005; 2006a; 2006b) for atorvastatin.

For the GG918 group, there was an increase in AUC of ERY compared to the control that resulted in nearly a 2-fold decrease in total clearance (Figure 3.9). Since ERY and N-demethyl-ERY appear to be substrates for the same transporters, the trend of the systemic metabolite profile follows that of the parent drug. When GG918 was present, the increased blood metabolite concentration is likely a result of increased ERY metabolism. In the liver, ERY and N-demethyl-ERY concentrations increased significantly when P-gp was inhibited by GG918, and the N-demethyl-ERY to ERY ratio increased indicating that ERY metabolism was increased compared to the control (Figure 3.12) although this increase was not reflected in the total clearance or CL(other) (Table

3.2). GG918 concentrations in the blood were lower than the detection limit of 250nM, thus, GG918 is unlikely to inhibit uptake transporters at this low concentration. As a consequence of lowered clearance in both treatment groups and no significant change in volume, the half-lives increased compared to their controls.

Bile concentrations of ERY and N-demethyl-ERY were lower than control for the rifampin group, resulting from inhibition of uptake transporters (Figure 3.10). Cell-line studies with MDCK-MDR1 show that rifampin does not inhibit human P-gp (Lau et al., 2006). Both ERY and metabolite bile concentrations were lower than control for the GG918 group (Figure 3.11), we believe as a consequence of inhibiting P-gp biliary elimination, which is consistent with the marked shift of peak time for ERY and N-demethyl-ERY compared to controls. Biliary clearances of both treatment groups significantly decreased versus the controls (Table 3.2); however, the rifampin effect was due to inhibition of uptake transporters, whereas the GG918 effect was due to inhibition of efflux transporters.

Renal clearances of ERY and N-demethyl-ERY didn't change significantly with rifampin co-administration. However, for the GG918 group, the renal clearances of ERY and its metabolite significantly decreased compared to their respective controls suggesting inhibition of P-gp in the kidney. This is consistent with previous findings (Hori et al., 1993) demonstrating that known P-gp inhibitors, quinidine and verapamil, decreased the ratio of fraction excreted to filtration fraction of digoxin in a dose-dependent manner in the isolated rat kidney.

Liver concentrations of ERY, N-demethyl-ERY and inhibitors were measured at the end of the PK study (Figure 3.12). Compared to the controls, there was a significant

decrease and increase in liver concentrations of both ERY and N-demethyl-ERY when rifampin or GG918 were co-administered, respectively. This correlated well with intracellular measurements of parent drug and metabolite in the hepatocyte studies (Table 3.1). For the rifampin group, the metabolite to parent drug ratio did not change significantly in the hepatocytes (Table 3.1) or in the liver (Figure 12) suggesting that the concentration of rifampin used for the in vitro and in vivo studies did not inhibit cyp3a and only inhibited Oatps. For the GG918 group, as observed for the intracellular hepatocyte measurements (Table 3.1), the metabolite to ERY ratio increased significantly in the liver indicating that ERY metabolism increased when P-gp was inhibited. Without affecting enzymatic activities, rifampin and GG918 altered the PK of ERY with similar trends but via very different mechanisms.

In conclusion, hepatic transporters play important roles in the disposition and metabolism of substrate compounds. In this study we used erythromycin as a model substrate. This class 3 drug (high solubility, low permeability with elimination primarily as unchanged drug in humans) as defined by Wu and Benet (2005) undergoes more extensive metabolism in rats and served as a good substrate for investigating both hepatic uptake and efflux transporter interplay with metabolic enzymes. In addition, since the N-demethyl-ERY metabolite is also a substrate for the same transporters, we could observe in vivo interactions of the metabolite that may not have been obvious from in vitro studies. The studies here should be important primarily for the many class 2 drugs (high permeability, low solubility, extensively metabolized compounds) where hepatic transporter-enzyme interplay will not be predicable from microsome studies alone.

Chapter 4

Elucidating the Effect of Final Day Dosing of Rifampin in Induction Studies on Hepatic Drug Disposition and Metabolism[1]

4.1 Introduction

Rifampin (RIF) is commonly used to treat tuberculosis and other mycobacterial infections. In clinical studies, it is frequently used as an inducer of several clinically significant cytochrome P450 isoforms as well as membrane transporters (Schuetz, 2001; Kullak-Ublick and Becker, 2003). The mechanism of activation is through the binding of nuclear receptor pregnane X receptor (PXR) (Kliewer et al., 1998; Lehmann et al., 1998). Recently, RIF has been shown to be an excellent substrate and inhibitor of hepatic uptake transporters that are localized on the sinusoidal membrane of hepatocytes (Tirona et al., 2003). These transporters are members of the solute carrier superfamily of transport

[1] A portion of this chapter was submitted in a manuscript entitled "Elucidating the effect of final day dosing of rifampin in induction studies on hepatic drug disposition and metabolism" Lam J.L., Shugarts S.B., Okochi H. and Benet L.Z. (2006) *J Pharmacol Exp Ther*

proteins. The isoforms that are most affected by RIF are organic anion transporting polypeptides (OATP in human/Oatp in rats). In the over-expressed oocyte system, RIF has been shown to inhibit the uptake of estradiol-17β-glucuronide by Oatp1a4 (formerly Oatp2) (K_i = 1.4 μM) (Fattinger et al., 2000) and the uptake of BSP by OATP1B1 (formerly OATP-C) (K_i = 7 μM) and OATP1B3 (formerly OATP8) (K_i = 5 μM) (Vavricka et al., 2002). In a transiently transfected cell-line, RIF potently inhibited: Oatp1a4 mediated uptake of digoxin (K_i = 1.46 ± 0.58 μM) (Shitara et al., 2002), OATP1B1 mediated uptake of estradiol-17β-glucuronide (EC_{50} = 0.94 μM) (Tirona et al., 2003) and atorvastatin (K_i = 2.88 ± 1.33 μM) (Lau et al., 2006b), as well as OATP-8 mediated uptake of BSP (K_i = 1.5 μM) and amanitin (IC_{50} =0.8 μM) (Letschert et al., 2006). In freshly isolated rat hepatocyte studies, RIF exhibited a strong inhibition effect on Oatp mediated uptake of digoxin and erythromycin (Chapter 2; Lam and Benet, 2004; Chapter 3; Lam et al., 2006). In the isolated perfused rat liver system, without affecting enzymatic activities, RIF reduced hepatic clearance of digoxin and atorvastatin by 1.3-fold and 2-fold, respectively(Lau et al., 2004; Lau et al., 2006b). In vivo, total clearance of erythromycin decreased 1.6-fold relative to the control when RIF was co-administered i.v. in rats (Chapter 3; Lam et al., 2006). Concomitant i.v. dosing of RIF with oral dosing of atorvastatin in rats and in humans reduced CL/F of atorvastatin by 3.5-fold and 6-fold, respectively (Lau et al., 2006a; Lau et al., 2006c).

Results from a clinical study conducted by Stone et al. (2004) suggested that RIF both induced and inhibited the disposition of caspofungin, which has been shown to be a substrate of OATP1B1 (Sandhu et al., 2005). In another clinical study, when RIF and repaglinide were co-administered, RIF acted as an inducer and inhibitor of repaglinide

metabolism (Bidstrup et al., 2004). When repaglinide was administered on the same day as the final (7th) inducing dose of RIF, repaglinide AUC decreased by 50% compared to the non-induced control; whereas, a sharper AUC decrease of 80% was observed when repaglinide was dosed one day after the last day of RIF dosing. Niemi et al. (2005) showed that OATP1B1 is important in the disposition of repaglinide by examining effects of transporter polymorphism on pharmacokinetics. Compared to measures for the 521TT reference genotype, the 521CC subjects exhibited a 152% increase in AUC and a 188% increase in C_{max}. Since it has been well demonstrated that RIF is an excellent inhibitor of OATP1B1, it is reasonable to speculate that the conflicting results from the Bidstrup study could be due in part to inhibition of OATP1B1 by RIF when administered on the same day with repaglinide. All of these findings lead to our hypothesis that because RIF induces hepatic enzymes and inhibits uptake transporters, dosing of a drug that is a dual substrate of enzymes and uptake transporters on the final day of an inducing regimen should exhibit less inductive effect than on the following day in the absence of RIF since the presence of RIF decreases drug uptake into the liver.

To test our hypothesis, in vitro and in vivo studies were conducted in rats using digoxin as a model compound. Chemical structures of digoxin and its metabolites are shown in Figure 2.1 (Chapter 2). Since the RIF inducing effect is species specific to human, dexamethasone (DEX) was used instead to induce cyp3a, p-gp and Oatp1a4 (Salphati and Benet, 1998; Guo et al., 2002). It has been shown that digoxin is an excellent substrate of Oatp1a4, cyp3a and p-gp (Tanigawara et al., 1992; Salphati and Benet, 1999; Shitara et al., 2002). We have previously demonstrated that up to 200 μM RIF does not inhibit digoxin cyp3a metabolism in microsome incubations (Chapter 2;

Lam and Benet, 2004). In this study, we examined the effects of RIF on digoxin disposition and subsequent metabolism in vitro using freshly isolated rat hepatocytes and in vivo comparing pharmacokinetic profiles.

4.2 Materials and Methods

4.2.1 Materials

Digoxin, digoxigenin (dg0), RIF, corticosterone, DEX, corn oil, HPLC grade methanol, acetonitrile (ACN) and *tert*-butyl-methyl-ether (MTBE) were purchased from Sigma-Aldrich (St Louis, MO). [^{3}H] digoxin (37 Ci/mmol) was obtained from Perkin Elmer Life Sciences (Boston, MA). Digoxigenin bis-digitoxoside (dg2) and digoxigenin mono-digitoxoside (dg1) were kind gifts from Professor Emil Lin, UCSF. Lanoxin (GlaxoSmithKline, Kirkland, Canada) and RIF (Bedford laboratories, Bedford, OH) for i.v. infusion were purchased from the UCSF pharmacy for research use only. Male Wistar rats (200-350 g) from Charles-River Laboratories (Wilmington, MA) were housed in the UCSF animal care facility with a 12 hour light/dark cycle and allowed free access to water and food. The studies described here were approved by the Committee on Animal Research, UCSF.

4.2.2 Study Design

For in vitro studies, control rats received 4 daily intraperitoneal (i.p.) injections of vehicle (corn oil) and induced rats received 4 daily i.p. injections of 80 mg/kg DEX (Salphati and Benet, 1998). On day 5, hepatocytes were isolated from the control rats and the induced rats. In vitro uptake studies and time course studies were carried out.

For in vivo studies, 18 rats were equally divided into 3 groups, the uninduced digoxin only control group, the induced digoxin alone group and the induced digoxin with RIF group. For the uninduced control group, rats received i.p. corn oil injections for 4 days followed by pharmacokinetic (PK) studies of 1 mg/kg digoxin on day 5 to obtain baseline PK values. For the two induced groups, rats received 80mg/kg of DEX for 4 days. On day 5, the induced digoxin alone group received 1 mg/kg digoxin, and PK studies were carried out to mimic the clinical situation where a test drug was administered one day after final dosing of RIF. The induced digoxin with RIF group received 1 mg/kg digoxin and 45 mg/kg RIF together on day 5 to simulate the situation in which a test drug was administered concomitantly with RIF on the last day of an induction regimen.

4.2.3 Hepatocyte Isolation

Cells from 6 rats per set were pooled for counting and subsequent studies. The cell isolation procedure is as follows: anesthesia was induced by intraperitoneal injection

with a 1 ml/kg dose of ketamine/xylazine (80 mg/ml, 12 mg/ml) prior to surgery. The portal vein was cannulated with an IV catheter (catalog number 2007-04, Becton Dickinson, Sandy, UT) and perfused with oxygenated liver perfusion buffer (Invitrogen, Carlsbad, CA) for 5 minutes at 30 ml/min followed by perfusion with an oxygenated hepatocyte washing buffer (Invitrogen, Carlsbad, CA) modified with 2 mM L-glutamine, 10 mM HEPES, and 1.2 U/ml collagenase (Sigma-Aldrich, St. Louis, MO) for 5 minutes at 20 ml/min. The digested livers were excised and broken down. Hepatocytes were then washed twice with an ice cold hepatocyte wash buffer containing 2 mM L-glutamine and 10 mM HEPES and centrifuged at 50 x g for 2-3 minutes. Cell viability was determined using the trypan blue exclusion method. Cells with viability of greater than 90% were used for further studies.

4.2.4 Hepatocyte Uptake Studies

Prior to each incubation, 2 million hepatocytes were pre-warmed in Krebs-Henseleit buffer (pH7.4) containing 0.21 g/L of sodium bicarbonate and supplemented with 1% BSA and 10 mM glucose for 5 minutes. For the digoxin uptake studies, [^{3}H] digoxin (500nM) with and without 100 μM RIF were added to the cells. After 2 minutes, each reactions was terminated by transferring 1 million hepatocytes into a centrifuge tube containing 150 μl of 2 N NaOH under a layer of 500 μl of a mixture of silicone oil and mineral oil (Shitara et al., 2003) and centrifuged at 13,000 × g for 10 seconds. The cell pellets were left at 65°C overnight to ensure complete lysis. After removing the oil layer,

150 µl of 2 N HCl and 5ml of scintillation cocktail were added to each sample and radioactivity was measured using a scintillation counter (LS6000TA, Beckman Coulter, Fullerton, CA).

To measure digoxin metabolite uptake, dg2 (500nM), dg1 (500nM) and dg0 (500nM) with and without 100 µM RIF were added to the cells. After 2 minutes, each reaction was stopped by transferring 1 million hepatocytes into a centrifuge tube containing 700 µl of a mixture of silicone oil and mineral oil and centrifuged at 13,000 x g for 10 seconds. After removing the oil layer, the cell pellet was resuspended in 100 µl of water to lyse the cells followed by addition of 200 µl of ACN to precipitate the protein. After a quick vortex, samples were spun down at 13,000 × g for 10 minutes. The supernatants were transferred into HPLC vials ready for LC-MS analysis. Protein concentrations of uninduced and induced cells were measured using a BCA protein assay kit (Pierce, Rockford, IL) according to the manufacturer's directions. All further hepatocyte calculations were normalized to protein concentration.

4.2.5 Hepatocyte Time Course Studies

Incubations were carried out in 50 ml round-bottom flasks undergoing continuous rotation while gassed with 95% O_2/5% CO_2 at 37°C (Li et al., 2002). At the end of the study, an aliquot of hepatocytes in Krebs-Henseleit buffer (pH7.4) containing 2.73 g/L of sodium bicarbonate and supplemented with 1% BSA and 10 mM glucose was removed from each flask to determine drug effects on cell viability using the trypan blue exclusion

method. At 5, 10, 15, 20, 30, 45 and 60 minute time points, two aliquots of two million hepatocytes were transferred to a glass cell culture tube containing 2 ml of MTBE and internal standard corticosterone, followed by a quick vortex to stop the reaction. All samples were spun down at 2000×g for 10 minutes. After quick-freezing the aqueous layer in a methanol/dry ice bath, the organic layer was poured into a new tube and evaporated under nitrogen gas. One group of aliquots was used to measure dg3 and metabolites by LC-MS analysis as described below. To each glass tube of the second group of aliquots, 150 µl of 4mM phosphate buffer (pH 6.8) containing 50 units of β-glucuronidase (Sigma-Aldrich, St. Louis, MO) was added to cleave possible glucuronide adducts. After a brief vortex, these samples were left in the 37°C incubator over night. ACN (150 µl) was added to each sample to stop the reaction followed by centrifugation at 13,000 × g for 10 minutes to precipitate the protein. The supernatants were transferred into HPLC vials ready for LC-MS analysis. All further hepatocyte calculations were normalized to protein concentrations.

4.2.6 Surgery and Pharmacokinetic Studies in Rats

Male Wistar rats (250g-300g) were under anesthesia induced by intraperitoneal injection with a 1 ml/kg dose of ketamine:xylazine (80 mg/ml:12 mg/ml, Sigma-Aldrich, St. Louis, MO) prior to surgery and several times during the 4 hour study to ensure complete anesthetization. The femoral vein and the femoral artery were cannulated using a 10 cm PE-10 tube (I.D. 0.28 mm, O.D. 0.61 mm, BD Intramedic, Sparks, MD) and a 10

cm SP-35 tube (I.D. 0.5 mm, O.D. 0.9 mm, Natume Co., Tokyo, Japan), respectively. The lines were washed immediately with saline containing 10 Unit/ml heparin to prevent clotting. Digoxin (1mg/kg) with either vehicle control (saline) or together with rifampin (45 mg/kg) was co-administered through the femoral vein. Blood (250 µl) samples were collected at time points 0, 3, 5, 15, 30, 60, 90, 120, 150, 180, and 240 minutes via femoral artery and transferred to heparin-pretreated microtainer tubes (Becton-Dickinson, Franklin Lakes, NJ). Plasma was obtained by centrifugation at 10,000×g for 5 minutes. Rat livers were excised at 240 min and weighed. To each 100 µl of plasma and liver homogenate sample, 200 µl of ACN containing IS was added, and samples were centrifuged for 15 minute at 13,000 rpm. The supernatants were transferred into HPLC vials and assayed using LC-MS.

4.2.7 Measurement of Drug Concentrations

Samples were analyzed on a liquid chromatography-mass selective detector system (Hewlett Packard) consisting of the 1100 HPLC components HPLCI and HPLCII as described previously (Christians et al., 2000). The two HPLC systems were connected via a 7240 Rheodyne six-port switching valve mounted on a step motor (Rheodyne, Cotati, CA). The system was controlled and data were processed using ChemStation Software revision A.06.01 (Hewlett Packard). Samples (100 µl) were injected onto a 10 x 6-mm extraction column (Keystone Scientific, Bellefonte, PA) filled with Hypersil ODS-1 of 5-µm particle size (Shandon, Chadwick, UK). Samples were washed with a mobile

phase of 0.1% formic acid supplemented with 1 mM sodium acetate. The flow was 1.5 ml/min, and the temperature for the extraction column was set to 65°C. After 0.9 minutes, the switching valve was activated, and the analytes were eluted with 100% ACN in the backflush mode from the extraction column onto a 100 x 4.6-mm C_8, 3.5-μm analytical column (Zorbax XDB, C_8; Hewlett Packard). The mobile phase consisted of methanol and 0.1% formic acid supplemented with 1 mM sodium acetate:ACN (80:20, v:v). The following gradient was run: time 0 min, 50% methanol; 6 min, 90% methanol. The flow rate was 0.5 ml/min. The analytical column was also maintained at 65°C. Two minutes after sample injection, the mass-selective detector was activated. The detection limits were 50 ng/ml, 5 ng/ml, 10 ng/ml, 10 ng/ml and 100 ng/ml for digoxin, dg2, dg1, dg0 and rifampin, respectively. A representative chromatogram was shown in Figure 2.2 (Chapter 2).

4.2.8 Transient Transfection and Uptake Transport Assays

The Oatp1a4 cDNA in pCI-neo mammalian expression plasmid (Promega, Madison, WI) was sequenced and its expression was verified using the Western blotting method. HEK293 cells (University of California Cell Culture Facility, San Francisco, CA) were cultured in Dulbecco's modified Eagle's medium H21 (4.5 g/liter glucose) supplemented with 10% fetal bovine serum (FBS, Invitrogen, Carlsbad, CA), 100 μg/mL streptomycin and 100 U/mL penicillin. Cells were seeded into poly-D-lysine-coated 12-well plates (BD Biosciences, Bedford, MA) at a density of 0.5×10^6 cells/well 1 day

prior to transfection. Transfection of the Oatp1a4 plasmid and the pCI-neo vector control using ExGen500 transfection reagents (Fermentas, Hanover, MD) were according to the manufacturer's direction. Cell culture media was replaced 24 hours prior to uptake studies. The cells were washed with 37°C transport medium (Hank's balanced salt solution containing 1% FBS and 25 mM HEPES, pH 7.4) for 5 minutes immediately before the uptake experiment. Uptake studies were initiated by adding 0.7 ml of 37°C transport medium containing substrates. The cells were incubated for 2 minutes at 37°C. Drug uptake was stopped by removing the incubation medium followed by washing three times with ice-cold phosphate buffered saline (pH 7.4). Air-dried cells were scraped off the plates and resuspended in 200 μL of double-distilled water. After adding ACN to precipitate the protein, the samples were spun down at 13,000 × g for 10 minutes at 4°C. The supernatants were transferred into HPLC vials ready for LC-MS analysis. Protein concentrations of cells were measured using a BCA protein assay kit (Pierce, Rockford, IL) according to the manufacturer's directions. All further calculations were normalized to protein concentrations.

4.2.9 Data Analysis

For the pharmacokinetic studies, terminal half-life ($T_{1/2}$) was determined from log linear regression. Area under the time-concentration curve (AUC) was calculated by the linear trapezoid rule and extrapolated to infinite time from the last measured concentration (C_{last}) by adding [$C_{last} \times T_{1/2}/0.693$]. Clearance (CL) was calculated as dose

divided by extrapolated AUC. Volume of distribution at steady-state (Vss) was calculated using moments (Benet and Galeazzi, 1979). Analysis of variance was used to analyze differences among the three groups. The significance between two means in these groups was evaluated using Tukey's multiple comparison test. The *p*-value for statistical significance was set at < 0.05.

4.3 Results

4.3.1 Uptake of [^{3}H]-Digoxin by Freshly Isolated Rat Hepatocytes

Effects of RIF on digoxin uptake were examined in the freshly isolated rat hepatocytes as depicted in Figure 4.1. Compared to that of the control in the uninduced cells (2.15 ± 0.17 nM/mg protein), there was a more than 5-fold increase in intracellular concentration of digoxin in the induced cells (12.6 ± 0.8 nM/mg protein, $p<0.001$) over 2 minutes. This finding is consistent with up-regulation of Oatp1a4 through PXR observed using RT-PCR (Guo et al., 2002). However, when 500 nM of [^{3}H]-digoxin was co-incubated with 100 μM RIF in the induced hepatocytes, the uptake was reduced more than 3-fold (3.55 ± 0.34 nM/mg protein, $p<0.001$) versus that without RIF (12.6 ± 0.8 nM/mg protein). Results from the uptake study indicate the importance of Oatp1a4 in the disposition of digoxin.

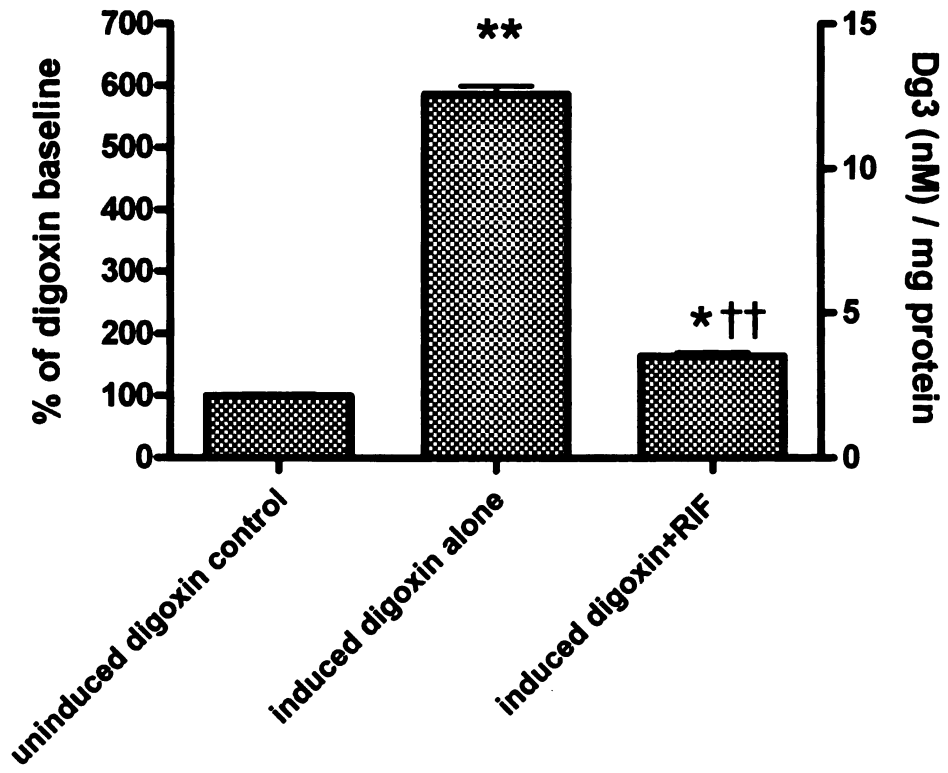

Figure 4.1 *Uptake of [^{3}H] digoxin into freshly isolated hepatocytes (right axis) for the three treatment groups expressed as a percentage of the uninduced control (left axis).* *, $p<0.05$; **, $p<0.001$, significantly different from the uninduced control group. ††, $p<0.001$, significantly different from the induced digoxin alone group. Data are depicted as the mean ± S.D., n=6.

4.3.2 Hepatocyte Time Course Studies

Three sets of time course studies were carried out. In the first set, digoxin with vehicle was incubated in hepatocytes that were not induced as control. In the second set,

digoxin with vehicle was incubated using induced cells to mimic clinical situations in which a test drug was administered one day after final dosing of RIF in induction studies. In the third set, digoxin was co-incubated with RIF in the induced cells to mimic conditions in which a test drug was administered concomitantly with RIF on the final day of an induction study. Total drug concentrations (cell and media) before and after glucuronidase treatment were measured over 60 minutes (Figures 4.2 and 4.3). Only digoxin and dg2 were found in the cell suspensions. Levels of dg1 and dg0 were below the detection limits.

Tables 4.1 and 4.2 summarizes the areas under the concentration-time curve over 60 minutes and related calculations for the 3 sets of studies for samples before and after glucuronidase cleavage, respectively. Compared to the digoxin (dg3) AUC of the uninduced control, AUC of digoxin decreased 2-fold when incubated alone in the induced cells. However, when RIF was co-incubated with digoxin in the induced cells, AUC increased 2-fold versus the digoxin alone to a level that overlapped with the control in the uninduced cells as shown in Figure 4.2A. Conversely, AUC of dg2 increased considerably (13-fold) for the induced group compared to the uninduced control, which indicates induction of cyp3a. Dg2 AUC decreased (3-fold) significantly with RIF compared to when no RIF was added to induced cells, as shown in Figure 4.2B. Ratios of dg2 AUC to dg3 AUC and mass balance were also calculated.

For the samples measured following glucuronidase cleavage (Figure 4.3, Table 4.2), none of the values changed significantly from that of Table 4.1 except for the mass balance percentage in the induced digoxin control set that increased from 43.3 ± 0.6% to 52.4 ± 1.2% ($p<0.05$).

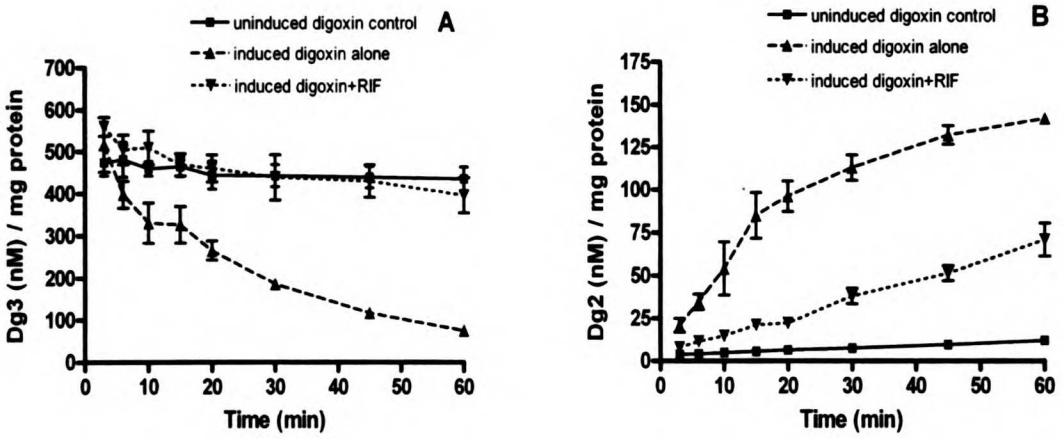

Figure 4.2 *Hepatocyte time course studies of the three treatment sets before glucuronidase cleavage.* Measurements of (A) digoxin (Dg3) and (B) Dg2 in the cell suspensions are shown. Data are depicted as the mean ± S.D., n=6.

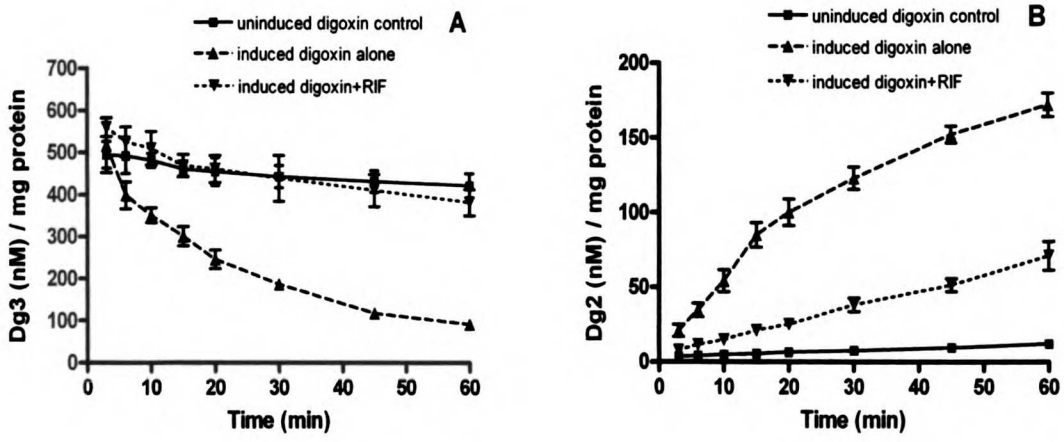

Figure 4.3 *Hepatocyte time course studies of the three treatment sets after glucuronidase cleavage.* Measurements of (A) digoxin (Dg3) and (B) Dg2 in the cell suspensions are shown. Data are depicted as the mean ± S.D., n=6.

	Uninduced digoxin control	Induced digoxin alone	Induced digoxin with RIF
$AUC_{(0\text{-}60)}$ of Dg3 (μM • min/mg)	26.9 ± 1.3	13.7 ± 0.9 *	27.3 ± 0.9 †
$AUC_{(0\text{-}60)}$ of Dg2 (μM • min/mg)	0.463 ± 0.009	6.06 ± 0.21 *	2.18 ± 0.87 * †
$AUC_{(0\text{-}60)}$ ratio (Dg2/Dg3)	0.0172 ± 0.0072	0.442 ± 0.294*	0.0799 ± 0.0950 †
Mass Balance (%)	89.3 ± 5.7	43.3 ± 0.6 *	93.3 ± 9.7†

Table 4.1 *Area under the curve (AUC) of digoxin (Dg3) and Dg2 in rat hepatocyte incubations were determined for the three treatment sets before glucuronidase cleavage.* Metabolite to digoxin ratio and mass balance were calculated. Each value represents mean ± S.D., n = 6. *, $p<0.01$, significantly different from the uninduced digoxin control set. †, $p<0.01$, significantly different from the induced digoxin alone group set.

	Uninduced digoxin control	Induced digoxin alone	Induced digoxin with RIF
$AUC_{(0\text{-}60)}$ of Dg3 (μM • min/mg)	26.8 ± 1.1	13.6 ± 0.6 *	26.9 ± 0.6 †
$AUC_{(0\text{-}60)}$ of Dg2 (μM • min/mg)	0.459 ± 0.009	6.74 ± 0.17 *	2.21 ± 0.25 * †
$AUC_{(0\text{-}60)}$ ratio (Dg2/Dg3)	0.0170 ± 0.0060	0.496 ± 0.187 *	0.0821 ± 0.0374 †
Mass Balance (%)	86.4 ± 6.5	52.4 ± 1.2 *	90.0 ± 5.7†

Table 4.2 *Area under the curve (AUC) of digoxin (Dg3) and Dg2 in rat hepatocyte incubations were determined for the three treatment sets after glucuronidase cleavage.* Metabolite to digoxin ratio and mass balance were calculated. Each value represents mean ± S.D., n = 6. *, $p<0.01$, significantly different from the uninduced digoxin control set. †, $p<0.01$, significantly different from the induced digoxin alone group set.

4.3.3 In Vivo Pharmacokinetic Study of Digoxin

To determine the effects of final day dosing of RIF on the pharmacokinetics of a representative drug, we tested our hypothesis in vivo in rats. Effects of RIF on digoxin metabolism were investigated in the induced rats. All three groups of rats received an i.v. bolus dose of digoxin (1mg/kg) with one induced group concomitantly receiving 45 mg/kg of RIF. Plasma concentrations of drugs were measured (Figure 4.4), and pharmacokinetic parameters were estimated (Table 4.3). Compared to that of the uninduced control rats, $AUC_{(0\text{-inf})}$ of digoxin decreased and CL increased 2- fold when digoxin alone was given to induced rats. Vss also increased significantly. However, when RIF was co-administered with digoxin in the induced rats, $AUC_{(0\text{-inf})}$ increased and CL decreased compared to that without RIF to levels close to that of uninduced controls. Vss also decreased significantly. Plasma levels of RIF were also measured (Figure 4.4A). Plasma levels of dg2 were only slightly and non-significantly lower in the induced rats than in the uninduced control rats. However, when RIF was co-administered with digoxin in the induced rats, dg2 levels increased substantially (Figure 4.4B, Table 4.3). As opposed to the hepatocyte studies, dg0 concentrations were measurable in the plasma in all three groups (Figure 4.4C, Table 4.3). Compared to the control dg0 level in the uninduced rats, dg0 concentrations in both induced groups were higher; however, levels of dg0 between digoxin with and without RIF in the induced rats were not significantly different. AUCs of dg2 and dg0 were summed and ratios of metabolite AUC to parent drug AUC were calculated (Table 4.3).

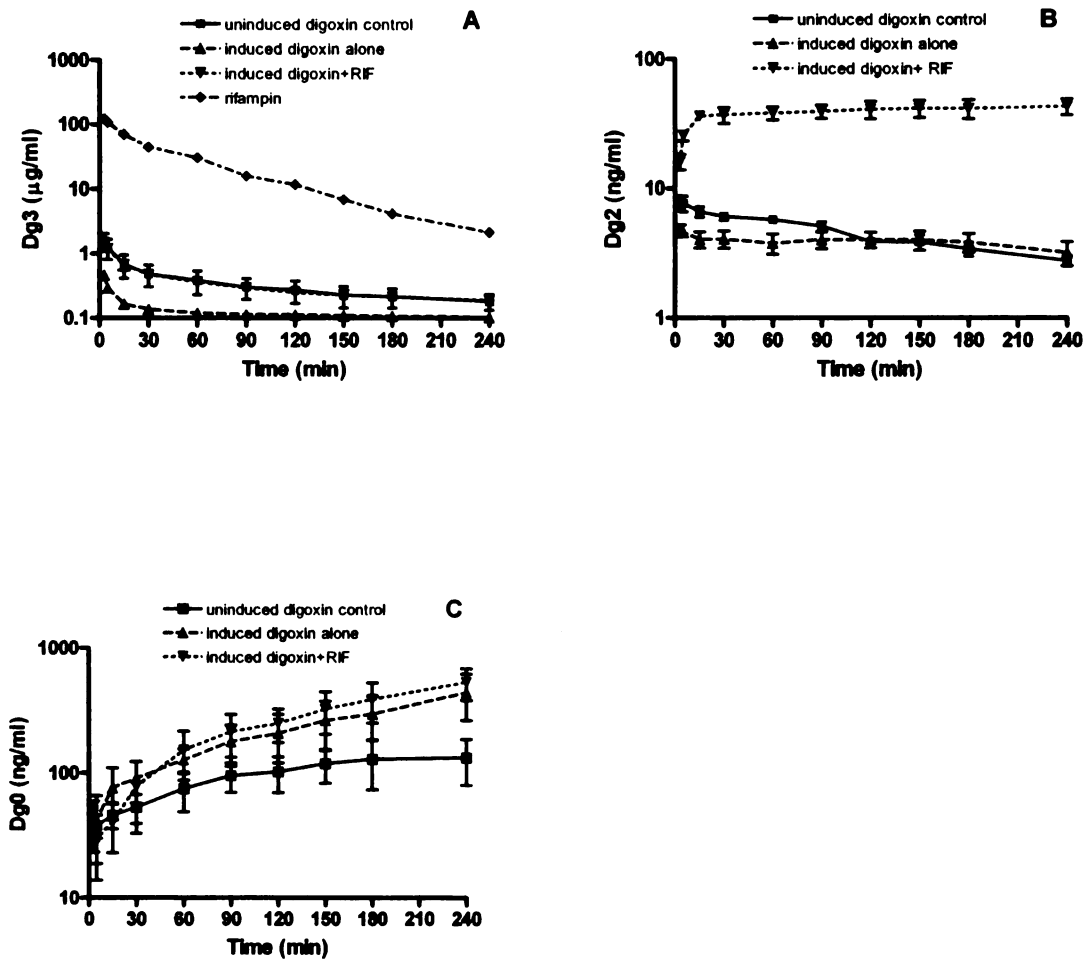

Figure 4.4 *Rat in vivo studies of the three treatment groups.* Plasma concentrations of (A) digoxin (Dg3) and RIF, (B) Dg2, and (C) Dg0 are shown. Data are depicted as the mean ± S.D., n=6.

	Uninduced digoxin control	Induced digoxin alone	Induced digoxin with RIF
$T_{1/2}$ (hr)	3.93 ± 1.07	4.97 ± 0.83	4.68 ± 1.18
$AUC_{0\text{-inf}}$ (μg/ml•min)	146 ± 25	66.9 ± 14.9 **	144 ± 30 ††
CL (ml/min/kg)	7.08 ± 1.57	15.6 ± 3.7 **	7.14 ± 1.24 ††
Vss (l)	0.616 ± 0.228	1.73 ± 0.21 **	0.613 ± 0.132 ††
Dg2 $AUC_{(0\text{-}240)}$ (μg/ml•min)	1.14 ± 0.15	1.01 ± 0.23	9.59 ± 1.17 ††**
Dg0 $AUC_{(0\text{-}240)}$ (μg/ml•min)	23.7 ± 8.7	48.1 ± 21.7	57.2 ± 27.0 *
$AUC_{(0\text{-}240)}$ ratio (met[a]/dg3)	0.266 ± 0.101	1.449 ± 0.621 *	0.803 ± 0.335 †*

Table 4.3 Pharmacokinetic parameters were calculated for the three treatment groups. Each value represents mean ± S.D., n = 6.
*, $p<0.05$; **, $p<0.001$, significantly different from the uninduced digoxin control group.
†, $p<0.05$; ††, $p<0.001$, significantly different from the induced digoxin alone group
[a] met: sum of Dg0 $AUC_{(0\text{-}240)}$ and Dg2 $AUC_{(0\text{-}240)}$.

The AUC ratio increased more than 5-fold in the induced digoxin alone group compared to the uninduced control rats. In the induced rats, when RIF was present, AUC ratio decreased significantly compared to induced without RIF. The trend of AUC ratio changes correlated well with that of hepatocyte studies.

Rat livers were excised and weighed immediately following the final blood draw at 240 minutes. Liver homogenates were made and concentrations of drugs were measured. Amounts of digoxin and its metabolites were expressed as percents of the original digoxin dose (Figure 4.5). The amount of digoxin did not differ significantly among the the 3 groups. However, dg2 levels were significantly higher in the induced digoxin alone group and the induced with RIF group compared to the uninduced control group. Furthermore, the amount of dg2 in the induced with RIF group was substantially higher than the without RIF group. RIF concentration was 254 ± 69 μg/ml/g liver (data not shown). The amount of dg0 in the induced with RIF group is significantly higher than that in the uninduced control group and the induced group.

4.3.4 Uptake of Digoxin Metabolites in Freshly Isolated Hepatocytes and in Oatp1a4 Transfected HEK293 Cells

To test whether digoxin metabolites are substrates of hepatic uptake transporters, 2 min uptake studies were carried out in the presence and the absence of RIF using freshly isolated hepatocytes. Results showed that in the presence of RIF, dg0 uptake was 55.1 ± 1.4 % of its control, dg1 uptake was 32.3 ± 5.1 % of its control, and dg2 uptake

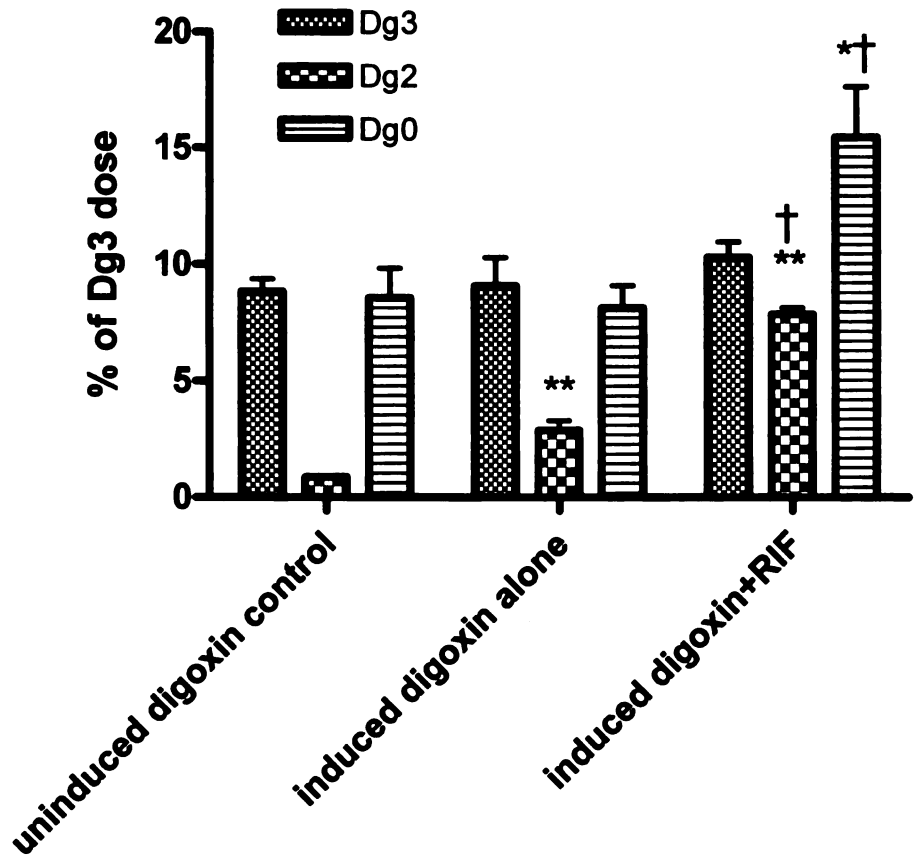

Figure 4.5 *Amounts of digoxin (Dg3), Dg2 and Dg0 retained in the liver at 240 minutes expressed as percentages of the original digoxin dose.* *, $p<0.05$; **, $p<0.001$, significantly different from the uninduced control group. †, $p<0.05$, significantly different from the induced digoxin alone group. Data are depicted as the mean ± S.D., n=6.

was 31.7 ± 0.8 % of its control (Figure 4.6A). To further investigate which uptake transporters are responsible for the uptake of the metabolites, Oatp1a4, Oatp1b2, and vector control plasmids were transiently transfected into HEK293 cells. Compared to each respective empty vector control, dg0 uptake was 188 ± 23 %, dg1 uptake was 380 ± 18 %, and dg2 uptake was 465 ± 39 % in Oatp1a4 transfected cells (Figure 4.6B). However, there were no significant changes in uptake found in Oatp1b2 transfected cells compared to vector controls for all three metabolites (data not shown). These data collectively indicate that digoxin metabolites are substrates of hepatic uptake transporters, specifically Oatp1a4 in rats.

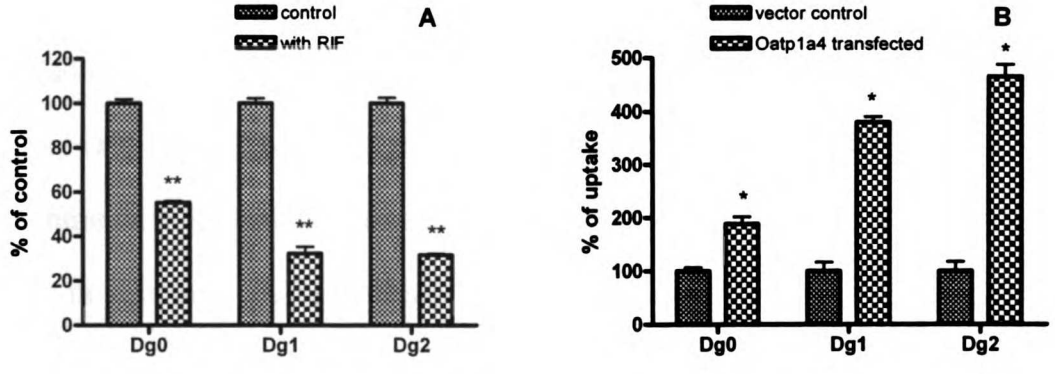

Figure 4.6 *Uptake of digoxin metabolites in (A) freshly isolated hepatocytes with and without the addition of RIF and (B) in Oatp1a4 transfected HEK293 cells and vector controls.* *, $p<0.005$; **, $p<0.0001$, significantly different from the respective control. Data are depicted as the mean ± S.D., n=3.

4.4 Discussion

The present study examined cellular and animal models that may predict the inhibitory effect of rifampin on metabolism of a test drug when dosed together on the final day of an induction regimen in humans. Three treatment groups were used to mimic clinical induction studies. First, the uninduced control group gives baseline values of metabolism for the test drug. Second, the induced group is representative of dosing the test drug alone one day following the final RIF dose of an induction regimen. Third, the induced with RIF group mimics concomitant dosing of the inducing agent RIF with the test drug on the last day of the induction regimen.

Digoxin was used to test our hypothesis because it is a substrate of Oatp1a4, cyp3a, and P-gp. DEX was used to induce cyp3a and the transporters instead of RIF due to species-specific differences between human and rats. In contrast to human OATPs, rat Oatp1a4 is under the regulation of PXR. As a result, 4 day treatment of DEX also induced Oatp1a4 as shown in Figure 4.1. There is a 5-fold increase in intracellular concentration of digoxin in induced cells versus the uninduced baseline control.

In vitro time course studies in hepatocytes showed that without affecting the enzymatic activity, concomitant dosing of rifampin and digoxin in induced cells diminished the induction effect on digoxin metabolism (Figures 4.2 and 4.3). When digoxin was given alone in the induced cells, a 2-fold decrease in digoxin AUC and a 14-fold increase in dg2 AUC were noted compared to that of the uninduced control cells. This profile is consistent with marked up-regulation of cyp3a. However, when RIF was concomitantly dosed with digoxin in the induced cells, digoxin AUC increased 2-fold to a

level no different from that of the uninduced control set. This significant change in AUC is most likely due to inhibition of Oatp1a4, because the RIF concentration used was 100 μM, a concentration previously shown to have minimum inhibitory effect on cyp3a and P-gp (Chapter 2; Lam and Benet, 2004). AUC of dg2 decreased significantly in the induced cells in the presence of RIF compared to induced cells without RIF, but was still significantly greater than that seen with the uninduced control cells. As expected, fewer drug molecules entered the cells and fewer metabolites were formed when the uptake transporters were inhibited. Only very small amounts of dg2 were formed, which resulted in greater changes in dg2 AUCs (13-fold) compared to digoxin AUCs (2-fold). Mass balance for the induced digoxin alone group was only 43% (Table 4.1). This is likely due to sequential metabolism of dg2; however, the levels of dg1 and dg0 were below the LC-MS detection limit. Glucuronidase assays were carried out to free digoxin and its metabolites from the glucuronide adduct for LC-MS measurement (Figure 4.3), however the treatment only improved the mass balance from 43% before digestion to 52% after digestion (Table 4.2). Thus, it appears that DEX may induce other unknown pathways that eliminate digoxin and its metabolites, but this change is not observed when RIF is present to decrease drug transport into hepatocytes, as no significant difference in mass balance is noted between control and induced digoxin with RIF (Table 4.2).

The in vivo rat studies showed that concomitant dosing of RIF and digoxin significantly reduced the apparent induction effects compared to that without RIF in the induced group by inhibiting Oatp1a4 (Figure 4.4). Total clearance (CL) for the induced digoxin alone group was 2-fold higher than that of the uninduced digoxin control group suggesting induction of cyp3a (Table 4.3). When RIF was co-administered with digoxin

in the induced rats, CL was no different than for the digoxin control group. Since rifampin concentrations in the blood (121-2.14 μg/ml) are at low levels that should not inhibit cyp3a, this decrease in CL is most likely due to inhibition of Oatp1a4. Half life for the induced digoxin alone group was expected to be significantly lower than that of the uninduced group, however $T_{1/2}$ for all 3 groups were not significantly different from each other. This results from the finding that volume of distribution increased (2.8-fold) significantly in the digoxin alone induced group versus that of the uninduced group, but in the presence of RIF, Vss returned to the control value. In rats, digoxin has a low hepatic extraction ratio, thus intrinsic clearance plays an important role in digoxin overall clearance. We previously showed that inhibition of Oatp1a4 can alter intrinsic clearance of digoxin by preventing drug entrance into the hepatocytes (Chapter 2, Lam and Benet, 2004). However, the increase in Vss with DEX induction suggests that upregulation of transporters throughout the animal leads to an overall increase in the space available in which digoxin may distribute. This is reversed when RIF is present to inhibit transporters.

Digoxin metabolites observed in the plasma were dg2 and dg0. Compared to the plasma concentrations of digoxin, dg2 concentrations were substantially lower, ranged from 1-12% of digoxin in the three groups, while dg0 concentrations ranged from 25-145% of digoxin concentrations (Figure 4.4). The lack of measurable dg1 reflects the fast conversion of digoxin to dg2 (V_{max}/K_m = 2.92 ± 0.42 μl/min/mg protein), dg1 to dg0 (V_{max}/K_m = 10.95 μl/min/mg protein), and slow formation of dg1 from dg2 (V_{max}/K_m = 0.11 ± 0.03 μl/min/mg protein) by cyp3a in rats (Salphati and Benet, 1999). Dg2 AUC for the induced digoxin alone group did not differ from that of uninduced control, but the

corresponding dg0 AUC was more than twice that of the uninduced control group indicating induction of cyp3a. In the presence of rifampin, AUC of dg2 increased significantly versus that of the induced digoxin alone group (Table 4.3). This finding does not follow the results from the hepatocyte time course study (Table 4.1); however, we have repeatedly observed results similar to those in Table 4.3 for our isolated perfused rat liver (Lau et al., 2006b) and in vivo studies (Chapter 3; Lam et al., 2006; Lau et al., 2006c). Since dg2 is also a substrate for Oatp1a4 (Figure 4.6), it is likely that in the presence of RIF, re-uptake of dg2 back into the liver after exiting into the blood is inhibited. AUC of dg0 for the induced digoxin with RIF group did not differ significantly from that of AUC for the induced digoxin alone group (Table 4.3). Metabolites to digoxin AUC ratios followed the same pattern as the ratios from the hepatocyte time course study. Compared to that of uninduced digoxin control group, AUC ratios increased significantly in the induced digoxin alone group suggesting increased metabolism due to induction of cyp3a; whereas without affecting cyp3a activity, inhibition of Oatp1a4 by RIF resulted in a decreased AUC ratio relative to that of the induced digoxin alone group indicating less metabolism occurred. Assays following glucuronidase cleavage were not conducted for in vivo samples due to sample size limitations.

Amounts of digoxin and its metabolites in the liver (at 240 minutes) were measured and expressed as percentages of the original dose. In all treatment groups, the amount of digoxin stayed relatively constant (Figure 4.5). The amount of dg2 in the induced digoxin alone group was markedly higher than that of the uninduced digoxin control group indicating induction of cyp3a; whereas little difference was observed for

dg0. Compared to that of the induced digoxin alone group, amounts of dg2 and dg0 in the induced digoxin with RIF group were significantly higher. In vitro, Oatp1a4 has been shown to be a bi-directional transporter (Li et al., 2000) depending on substrate gradient and intracellular level of glutathione. At 240 minutes, plasma concentrations of RIF were 2.13 ± 0.55 μg/ml, and liver concentrations were 254 ± 69 μg/ml/g liver. It is likely that the liver concentration of RIF is high enough to inhibit basolateral efflux of the metabolites into the blood. The basolateral inhibition should be more prominent for the metabolites since they are more polar than digoxin.

During early-phase drug development, the hepatic uptake transporters should be taken into consideration for their potential effects on drug disposition and metabolism of substrates. Currently, induction study protocols in humans are designed to administer a test drug either on the last day of the 7-day inducing regiment with RIF or a day later. However, our studies with digoxin, a drug that is both metabolized and transported in rats, suggest that these two study designs would yield confusing and possibly contradictory information about drugs with such elimination pathways. Here we showed that concomitant dosing of RIF and digoxin completely diminished the induction effect. In order to observe the full induction effect, a test drug (an OATP substrate) should be administered on day 8, one day following the completion of the inducing regimen.

Chapter 5

References

Akita H, Suzuki H, Ito K, Kinoshita S, Sato N, Takikawa H and Sugiyama Y (2001) Characterization of bile acid transport mediated by multidrug resistance associated protein 2 and bile salt export pump. *Biochim Biophys Acta* **1511**:7-16.

Allen JD and Schinkel AH (2002) Multidrug resistance and pharmacological protection mediated by the breast cancer resistance protein (BCRP/ABCG2). *Mol Cancer Ther* **1**:427-434.

Ambudkar SV, Dey S, Hrycyna CA, Ramachandra M, Pastan I and Gottesman MM (1999) Biochemical, cellular, and pharmacological aspects of the multidrug transporter. *Annu Rev Pharmacol Toxicol* **39**:361-398.

Annaert PP, Turncliff RZ, Booth CL, Thakker DR and Brouwer KL (2001) P-glycoprotein-mediated in vitro biliary excretion in sandwich-cultured rat hepatocytes. *Drug Metab Dispos* **29**:1277-1283.

Antman EM and Smith TW (1985) Digitalis toxicity. *Annu Rev Med* **36**:357-367.

Asberg A, Hartmann A, Fjeldsa E, Bergan S and Holdaas H (2001) Bilateral pharmacokinetic interaction between cyclosporine A and atorvastatin in renal transplant recipients. *Am J Transplant* **1**:382-386.

Backman JT, Kyrklund C, Kivisto KT, Wang JS and Neuvonen PJ (2000) Plasma concentrations of active simvastatin acid are increased by gemfibrozil. *Clin Pharmacol Ther* **68:**122-129.

Backman JT, Kyrklund C, Neuvonen M and Neuvonen PJ (2002) Gemfibrozil greatly increases plasma concentrations of cerivastatin. *Clin Pharmacol Ther* **72:**685-691.

Bauer B, Hartz AM, Fricker G and Miller DS (2004) Pregnane X receptor up-regulation of P-glycoprotein expression and transport function at the blood-brain barrier. *Mol Pharmacol* **66:**413-419.

Bayliss MK, Bell JA, Jenner WN, Park GR and Wilson K (1999) Utility of hepatocytes to model species differences in the metabolism of loxtidine and to predict pharmacokinetic parameters in rat, dog and man. *Xenobiotica* **29:**253-268.

Belinsky MG, Dawson PA, Shchaveleva I, Bain LJ, Wang R, Ling V, Chen ZS, Grinberg A, Westphal H, Klein-Szanto A, Lerro A and Kruh GD (2005) Analysis of the in vivo functions of Mrp3. *Mol Pharmacol* **68:**160-168.

Benedetti MS (2001) Biotransformation of xenobiotics by amine oxidases. *Fundam Clin Pharmacol* **15:**75-84.

Benet LZ and Galeazzi RL (1979) Noncompartmental determination of the steady-state volume of distribution. *J Pharm Sci* **68:**1071-1074.

Benet LZ, Cummins CL and Wu CY (2003) Transporter-enzyme interactions: implications for predicting drug-drug interactions from in vitro data. *Curr Drug Metab* **4:**393-398.

Benet LZ, Cummins CL and Wu CY (2004) Unmasking the dynamic interplay between efflux transporters and metabolic enzymes. *Int J Pharm* **277:**3-9.

Bidstrup TB, Stilling N, Damkier P, Scharling B, Thomsen MS and Brosen K (2004) Rifampicin seems to act as both an inducer and an inhibitor of the metabolism of repaglinide. *Eur J Clin Pharmacol* **60:**109-114.

Bigger JT, Jr. and Leahey EB, Jr. (1982) Quinidine and digoxin. An important interaction. *Drugs* **24:**229-239.

Blanchard RL, Freimuth RR, Buck J, Weinshilboum RM and Coughtrie MW (2004) A proposed nomenclature system for the cytosolic sulfotransferase (SULT) superfamily. *Pharmacogenetics* **14:**199-211.

Borges-Walmsley MI, McKeegan KS and Walmsley AR (2003) Structure and function of efflux pumps that confer resistance to drugs. *Biochem J* **376:**313-338.

Brown GR (1993) Cephalosporin-probenecid drug interactions. *Clin Pharmacokinet* **24:**289-300.

Chambers HF (2001) Antimicrobial Agents, in: *Goodman and Gilman's The Pharmacological Basis of Therapeutics (10th edition)* (Hardman JG, Limbird LE and Gilman AG eds), pp 1250-1256, McGraw-Hill, New York.

Chang JH and Benet LZ (2005) Glucuronidation and the transport of the glucuronide metabolites in LLC-PK1 cells. *Mol Pharm* **2:**428-434.

Christians U, Jacobsen W, Serkova N, Benet LZ, Vidal C, Sewing KF, Manns MP and Kirchner GI (2000) Automated, fast and sensitive quantification of drugs in blood by liquid chromatography-mass spectrometry with on-line extraction: immunosuppressants. *J Chromatogr B Biomed Sci Appl* **748:**41-53.

Coffman BL, Rios GR and Tephly TR (1996) Purification and properties of two rat liver phenobarbital-inducible UDP-glucuronosyltransferases that catalyze the glucuronidation of opioids. *Drug Metab Dispos* **24:**329-333.

Cui Y, Konig J, Leier I, Buchholz U and Keppler D (2001) Hepatic uptake of bilirubin and its conjugates by the human organic anion transporter SLC21A6. *J Biol Chem* **276:**9626-9630.

Cummins CL, Mangravite LM and Benet LZ (2001) Characterizing the expression of CYP3A4 and efflux transporters (P-gp, MRP1, and MRP2) in CYP3A4-transfected Caco-2 cells after induction with sodium butyrate and the phorbol ester 12-O-tetradecanoylphorbol-13-acetate. *Pharm Res* **18:**1102-1109.

Cummins CL, Jacobsen W and Benet LZ (2002a) Unmasking the dynamic interplay between intestinal P-glycoprotein and CYP3A4. *J Pharmacol Exp Ther* **300:**1036-1045.

Cummins CL, Wu CY and Benet LZ (2002b) Sex-related differences in the clearance of cytochrome P450 3A4 substrates may be caused by P-glycoprotein. *Clin Pharmacol Ther* **72:**474-489.

Cummins CL, Salphati L, Reid MJ and Benet LZ (2003) In vivo modulation of intestinal CYP3A metabolism by P-glycoprotein: studies using the rat single-pass intestinal perfusion model. *J Pharmacol Exp Ther* **305:**306-314.

Cummins CL, Jacobsen W, Christians U and Benet LZ (2004) CYP3A4-transfected Caco-2 cells as a tool for understanding biochemical absorption barriers: studies with sirolimus and midazolam. *J Pharmacol Exp Ther* **308:**143-155.

de Vree JM, Jacquemin E, Sturm E, Cresteil D, Bosma PJ, Aten J, Deleuze JF, Desrochers M, Burdelski M, Bernard O, Oude Elferink RP and Hadchouel M (1998) Mutations in the MDR3 gene cause progressive familial intrahepatic cholestasis. *Proc Natl Acad Sci U S A* **95**:282-287.

Dean M, Hamon Y and Chimini G (2001) The human ATP-binding cassette (ABC) transporter superfamily. *J Lipid Res* **42**:1007-1017.

Duthu GS (1985) Interspecies correlation of the pharmacokinetics of erythromycin, oleandomycin, and tylosin. *J Pharm Sci* **74**:943-946.

Eichelbaum M, Ingelman-Sundberg M and Evans WE (2006) Pharmacogenomics and Individualized Drug Therapy. *Annu Rev Med* **57**:119-137.

Faber KN, Muller M and Jansen PL (2003) Drug transport proteins in the liver. *Adv Drug Deliv Rev* **55**:107-124.

Fattinger K, Cattori V, Hagenbuch B, Meier PJ and Stieger B (2000) Rifamycin SV and rifampicin exhibit differential inhibition of the hepatic rat organic anion transporting polypeptides, Oatp1 and Oatp2. *Hepatology* **32**:82-86.

Fisher MB, Vandenbranden M, Findlay K, Burchell B, Thummel KE, Hall SD and Wrighton SA (2000) Tissue distribution and interindividual variation in human UDP-glucuronosyltransferase activity: relationship between UGT1A1 promoter genotype and variability in a liver bank. *Pharmacogenetics* **10**:727-739.

Fisher MB, Paine MF, Strelevitz TJ and Wrighton SA (2001) The role of hepatic and extrahepatic UDP-glucuronosyltransferases in human drug metabolism. *Drug Metab Rev* **33**:273-297.

Foradori A, Mezzano S, Videla C, Pefaur J and Elberg A (1998) Modification of the pharmacokinetics of cyclosporine A and metabolites by the concomitant use of Neoral and diltiazem or ketoconazol in stable adult kidney transplants. *Transplant Proc* **30:**1685-1687.

Frassetto L, Baluom M, Jacobsen W, Christians U, Roland ME, Stock PG, Carlson L and Benet LZ (2005) Cyclosporine pharmacokinetics and dosing modifications in human immunodeficiency virus-infected liver and kidney transplant recipients. *Transplantation* **80:**13-17.

Frelet A and Klein M (2006) Insight in eukaryotic ABC transporter function by mutation analysis. *FEBS Lett* **580:**1064-1084.

Fromm MF, Kim RB, Stein CM, Wilkinson GR and Roden DM (1999) Inhibition of P-glycoprotein-mediated drug transport: A unifying mechanism to explain the interaction between digoxin and quinidine [seecomments]. *Circulation* **99:**552-557.

Fujino H, Saito T, Tsunenari Y, Kojima J and Sakaeda T (2004) Metabolic properties of the acid and lactone forms of HMG-CoA reductase inhibitors. *Xenobiotica* **34:**961-971.

Furst DE (1995) Practical clinical pharmacology and drug interactions of low-dose methotrexate therapy in rheumatoid arthritis. *Br J Rheumatol* **34 Suppl 2:**20-25.

Garfinkel D (1958) Studies on pig liver microsomes. I. Enzymic and pigment composition of different microsomal fractions. *Arch Biochem Biophys* **77:**493-509.

Gerber NC and Sligar SG (1994) A role for Asp-251 in cytochrome P-450cam oxygen activation. *J Biol Chem* **269:**4260-4266.

Gerlach JH, Endicott JA, Juranka PF, Henderson G, Sarangi F, Deuchars KL and Ling V (1986) Homology between P-glycoprotein and a bacterial haemolysin transport protein suggests a model for multidrug resistance. *Nature* **324:**485-489.

Gerloff T, Stieger B, Hagenbuch B, Madon J, Landmann L, Roth J, Hofmann AF and Meier PJ (1998) The sister of P-glycoprotein represents the canalicular bile salt export pump of mammalian liver. *J Biol Chem* **273:**10046-10050.

Glass CK and Rosenfeld MG (2000) The coregulator exchange in transcriptional functions of nuclear receptors. *Genes Dev* **14:**121-141.

Gramatte T and Oertel R (1999) Intestinal secretion of intravenous talinolol is inhibited by luminal R-verapamil. *Clin Pharmacol Ther* **66:**239-245.

Gros, P., M. Raymond, J. Bell, and D. Housman. 1988. Cloning and characterization of a second member of the mouse mdr gene family. *Mol Cell Bio* **8**:2770-2778

Gu YZ, Hogenesch JB and Bradfield CA (2000) The PAS superfamily: sensors of environmental and developmental signals. *Annu Rev Pharmacol Toxicol* **40:**519-561.

Guengerich FP (2005) *Cytochrome P450 Structure, Mechanism, and Biochemistry.* Kluwer Academic / Plenum Publishers, New York.

Guo GL, Choudhuri S and Klaassen CD (2002) Induction profile of rat organic anion transporting polypeptide 2 (oatp2) by prototypical drug-metabolizing enzyme inducers that activate gene expression through ligand-activated transcription factor pathways. *J Pharmacol Exp Ther* **300:**206-212.

Hagenbuch B and Meier PJ (2003) The superfamily of organic anion transporting polypeptides. *Biochim Biophys Acta* **1609:**1-18.

Hagenbuch B and Meier PJ (2004) Organic anion transporting polypeptides of the OATP/ SLC21 family: phylogenetic classification as OATP/ SLCO superfamily, new nomenclature and molecular/functional properties. *Pflugers Arch* **447:**653-665.

Harrison LI and Gibaldi M (1976) Pharmacokinetics of digoxin in the rat. *Drug Metab Dispos* **4:**88-93.

Hasunuma T NM, Yachi T, Arisawa N, Fukushima K (2003) The drug-drug interactions of pitavastatin (NK-104), a novel HMG-CoA reductase in hibitor and cyclosporine. *J Clin Ther Med* **19:**381-389.

Heller M (1990) Cardiac glycosides. New/old ideas about old drugs. *Biochem Pharmacol* **40:**919-925.

Higgis CF (1992) ABC transporters: from microorganisms to man. *Annu Rev Cell Biol* **8**:67-113

Hinderling PH (1984) Kinetics of partitioning and binding of digoxin and its analogues in the subcompartments of blood. *J Pharm Sci* **73:**1042-1053.

Hoffmeyer S, Burk O, von Richter O, Arnold HP, Brockmoller J, Johne A, Cascorbi I, Gerloff T, Roots I, Eichelbaum M and Brinkmann U (2000) Functional polymorphisms of the human multidrug-resistance gene: multiple sequence variations and correlation of one allele with P-glycoprotein expression and activity in vivo. *Proc Natl Acad Sci U S A* **97:**3473-3478.

Hori R, Okamura N, Aiba T and Tanigawara Y (1993) Role of P-glycoprotein in renal tubular secretion of digoxin in the isolated perfused rat kidney. *J Pharmacol Exp Ther* **266:**1620-1625.

Horinouchi M, Sakaeda T, Nakamura T, Morita Y, Tamura T, Aoyama N, Kasuga M and Okumura K (2002) Significant genetic linkage of MDR1 polymorphisms at positions 3435 and 2677: functional relevance to pharmacokinetics of digoxin. *Pharm Res* **19:**1581-1585.

Hyde SC, Emsley P, Hartshorn MJ, Mimmack MM, Gileadi U, Pearce SR, Gallagher MP, Gill DR, Hubbard RE and Higgins CF (1990) Structural model of ATP-binding proteins associated with cystic fibrosis, multidrug resistance and bacterial transport. *Nature* **346:**362-365.

Ismair MG, Stieger B, Cattori V, Hagenbuch B, Fried M, Meier PJ and Kullak-Ublick GA (2001) Hepatic uptake of cholecystokinin octapeptide by organic anion-transporting polypeptides OATP4 and OATP8 of rat and human liver. *Gastroenterology* **121:**1185-1190.

Ito K, Suzuki H, Horie T and Sugiyama Y (2005) Apical/basolateral surface expression of drug transporters and its role in vectorial drug transport. *Pharm Res* **22:**1559-1577.

Iyer L, Hall D, Das S, Mortell MA, Ramirez J, Kim S, Di Rienzo A and Ratain MJ (1999) Phenotype-genotype correlation of in vitro SN-38 (active metabolite of irinotecan) and bilirubin glucuronidation in human liver tissue with UGT1A1 promoter polymorphism. *Clin Pharmacol Ther* **65:**576-582.

Jacquemin E, Hagenbuch B, Stieger B, Wolkoff AW and Meier PJ (1994) Expression cloning of a rat liver Na(+)-independent organic anion transporter. *Proc Natl Acad Sci U S A* **91:**133-137.

Jung D, Hagenbuch B, Gresh L, Pontoglio M, Meier PJ and Kullak-Ublick GA (2001) Characterization of the human OATP-C (SLC21A6) gene promoter and regulation of liver-specific OATP genes by hepatocyte nuclear factor 1 alpha. *J Biol Chem* **276:**37206-37214.

Kajosaari LI, Laitila J, Neuvonen PJ and Backman JT (2005) Metabolism of repaglinide by CYP2C8 and CYP3A4 in vitro: effect of fibrates and rifampicin. *Basic Clin Pharmacol Toxicol* **97:**249-256.

Karpen SJ, Sun AQ, Kudish B, Hagenbuch B, Meier PJ, Ananthanarayanan M and Suchy FJ (1996) Multiple factors regulate the rat liver basolateral sodium-dependent bile acid cotransporter gene promoter. *J Biol Chem* **271:**15211-15221.

Kim RB, Leake BF, Choo EF, Dresser GK, Kubba SV, Schwarz UI, Taylor A, Xie HG, McKinsey J, Zhou S, Lan LB, Schuetz JD, Schuetz EG and Wilkinson GR (2001) Identification of functionally variant MDR1 alleles among European Americans and African Americans. *Clin Pharmacol Ther* **70:**189-199.

Kliewer SA, Moore JT, Wade L, Staudinger JL, Watson MA, Jones SA, McKee DD, Oliver BB, Willson TM, Zetterstrom RH, Perlmann T and Lehmann JM (1998) An orphan nuclear receptor activated by pregnanes defines a novel steroid signaling pathway. *Cell* **92:**73-82.

Klingenberg M (1958) Pigments of rat liver microsomes. *Arch Biochem Biophys* **75:**376-386.

Konig J, Nies AT, Cui Y, Leier I and Keppler D (1999a) Conjugate export pumps of the multidrug resistance protein (MRP) family: localization, substrate specificity, and MRP2-mediated drug resistance. *Biochim Biophys Acta* **1461:**377-394.

Konig J, Rost D, Cui Y and Keppler D (1999b) Characterization of the human multidrug resistance protein isoform MRP3 localized to the basolateral hepatocyte membrane. *Hepatology* **29:**1156-1163.

Kremer JM and Hamilton RA (1995) The effects of nonsteroidal antiinflammatory drugs on methotrexate (MTX) pharmacokinetics: impairment of renal clearance of MTX at weekly maintenance doses but not at 7.5 mg. *J Rheumatol* **22:**2072-2077.

Kruh GD and Belinsky MG (2003) The MRP family of drug efflux pumps. *Oncogene* **22:**7537-7552.

Kullak-Ublick GA, Ismair MG, Stieger B, Landmann L, Huber R, Pizzagalli F, Fattinger K, Meier PJ and Hagenbuch B (2001) Organic anion-transporting polypeptide B (OATP-B) and its functional comparison with three other OATPs of human liver. *Gastroenterology* **120:**525-533.

Kullak-Ublick GA and Becker MB (2003) Regulation of drug and bile salt transporters in liver and intestine. *Drug Metab Rev* **35:**305-317.

Lage H (2003) ABC-transporters: implications on drug resistance from microorganisms to human cancers. *Int J Antimicrob Agents* **22:**188-199.

Lam JL and Benet LZ (2004) Hepatic microsome studies are insufficient to characterize in vivo hepatic metabolic clearance and metabolic drug-drug interactions: studies of digoxin metabolism in primary rat hepatocytes versus microsomes. *Drug Metab Dispos* **32:**1311-1316.

Lam JL, Okochi H, Huang Y and Benet LZ (2006) In vitro and in vivo correlation of hepatic transporter effects on erythromycin metabolism: characterizing the importance of transporter-enzyme interplay. *Drug Metab Dispos* **[Fast Forward May 12]**.

Lan LB, Dalton JT and Schuetz EG (2000) Mdr1 limits CYP3A metabolism in vivo. *Mol Pharmacol* **58:**863-869.

Lau YY, Wu CY, Okochi H and Benet LZ (2004) Ex situ inhibition of hepatic uptake and efflux significantly changes metabolism: hepatic enzyme-transporter interplay. *J Pharmacol Exp Ther* **308:**1040-1045.

Lau YY, Huang Y, Frassetto L and Benet LZ (2006a) Effects of OATP1B1 inhibition of the disposition and metabolism of atorvastatin in healthy volunteers. *Clin Pharmacol Ther* **Submitted.**

Lau YY, Okochi H, Huang Y and Benet LZ (2006b) Multiple transporters affect the disposition of atorvastatin and its two active hydroxy metabolites: application of in vitro and ex situ systems. *J Pharmacol Exp Ther* **316:**762-771.

Lau YY, Okochi H, Huang Y and Benet LZ (2006c) Pharmacokinetics of atorvastatin and its hydroxy metabolites in rats and the effects of concomitant rifampicin single doses: Relevance of first-pass effect from hepatic uptake transporters, intestinal and hepatic metabolism. *Drug Metab Dispos* **[Fast Forward, April 19]**.

Lehmann JM, McKee DD, Watson MA, Willson TM, Moore JT and Kliewer SA (1998) The human orphan nuclear receptor PXR is activated by compounds that regulate CYP3A4 gene expression and cause drug interactions. *J Clin Invest* **102:**1016-1023.

Letschert K, Faulstich H, Keller D and Keppler D (2006) Molecular Characterization and Inhibition of Amanitin Uptake into Human Hepatocytes. *Toxicol Sci.*

Lewis DFV (2001) *Guide to Cytochromes P450 Structure and Function.* Taylor and Francis Inc., London and New York.

Li C, Benet LZ and Grillo MP (2002) Enantioselective covalent binding of 2-phenylpropionic Acid to protein in vitro in rat hepatocytes. *Chem Res Toxicol* **15:**1480-1487.

Li L, Meier PJ and Ballatori N (2000) Oatp2 mediates bidirectional organic solute transport: a role for intracellular glutathione. *Mol Pharmacol* **58:**335-340.

Ling V and Thompson LH (1974) Reduced permeability in CHO cells as a mechanism of resistance to colchicine. *J Cell Physiol* **83:**103-116.

Loo TW and Clarke DM (2005) Recent progress in understanding the mechanism of P-glycoprotein-mediated drug efflux. *J Membr Biol* **206:**173-185.

Luo FR, Paranjpe PV, Guo A, Rubin E and Sinko P (2002) Intestinal transport of irinotecan in Caco-2 cells and MDCK II cells overexpressing efflux transporters Pgp, cMOAT, and MRP1. *Drug Metab Dispos* **30:**763-770.

Marzolini C, Paus E, Buclin T and Kim RB (2004) Polymorphisms in human MDR1 (P-glycoprotein): recent advances and clinical relevance. *Clin Pharmacol Ther* **75:**13-33.

McKenna NJ and O'Malley BW (2002) Combinatorial control of gene expression by nuclear receptors and coregulators. *Cell* **108:**465-474.

Meier PJ, Eckhardt U, Schroeder A, Hagenbuch B and Stieger B (1997) Substrate specificity of sinusoidal bile acid and organic anion uptake systems in rat and human liver. *Hepatology* **26:**1667-1677.

Mikkaichi T, Suzuki T, Tanemoto M, Ito S and Abe T (2004) The organic anion transporter (OATP) family. *Drug Metab Pharmacokinet* **19:**171-179.

Naritomi Y, Terashita S, Kimura S, Suzuki A, Kagayama A and Sugiyama Y (2001) Prediction of human hepatic clearance from in vivo animal experiments and in vitro metabolic studies with liver microsomes from animals and humans. *Drug Metab Dispos* **29:**1316-1324.

Nie W, Sweetser S, Rinella M and Green RM (2005) Transcriptional regulation of murine Slc22a1 (Oct1) by peroxisome proliferator agonist receptor-alpha and -gamma. *Am J Physiol Gastrointest Liver Physiol* **288:**G207-212.

Niemi M, Schaeffeler E, Lang T, Fromm MF, Neuvonen M, Kyrklund C, Backman JT, Kerb R, Schwab M, Neuvonen PJ, Eichelbaum M and Kivisto KT (2004) High plasma pravastatin concentrations are associated with single nucleotide polymorphisms and haplotypes of organic anion transporting polypeptide-C (OATP-C, SLCO1B1). *Pharmacogenetics* **14:**429-440.

Niemi M, Backman JT, Kajosaari LI, Leathart JB, Neuvonen M, Daly AK, Eichelbaum M, Kivisto KT and Neuvonen PJ (2005a) Polymorphic organic anion transporting polypeptide 1B1 is a major determinant of repaglinide pharmacokinetics. *Clin Pharmacol Ther* **77:**468-478.

Niemi M, Neuvonen PJ, Hofmann U, Backman JT, Schwab M, Lutjohann D, von Bergmann K, Eichelbaum M and Kivisto KT (2005b) Acute effects of pravastatin

on cholesterol synthesis are associated with SLCO1B1 (encoding OATP1B1) haplotype *17. *Pharmacogenet Genomics* **15:**303-309.

Nishizato Y, Ieiri I, Suzuki H, Kimura M, Kawabata K, Hirota T, Takane H, Irie S, Kusuhara H, Urasaki Y, Urae A, Higuchi S, Otsubo K and Sugiyama Y (2003) Polymorphisms of OATP-C (SLC21A6) and OAT3 (SLC22A8) genes: consequences for pravastatin pharmacokinetics. *Clin Pharmacol Ther* **73:**554-565.

Noe B, Hagenbuch B, Stieger B and Meier PJ (1997) Isolation of a multispecific organic anion and cardiac glycoside transporter from rat brain. *Proc Natl Acad Sci U S A* **94:**10346-10350.

Nozawa T, Nakajima M, Tamai I, Noda K, Nezu J, Sai Y, Tsuji A and Yokoi T (2002) Genetic polymorphisms of human organic anion transporters OATP-C (SLC21A6) and OATP-B (SLC21A9): allele frequencies in the Japanese population and functional analysis. *J Pharmacol Exp Ther* **302:**804-813.

Omura T and Sato R (1962) A new cytochrome in liver microsomes. *J Biol Chem* **237:**1375-1376.

Omura T and Sato R (1964a) The carbon monoxide-binding pigment of liver microsomes. I. Evidence for its hemoprotein nature. *J Biol Chem* **239:**2370-2378.

Omura T and Sato R (1964b) The carbon monoxide-binding pigment of liver microsomes. II. Solubilization, purification, and properties. *J Biol Chem* **239:**2379-2385.

Ortiz de Montellano PR (2005) *Cytochrome P450 Structure, Mechanism, and Biochemistry*. Kluwer Academic / Plenum Publishers, New York.

Ortiz de Montellano PR and De Voss JJ (2002) Oxidizing species in the mechanism of cytochrome P450. *Nat Prod Rep* **19:**477-493.

Paulusma CC, Kool M, Bosma PJ, Scheffer GL, ter Borg F, Scheper RJ, Tytgat GN, Borst P, Baas F and Oude Elferink RP (1997) A mutation in the human canalicular multispecific organic anion transporter gene causes the Dubin-Johnson syndrome. *Hepatology* **25:**1539-1542.

Pizzagalli F, Hagenbuch B, Stieger B, Klenk U, Folkers G and Meier PJ (2002) Identification of a novel human organic anion transporting polypeptide as a high affinity thyroxine transporter. *Mol Endocrinol* **16:**2283-2296.

Regazzi MB, Iacona I, Campana C, Raddato V, Lesi C, Perani G, Gavazzi A and Vigano M (1993) Altered disposition of pravastatin following concomitant drug therapy with cyclosporin A in transplant recipients. *Transplant Proc* **25:**2732-2734.

Renes J, de Vries EE, Hooiveld GJ, Krikken I, Jansen PL and Muller M (2000) Multidrug resistance protein MRP1 protects against the toxicity of the major lipid peroxidation product 4-hydroxynonenal. *Biochem J* **350 Pt 2:**555-561.

Rettie A (1999) *Handbook of Drug Metabolism*. Marcel Dekker, New York.

Robin MA, Anandatheerthavarada HK, Biswas G, Sepuri NB, Gordon DM, Pain D and Avadhani NG (2002) Bimodal targeting of microsomal CYP2E1 to mitochondria through activation of an N-terminal chimeric signal by cAMP-mediated phosphorylation. *J Biol Chem* **277:**40583-40593.

Rodrigues-Lima F, Blomeke B, Sim E and Dupret JM (2002) NAT--from bugs to brains. An overview of the 2nd International Workshop on the arylamine N-acetyltransferases. *Pharmacogenomics J* **2:**152-155.

Roninson IB, Chin JE, Choi KG, Gros P, Housman DE, Fojo A, Shen DW, Gottesman MM and Pastan I (1986) Isolation of human mdr DNA sequences amplified in multidrug-resistant KB carcinoma cells. *Proc Natl Acad Sci U S A* **83:**4538-4542.

Saborowski M, Kullak-Ublick GA and Eloranta JJ (2006) The human organic cation transporter 1 gene is transactivated by hepatocyte nuclear factor-4{alpha}. *J Pharmacol Exp Ther.* **317**:778-85.

Sadeque AJ, Wandel C, He H, Shah S and Wood AJ (2000) Increased drug delivery to the brain by P-glycoprotein inhibition. *Clin Pharmacol Ther* **68:**231-237.

Sakai K, Yamazaki T and Hinohara Y (1988) Effects of AN-132 and quinidine, antiarrhythmic agents, on plasma digoxin concentrations in rats. *J Pharm Pharmacol* **40:**68-69.

Salphati L and Benet LZ (1998a) Effects of ketoconazole on digoxin absorption and disposition in rat. *Pharmacology* **56:**308-313.

Salphati L and Benet LZ (1998b) Modulation of P-glycoprotein expression by cytochrome P450 3A inducers in male and female rat livers. *Biochem Pharmacol* **55:**387-395.

Salphati L and Benet LZ (1999) Metabolism of digoxin and digoxigenin digitoxosides in rat liver microsomes: involvement of cytochrome P4503A. *Xenobiotica* **29:**171-185.

Sandhu P, Lee W, Xu X, Leake BF, Yamazaki M, Stone JA, Lin JH, Pearson PG and Kim RB (2005) Hepatic uptake of the novel antifungal agent caspofungin. *Drug Metab Dispos* **33:**676-682.

Sarkadi B, Ozvegy-Laczka C, Nemet K and Varadi A (2004) ABCG2 -- a transporter for all seasons. *FEBS Lett* **567:**116-120.

Sasaki M, Suzuki H, Ito K, Abe T and Sugiyama Y (2002) Transcellular transport of organic anions across a double-transfected Madin-Darby canine kidney II cell monolayer expressing both human organic anion-transporting polypeptide (OATP2/SLC21A6) and Multidrug resistance-associated protein 2 (MRP2/ABCC2). *J Biol Chem* **277:**6497-6503.

Satlin LM, Amin V and Wolkoff AW (1997) Organic anion transporting polypeptide mediates organic anion/HCO3- exchange. *J Biol Chem* **272:**26340-26345.

Savolainen J, Edwards JE, Morgan ME, McNamara PJ and Anderson BD (2002) Effects of a P-glycoprotein inhibitor on brain and plasma concentrations of anti-human immunodeficiency virus drugs administered in combination in rats. *Drug Metab Dispos* **30:**479-482.

Schinkel AH, Smit JJ, van Tellingen O, Beijnen JH, Wagenaar E, van Deemter L, Mol CA, van der Valk MA, Robanus-Maandag EC, te Riele HP and et al. (1994) Disruption of the mouse mdr1a P-glycoprotein gene leads to a deficiency in the blood-brain barrier and to increased sensitivity to drugs. *Cell* **77:**491-502.

Schinkel AH, Mayer U, Wagenaar E, Mol CA, van Deemter L, Smit JJ, van der Valk MA, Voordouw AC, Spits H, van Tellingen O, Zijlmans JM, Fibbe WE and Borst P (1997) Normal viability and altered pharmacokinetics in mice lacking mdr1-type (drug-transporting) P-glycoproteins. *Proc Natl Acad Sci U S A* **94:**4028-4033.

Schuetz EG (2001) Induction of cytochromes P450. *Curr Drug Metab* **2:**139-147.

Schuetz EG, Yasuda K, Arimori K and Schuetz JD (1998) Human MDR1 and mouse mdr1a P-glycoprotein alter the cellular retention and disposition of erythromycin, but not of retinoic acid or benzo(a)pyrene. *Arch Biochem Biophys* **350**:340-347.

See YP, Carlsen SA, Till JE and Ling V (1974) Increased drug permeability in Chinese hamster ovary cells in the presence of cyanide. *Biochim Biophys Acta* **373**:242-252.

Seglen PO (1976) Preparation of isolated rat liver cells. *Methods Cell Biol* **13**:29-83.

Sekine T, Cha SH, Tsuda M, Apiwattanakul N, Nakajima N, Kanai Y and Endou H (1998) Identification of multispecific organic anion transporter 2 expressed predominantly in the liver. *FEBS Lett* **429**:179-182.

Shi X, Bai S, Ford AC, Burk RD, Jacquemin E, Hagenbuch B, Meier PJ and Wolkoff AW (1995) Stable inducible expression of a functional rat liver organic anion transport protein in HeLa cells. *J Biol Chem* **270**:25591-25595.

Shih DQ, Bussen M, Sehayek E, Ananthanarayanan M, Shneider BL, Suchy FJ, Shefer S, Bollileni JS, Gonzalez FJ, Breslow JL and Stoffel M (2001) Hepatocyte nuclear factor-1alpha is an essential regulator of bile acid and plasma cholesterol metabolism. *Nat Genet* **27**:375-382.

Shitara Y, Sugiyama D, Kusuhara H, Kato Y, Abe T, Meier PJ, Itoh T and Sugiyama Y (2002) Comparative inhibitory effects of different compounds on rat oatpl (slc21a1)- and Oatp2 (Slc21a5)-mediated transport. *Pharm Res* **19**:147-153.

Shitara Y, Itoh T, Sato H, Li AP and Sugiyama Y (2003) Inhibition of transporter-mediated hepatic uptake as a mechanism for drug-drug interaction between cerivastatin and cyclosporin A. *J Pharmacol Exp Ther* **304**:610-616.

Shitara Y, Hirano M, Adachi Y, Itoh T, Sato H and Sugiyama Y (2004a) In vitro and in vivo correlation of the inhibitory effect of cyclosporin A on the transporter-mediated hepatic uptake of cerivastatin in rats. *Drug Metab Dispos* **32:**1468-1475.

Shitara Y, Hirano M, Sato H and Sugiyama Y (2004b) Gemfibrozil and its glucuronide inhibit the organic anion transporting polypeptide 2 (OATP2/OATP1B1:SLC21A6)-mediated hepatic uptake and CYP2C8-mediated metabolism of cerivastatin: analysis of the mechanism of the clinically relevant drug-drug interaction between cerivastatin and gemfibrozil. *J Pharmacol Exp Ther* **311:**228-236.

Shitara Y, Sato H and Sugiyama Y (2005) Evaluation of drug-drug interaction in the hepatobiliary and renal transport of drugs. *Annu Rev Pharmacol Toxicol* **45:**689-723.

Smith AJ, Timmermans-Hereijgers JL, Roelofsen B, Wirtz KW, van Blitterswijk WJ, Smit JJ, Schinkel AH and Borst P (1994) The human MDR3 P-glycoprotein promotes translocation of phosphatidylcholine through the plasma membrane of fibroblasts from transgenic mice. *FEBS Lett* **354:**263-266.

Smith AJ, van Helvoort A, van Meer G, Szabo K, Welker E, Szakacs G, Varadi A, Sarkadi B and Borst P (2000) MDR3 P-glycoprotein, a phosphatidylcholine translocase, transports several cytotoxic drugs and directly interacts with drugs as judged by interference with nucleotide trapping. *J Biol Chem* **275:**23530-23539.

Soroka CJ, Lee JM, Azzaroli F and Boyer JL (2001) Cellular localization and up-regulation of multidrug resistance-associated protein 3 in hepatocytes and cholangiocytes during obstructive cholestasis in rat liver. *Hepatology* **33:**783-791.

Staudinger JL, Madan A, Carol KM and Parkinson A (2003) Regulation of drug transporter gene expression by nuclear receptors. *Drug Metab Dispos* **31:**523-527.

Stone JA, Migoya EM, Hickey L, Winchell GA, Deutsch PJ, Ghosh K, Freeman A, Bi S, Desai R, Dilzer SC, Lasseter KC, Kraft WK, Greenberg H and Waldman SA (2004) Potential for interactions between caspofungin and nelfinavir or rifampin. *Antimicrob Agents Chemother* **48:**4306-4314.

Strange RC, Spiteri MA, Ramachandran S and Fryer AA (2001) Glutathione-S-transferase family of enzymes. *Mutat Res* **482:**21-26.

Strautnieks SS, Bull LN, Knisely AS, Kocoshis SA, Dahl N, Arnell H, Sokal E, Dahan K, Childs S, Ling V, Tanner MS, Kagalwalla AF, Nemeth A, Pawlowska J, Baker A, Mieli-Vergani G, Freimer NB, Gardiner RM and Thompson RJ (1998) A gene encoding a liver-specific ABC transporter is mutated in progressive familial intrahepatic cholestasis. *Nat Genet* **20:**233-238.

Su SF and Huang JD (1996) Inhibition of the intestinal digoxin absorption and exsorption by quinidine. *Drug Metab Dispos* **24:**142-147.

Sun H, Huang Y, Frassetto L and Benet LZ (2004) Effects of uremic toxins on hepatic uptake and metabolism of erythromycin. *Drug Metab Dispos* **32:**1239-1246.

Tanabe M, Ieiri I, Nagata N, Inoue K, Ito S, Kanamori Y, Takahashi M, Kurata Y, Kigawa J, Higuchi S, Terakawa N and Otsubo K (2001) Expression of P-glycoprotein in human placenta: relation to genetic polymorphism of the multidrug resistance (MDR)-1 gene. *J Pharmacol Exp Ther* **297:**1137-1143.

Tanigawara Y, Okamura N, Hirai M, Yasuhara M, Ueda K, Kioka N, Komano T and Hori R (1992) Transport of digoxin by human P-glycoprotein expressed in a

porcine kidney epithelial cell line (LLC-PK1). *J Pharmacol Exp Ther* **263:**840-845.

Tirona RG, Leake BF, Merino G and Kim RB (2001) Polymorphisms in OATP-C: identification of multiple allelic variants associated with altered transport activity among European- and African-Americans. *J Biol Chem* **276:**35669-35675.

Tirona RG, Leake BF, Wolkoff AW and Kim RB (2003) Human organic anion transporting polypeptide-C (SLC21A6) is a major determinant of rifampin-mediated pregnane X receptor activation. *J Pharmacol Exp Ther* **304:**223-228.

Tracy TS, Krohn K, Jones DR, Bradley JD, Hall SD and Brater DC (1992) The effects of a salicylate, ibuprofen, and naproxen on the disposition of methotrexate in patients with rheumatoid arthritis. *Eur J Clin Pharmacol* **42:**121-125.

Treiber A, Schneiter R, Delahaye S and Clozel M (2004) Inhibition of organic anion transporting polypeptide-mediated hepatic uptake is the major determinant in the pharmacokinetic interaction between bosentan and cyclosporin A in the rat. *J Pharmacol Exp Ther* **308:**1121-1129.

van Montfoort JE, Hagenbuch B, Groothuis GM, Koepsell H, Meier PJ and Meijer DK (2003) Drug uptake systems in liver and kidney. *Curr Drug Metab* **4:**185-211.

Vavricka SR, Van Montfoort J, Ha HR, Meier PJ and Fattinger K (2002) Interactions of rifamycin SV and rifampicin with organic anion uptake systems of human liver. *Hepatology* **36:**164-172.

Vavricka SR, Jung D, Fried M, Grutzner U, Meier PJ and Kullak-Ublick GA (2004) The human organic anion transporting polypeptide 8 (SLCO1B3) gene is

transcriptionally repressed by hepatocyte nuclear factor 3beta in hepatocellular carcinoma. *J Hepatol* **40:**212-218.

Wacher VJ, Wu CY and Benet LZ (1995) Overlapping substrate specificities and tissue distribution of cytochrome P450 3A and P-glycoprotein: implications for drug delivery and activity in cancer chemotherapy. *Mol Carcinog* **13:**129-134.

Walters HC, Craddock AL, Fusegawa H, Willingham MC and Dawson PA (2000) Expression, transport properties, and chromosomal location of organic anion transporter subtype 3. *Am J Physiol Gastrointest Liver Physiol* **279:**G1188-1200.

Waxman DJ (1999) P450 gene induction by structurally diverse xenochemicals: central role of nuclear receptors CAR, PXR, and PPAR. *Arch Biochem Biophys* **369:**11-23.

Weinshilboum RM, Otterness DM, Aksoy IA, Wood TC, Her C and Raftogianis RB (1997) Sulfation and sulfotransferases 1: Sulfotransferase molecular biology: cDNAs and genes. *FASEB J* **11:**3-14.

Wu CY and Benet LZ (2003) Disposition of tacrolimus in isolated perfused rat liver: influence of troleandomycin, cyclosporine, and gg918. *Drug Metab Dispos* **31:**1292-1295.

Wu CY and Benet LZ (2005) Predicting drug disposition via application of BCS: transport/absorption/ elimination interplay and development of a biopharmaceutics drug disposition classification system. *Pharm Res* **22:**11-23.

Youdim MB, Maruyama W and Naoi M (2005) Neuropharmacological, neuroprotective and amyloid precursor processing properties of selective MAO-B inhibitor antiparkinsonian drug, rasagiline. *Drugs Today (Barc)* **41:**369-391.

Zhang L, Dresser MJ, Gray AT, Yost SC, Terashita S and Giacomini KM (1997) Cloning and functional expression of a human liver organic cation transporter. *Mol Pharmacol* **51:**913-921.

Ziegler DM (1993) Recent studies on the structure and function of multisubstrate flavin-containing monooxygenases. *Annu Rev Pharmacol Toxicol* **33:**179-199.

Zong J and Pollack GM (2003) Modulation of P-glycoprotein transport activity in the mouse blood-brain barrier by rifampin. *J Pharmacol Exp Ther* **306:**556-562.

LIBRARY
7541827
3 1378 00754 1827
San Francisco
For reference
Not to be taken from the room.